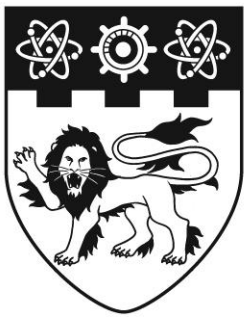

NANYANG TECHNOLOGICAL UNIVERSITY

SYNTHESIS AND CHARACTERIZATION OF POLYSACCHARIDE-BASED ANTIMICROBIAL MATERIALS

LI PENG

SCHOOL OF CHEMICAL AND BIOMEDICAL ENGINEERING

2012

SYNTHESIS AND CHARACTERIZATION OF POLYSACCHARIDE-BASED ANTIMICROBIAL MATERIALS

LI PENG

School of Chemical and Biomedical Engineering

A thesis submitted to the Nanyang Technological University

in partial fulfillment of the requirement for the degree of

Doctor of Philosophy

2012

Acknowledgements

First, I wish to thank my supervisor, Professor Chan Bee Eng, Mary, for her extensive guidance and support throughout my PhD study. It has been an honor to be her student, and I will always be grateful for her help.

Then I need acknowledge and appreciate Prof. Susanna Leong Su Jan for her invaluable advices and support in my research.

I would like to thank the colleagues in my research group, including Dr. Poon Yinfun, Dr. Zhou Chuncai, Dr. Qi Xiaobao, Dr. Yan Liangyu, Dr. Liu Yunxiao, Dr. Yuan Wei, Dr. Daniel Heath, Dr. Shahrzad Rayatpisheh, Mr. Wang Yilei, Ms. Wang Jing, and all other group members for their generous help in my PhD study.

I would also like to acknowledge Prof. Roger W. Beuerman, Prof. Duan Hongwei, Prof. Mu Yuguang, Prof. Matthew Chang, Dr. Zhu Hong-yuan, Mr. Ye Kai, Mr. Li Weifeng, Mr. Li Xiang, for their grateful assistance in my research project.

In addition, I would like to acknowledge the scholarship from Nanyang Technological University and all the facilities provided by School of Chemical and Biomedical Engineering.

Finally, a special thanks to my family and friends for their endless encouragement and support.

Table of Contents

List of Abbreviations

AFM	atomic force microscopy
AMPs	antimicrobial peptides
Ar	argon
ATR	attenuated total reflectance
C. albicans	*Candida. albicans*
CFU	colony forming unit
CS	chitosan
DEGDA	diethylene glycol diacrylate
DI H_2O	de-ionized water
DMAc	*N, N'*-dimethylacetamide
DMDC	dimethyldecylammonium chitosan
DMHC	dimethyldhexylammonium chitosan
DMF	dimethylformadie
DMSO	dimethyl sulfoxide
DPPH	2,2-diphenyl-1-picrylhydrazyl
E. coli	*Escherichia coli*
EDC	1-ethyl-3-(3-dimethylaminopropyl) carbodiimide
F. solani	*Fusarium solani*
FE-SEM	field emission scanning electron microscope
FTIR	fourier transform infrared spectroscopy
GO	graphene oxides
GPC	gel permeation chromatography
GSH	glutathione
H&E	hematoxylin and eosin
IPA	isopropyl alcohol
LB	Luria-Bertani
LPS	lipopolysaccharide

LTA	lipoteichoic acid
MHB	mueller Hinton Broth
MK	microbial keratitis
MRSA	methicillin-resistant *Staphylococcus aureus*
Mw	molecular weight
MTT	methyl tetrazolium
NCA	*N*-carboxyanhydride
NHS	*N*-hydroxysuccinimide
NM	nanomaterials
NMR	nuclear magnetic resonance
NP	nano-particle
P. aeruginosa	*Pseudomonas aeruginosa*
PDI	polydispersity index
PEGDA	poly(ethylene glycol) diacrylate
PEGMA	poly(ethylene glycol) methacrylate
PO	post-operation
PTFE	poly(tetrafluoro ethylene)
QC	quaternized chitosan
RBC	red blood cell
RF	radio frequency
S. aureus	*Staphylococcus aureus*
sccm	standard cubic centimetres per minute
SEM	scanning electron microscopy
SMAMPS	synthetic mimics of antimicrobial peptides
SMC	smooth muscle cell
TCPS	tissue culture polystyrene dish
TGA	thermogravimetric analysis
TMS	trimethyl chitosan
US	United States

UV	ultra-violet
XPS	X-ray photoelectron spectroscopy
YM	yeast-malt

List of Figures

List of Tables

Summary

Microbial infections endanger public health unremittingly and give rise to a huge economic burden to our society. Hence numerous efforts have been made to develop molecules which are able to inhibit pathogens. In this thesis we report the synthesis and characterization of antimicrobial materials based on the natural polysaccharide chitosan.

Despite advanced sterilization and aseptic techniques and procedures, infections associated with medical implants/devices have not been eradicated, particularly in long-term implants. Antimicrobial coatings, which adhere permanently to an implant/device surface, inhibit microorganism colonization and have low toxicity to human cells are a promising approach to lower the incidence of infections. We developed a new class of antimicrobial coating based on hydrogels of quaternized ammonium chitosan-graft-poly(ethylene glycol) methacrylate (qC-g-EM) and poly(ethylene glycol) diacrylate. The hydrogel coating formed by plasma-ultraviolet (UV) induced surface grafting adheres to the substrate surface by covalent bonds, and shows excellent antimicrobial efficacy of more than 99% kill (2 log reductions) against four clinically significant bacteria and fungi: *Pseudomonas aeruginosa* (*P. aeruginosa*), *Escherichia coli* (*E. coli*), *Staphylococcus aureus* (*S. aureus*) and *Fusarium solani* (*F. solani*). Further, a new killing mechanism which is active in this new class of highly hydrated cationic antimicrobial hydrogels has been proposed and tested experimentally: these materials attract parts of the anionic microbial membrane into

internal nanopores of the gels, like an "anion sponge", leading to microbial membrane disruption and apoptosis. *In vitro* and *in vivo* studies suggest that this kind of antimicrobial hydrogel coating is biocompatible with human primary keratinocyte and is non-toxic to the epithelial cells or the underlying stroma of rabbit conjunctiva. In addition to its good antimicrobial activity, this hydrogel is reusable.

The emergence of antibiotic-resistant microorganism strains calls for continuing development of novel antimicrobial molecules. The cytoplasmic membrane of microbes is surrounded by cell wall, a barrier which must be penetrated by all effective antimicrobial molecules. However, the structural affinity of antimicrobial molecules with the microbial cell wall has generally not been considered in previous designs of cationic antimicrobial polymers. Peptidoglycan is a common component of the bacteria cell wall, a feature absent from animal cells, so that peptidoglycan-mimicry may be exploited to achieve high antimicrobial activity with low hemolytic activity. Here, we report a new class of antimicrobial polymers based on cationic peptidopolysaccharides that mimic the peptidoglycan structure and that show excellent antimicrobial activity and high selectivity. The optimum tested peptidopolysaccharide, specifically a copolymer of chitosan and polylysine (CS-*g*-K_{16}), is effective against clinically significant Gram-negative and Gram-positive bacteria and fungi with low minimum inhibitory concentrations (5-20 μg ml^{-1}), and high selectivity (> 5,000-10,000). The *in vitro* and *in vivo* tests suggest non/low-toxicity of CS-g-K_{16} with mammalian cells. Preliminary results also suggest that the compound stimulates little or no inflammatory response. The cationic charge of our peptidopolysaccharides causes them to target the

anionic microbial cell envelope, and their structural affinity with microbial cell wall constituents promotes their penetration of the cell wall to reach the cytoplasmic membrane, where the peptidopolysaccharide acts as an effective membrane disruptor. The combination of these features results in excellent antimicrobial activity and selectivity. This class of antimicrobial peptidopolysaccharides reveals a new direction for the design of antimicrobial molecules.

Although our previous antimicrobial hydrogel coating is highly effective and biocompatible, its application is limited by the weak mechanical strength and requirement of hydrated environments. In order to develop a dry form antimicrobial coating for harsher environments, nanomaterial (NM, this material is being patented at this moment) was grafted with quaternized chitosan (QC) by a facile single-step carbodiimide coupling reaction. The NM-QC nanosheet shows broad-spectrum antimicrobial activity for Gram-negative /positive bacteria, and fungi. The antimicrobial efficacy of NM-QC is superior to pristine NM. FESEM analysis shows that NM-QC induces more significant microbial cell wall/membrane damage than NM and QC, where obvious holes can be observed with NM-QC treated cells. QC appeared to have only a membrane-wrinkling effect while NM incurred only relatively minor morphology changes. The synergistic combination of NM and QC confers the NM-QC nanosheet with unique properties: it comprises a condensed carrier of quaterinzed chitosan, where the cationic charge of the QC groups is responsible for electrostatic-driven contact with the anionic microbial cell envelope and the sharp edges of the single atom layer nanosheet would further enhance membrane disruption.

Importantly, the chitosan groups confer the NM-QC nanosheet good biocompatibility properties, as demonstrated by the reduced hemolytic activity. A transparent coating of NM-QC was fabricated on glass surface and shows broad-spectrum antimicrobial activity of more than 99%kill (2 log reduction) against Gram-negative/positive bacteria and fungi. This dry form antimicrobial coating definitely has a hopeful outlook in healthcare and household applications.

Chapter 1 Introduction

1.1 Background

1.1.1 Call for novel antimicrobial molecules

A multitude of microorganisms populate our planet, and although many of them co-exist together peacefully with us, some are pathogenic and threaten our human lives.[1] Human beings have been suffering and fighting against pathogenic microbial strains.[2] The use of penicillin in the 1940s marks the beginning of the antibiotics era, and many life-saving antibiotics have been discovered and invented since then.[2] Antibiotics fight against infections by the killing or inhibition of the growth of pathogenic microbial strains, resulting in millions of lives being saved and great reduction in patient's suffering.[3] However, the excessive use of antibiotics in human therapeutics, veterinary practices and agriculture over the past decades has triggered the emergence of antibiotic-resistant strains, and some of these are non-treatable with conventional antibiotics.[4] In 2002, approximately 70% of nosocomial infections acquired in the United States (US) are already resistant to at least one antibiotic.[5] The in-hospital deaths associated with methicillin-resistant *Staphylococcus aureus* (MRSA) is estimated to be up to 18,650 cases per year, which even exceeds the deaths associated with HIV in US.[6] Among the *Escherichia coli* isolates from China and India, more than 50% of them are resistant to commonly used antibiotics (*e. g.* Ciprofloxacin and Cephalosporins). With the rapid rise of antibiotic-resistant strains,

microbe antibiotic resistance is now considered to be one of the most imperative public heath issue that needs a new solution.[7] The development of a new class of antimicrobial agents is critically important for public health.

Antimicrobial peptides (AMPs) are a group of ubiquitous host defense molecules that exist in various organisms, and they play an essential role in the innate immune system.[8] After the first discovery of cecropins from silk moth in 1980s, hundreds of natural AMPs were isolated from plants, insects, amphibians, mammals, and prokaryotes.[9-10] AMPs protect their hosts from invasion by a wide variety of pathogenic microorganisms, without incurring microbial resistance after millions of years.[11] Conventional antibiotics act on specific inner targets or metabolic pathways, so that microorganisms deactivate these specific actions in a variety of ways such as modification or overproduction of targets, metabolic bypass of the targeted pathway, drug sequestering, enzymatic alteration, reducing drug uptake, or pumping of drugs extracellularly, *etc*.[12] On the other hand, AMPs generally kill by a completely different mechanism targeting the microbial cell membrane, a previously under-appreciated target of conventional antibiotics.[13] It is challenging for microorganisms to strike back the action mode of AMP, as this will involve redesign of its membrane, e.g. by changing the organization or composition of the bi-layer lipids. Studies both in laboratories and clinics confirmed that the emerging resistance against AMPs is significantly less probable than against conventional antibiotics.[11] AMPs are generally believed to be a promising new class of antimicrobial molecules in the antibiotic-resistance era.

Although AMPs show rapid and broad-spectrum antimicrobial activities, their applications are still limited by some disadvantages such as toxicity, high costs, impurity, proteolysis and salt-senstivity.[14] To overcome some of these limitations, synthetic cationic oligomers and polymers which able to mimic the action mode of AMPs have been developed.

1.1.2 Biomedical implants/devices related infections

Biomedical implants and devices such as contact lenses, catheters, prostheses, arteriovenous shunts, pacemakers and other devices are extensively used in medical care nowadays, to restore the quality of life or save lives.[15-16] Despite advanced sterilization and aseptic techniques and extreme care taken during the implantation procedure, some implants and medical devices can still be infected by bacteria or fungi which can lead to severe infections or life threats.[17-19] Hospital-acquired infections related with biomedical devices and implants have been reported to result in approximately 99,000 deaths per year in US.[5]

The discovery of new antimicrobial materials will also be significant to a large fraction of the world's population. It has been estimated that 125 million people (approximately 2% of the population) wear contact lenses worldwide (2005).[20] However, contact lens wearers are challenged by various microorganisms in the environment and human host constantly.[21] The rate of contact lens related microbial keratitis (MK), which are corneal infections, increased rapidly from 0% to 52%

between 1950s and 1980s, along with the growing popularity of contact lens wearing.[22] 20% of MK cases result in permanent vision damage, due to corneal perforation or scarring caused by the infections.[23-24]

Urinary and intravascular catheters are the most common sources of nosocomial blood stream infections.[25] More than 35 million urinary and venous catheters are inserted in patient's body annually with an infection rate at 10%-30%, and up to 5% of the infected cases lead to death.[26] For orthopedic implants, approximately 4.3% (*i.e.* 112,000 cases) become infected per year, among the 2.6 million implants inserted into humans annually in US.[27]

In serious infections, implant removal or even amputation is inescapable, causing additional suffering to patients, and prolonged hospitalization for typically another 10-20 days.[28-29] Meanwhile, biomedical implant/device-related infections bring a heavy economic burden to the society, and it has cost up to $24 billion in public health spending annually in US (2002).[5] Proper hygiene could only reduce the incidence of infections by two thirds, but not eradicate it. The healthcare system has been longing for minimization of the risk of biomedical devices/implant related infection, particularly without the use of antibiotics.[30] Novel antimicrobial surface coatings for medical devices and implants which are not based on antibiotics or other contaminating or toxic chemicals seem highly attractive for preventing infections and deaths.

1.2 Objectives of Thesis

The objectives of this thesis are to develop novel contact-active antimicrobial materials, in both solution and coating forms, with low hemolysis and toxicity towards mammalian cells. For the coatings, they should adhere permanently on the biomedical device surfaces, inhibit microorganisms from colonizing on the surface and be biocompatible with human cells. This thesis also seeks to understand the mechanisms of their antimicrobial activity and mammalian toxicity. These inventions can potentially act as antimicrobial drugs, minimize the risk of biomedical device/implant related infections, and will significantly reduce the spending in infections-related health care.

Firstly, novel broad-spectrum antimicrobial materials were developed based on the natural polysaccharide chitosan. The antimicrobial activity was significantly promoted by quaternization and alkylation of chitosan, and the biocompatibility was improved by PEGylation. An argon plasma-ultraviolet (UV) induced coating method for hydrogel surface immobilization was developed, which can be applied on diverse soft biomedical surfaces. A novel mechanism of these hydrogels based on “anion sponge” concept was proposed and proven. The optimized coating formulation and conditions show excellent antimicrobial potency. The *in vitro* and *in vivo* studies suggest this antimicrobial coating is biocompatible with mammalian cells.

Secondly, a peptidopolysaccharide that mimics the bacterial peptidoglycan structure, which is a feature unique to bacterial membrane but absent in mammalian cells, was designed, synthesized and tested. By the ring-opening polymerization of

N-carboxyanhydrides (NCA), a polysaccharide backbone was copolymerized with cationic polylysine, and the resulting optimized peptidopolysacchride shows high selectivity to bacteria over mammalian cell.

Thirdly, a polysaccharide-nanomaterial hybrid was designed by combining quaternized chitosan and the nanomaterial (this material is being patented at this moment). The huge specific surface area of the nanomaterial enables high surface density of the cationic polymers, and the nanomaterial act as the delivery vehicle for the targeted anionic bacterial membrane, thus enhancing the antimicrobial properties.

For the three inventions, fundamental studies were also carried out to investigate the interaction between the bacterial membrane and the antimicrobial materials. The mechanisms of the antimicrobial activity and mammalian cytotoxicity were proposed based on experimental and computer simulation results.

1.3 Organization of Thesis

This thesis is organized into 7 Chapters. Chapter 1 is the introduction which covers the background and objectives of this work. Chapter 2 presents a literature review on antimicrobial peptides, oligomers, polymers and hybrid materials and their applications in surface coatings. Chapter 3 describes the experimental details of bacteria and fungi culture, antimicrobial assays and characterization techniques used in this thesis. Chapter 4 is about a contact-active antimicrobial and biocompatible hydrogel of cationic polysaccharide derivatives for covalent surface immobilization.

Chapter 5 describes a series of cationic peptidopolysaccharides which show excellent broad-spectrum antimicrobial activities and high selectivity. Chapter 6 is about a polysaccharide-nanomaterial hybrid with enhanced antimicrobial activity. And Chapter 7 presents the conclusions of this thesis and prospects for further research.

Chapter 2 Literature Review

2.1 Antimicrobial Peptides

Antimicrobial peptides (AMPs) exist widely throughout the plant and animal kingdoms, and have rapid action mode and broad-spectrum antimicrobial activities against bacteria, fungi, viruses and parasites.[11, 31] Hundreds of AMPs have been discovered in the past two decades and they play an essential part in the innate immunity system of most living organisms.[32] Unlike conventional antibiotics such as penicillin, which microbial strains tend to circumvent after decades of clinical use, AMPs are still effective after a history of up to billions of years. Despite the diversity of forms of hundreds of AMPs, most of them have an amphiphilic structure due to the organization of cationic, hydrophobic and hydrophilic amino acids present (Figure 2.1).

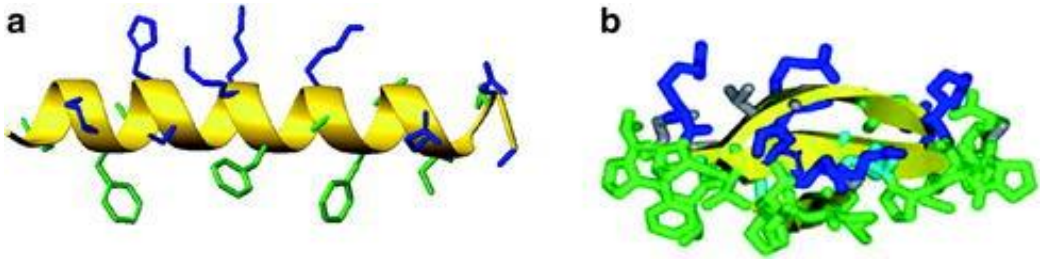

Figure 2.1 The natural antimicrobial peptides (a) Magainin with an α-helix structure;[33] (b) Defensin with a β-sheet structure.[34] Both of them have a facially amphiphilic structure constituting hydrophobic (Green) and hydrophilic (Blue) amino acids.

In spite of the diversity of protocols to determine the cytotoxicity of AMPs to mammalian cells, the most commonly reported "mammalian toxicity" in AMPs and their synthetic mimics is measured by exposing them to red blood cells (RBCs) and then determining the percentage of hemolysis. The concentration which induced 50% lysis of RBCs is commonly labeled as HC_{50}, which is the most frequently used value to gage cytotoxicity to mammalian cells. The preferential tendency of an agent against microbes rather than mammalian cells is typically named as selectivity, which is normally calculated by dividing the value of HC_{50} by the minimum inhibitory concentration (MIC).

2.1.1 Structure of bacteria cell membrane

Phospholipids can be classified as anionic or zwitterionic by their head groups.[35] The composition of phospholipids present in most mammalian cell membranes is different from that of bacterial or fungal cell membranes.[36-37] For the mammalian cell, the outer leaflet of the lipid bilayer usually lacks anionic phospholipids making it neutral, in spite of the inner leaflet of mammalian cells typically contains both zwitterionic and anionic lipids. For example, the outer leaflet of a human erythrocyte cell is composed of zwitterionic sphingomyelin (43%) and phosphatidylcholine (PC, 57%) without any anionic phospholipid, while the inner leaftlet is composed of anionic phosphatidylserine (PS, 30%) with the remaining being zwitterionic phospholipids.[38]

Bacterial and fungal membrane outermost leaflets are negatively charged because they are constituted of anionic phospholipids, usually together with zwitterionic phospholipids.[36-37] For example, Gram-negative bacteria *P. aeruginosa* cell membrane is composed of 13% anionic phosphatidylglycerol (PG), 2% anionic phosphatidic acid (PA), 12% zwitterionic phosphatidyl-choline (PC) and 73% zwitterionic phosphatidylethanolamine (PE).[39] Gram-positive bacteria *S. aureus* cell membrane is composed of PG (57%) and cardiolipin (CL, 43%), both of which are anionic.[38]

Moreover, Gram-negative and Gram-positive bacteria differ in membrane structures as well as phospholipid compositions (Figure 2.2). Gram-negative bacteria have two concentric lipid bilayer membranes: the cytoplasmic (inner) membrane and the outer membrane (Figure 2.2a).[40] Phospholipids distribute equally between the two leaflets of the cytoplasmic membrane, but the outer membrane is highly asymmetric.[40] The outer leaflet is mainly composed of lipopolysaccharides (LPS), while the inner leaflet of outer membrane has the same composition as the cytoplasmic membrane.[41] LPS are highly negatively charged molecules, even more anionic than any phospholipids.[40] Unlike Gram-negative bacteria, Gram-positive bacteria typically possess a single membrane and a thick peptidoglycan layer outside the membrane (Figure 2.2b).[42] This outermost peptidoglycan layer is rich in teichoic acid, which is either covalently linked to the peptidoglycan (as in wall teichoic acid, WTA) or anchored to the membrane phospholipids (as in lipoteichoic acid, LTA).[43]

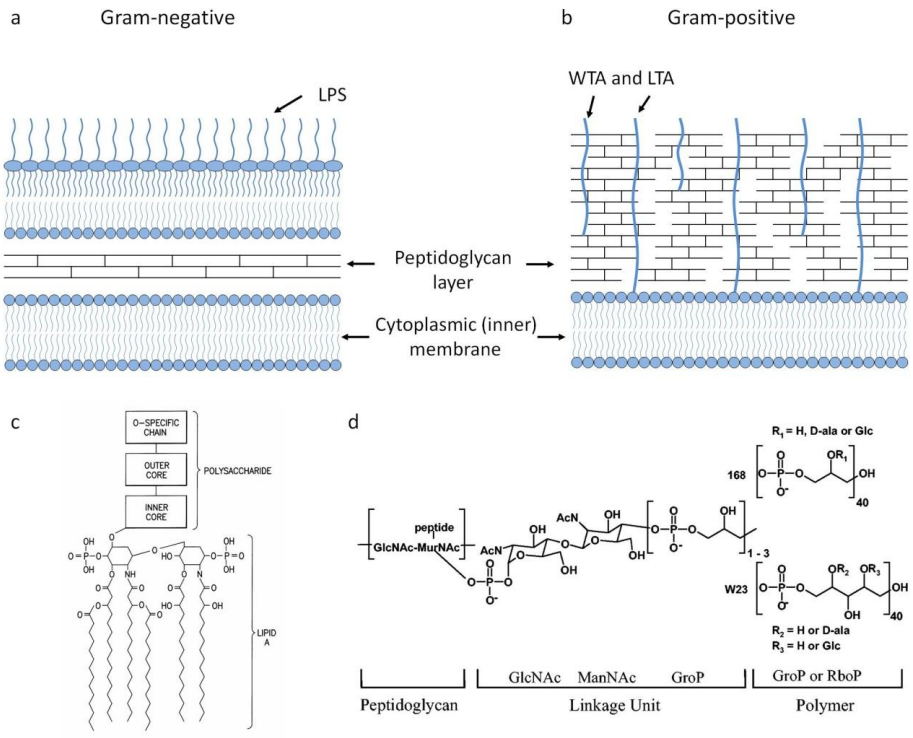

Figure 2.2 Cell wall structures of (a) Gram-negative bacteria and (b) Gram-positive bacteria. Chemical structure of (c) lipopolysaccharide (LPS)[44] (d) teichoic acid and peptidoglycan[45].

2.1.2 Action modes of antimicrobial peptides

Numerous studies have shown that that the amphiphilic structure of AMPs underlies their antimicrobial activities.[46-47] The target of AMPs has been shown to be the cytoplasmic membrane, and the amphiphilic structure plays an essential role for the insertion and disruption of membranes. Firstly, the cationic peptides bind to the anionic bacterial membrane electrostatically. At a low peptide/lipid ratio, peptides bind parallel to the lipid bilayer. When the ratio increases, the amphiphilic peptides change direction and insert into the bilayer, disrupting the membrane or forming transmembrane pores.

Several models have been hypothesized to explain this complex mechanism, and these include the *toroidal pore*, *barrel stave*, or *carpet* models (Figure 2.3).[11, 13, 31, 48]

As many AMPs effect their antimicrobial action through the membrane-active mode, one potential shortcoming is their potential cytotoxicity to mammalian cells and their resulting toxicity. Antimicrobials peptides which kill microbes by a membrane-disturbing mechanism, can potentially also act the same on mammalian cells. But there are AMPs such as magainins, which have selectivity to prokaryocytes over eucaryotes, and kill bacteria efficiently without present significant toxicity for mammalian cells.[49] The mechanism is still little understood, and in-depth studies of the differential interactions of AMPs between bacteria and mammalian membranes will help the design of high selective synthetic AMPs. Another shortcoming of AMPs is their instability to proteases.[32] The other issue about the application of AMPs is the extremely high cost of manufacturing. It is expensive to make AMPs by solid-phase chemical synthesis. So there are many attempts to produce antimicrobial peptide inexpensively, by other methods such as chemical synthesis and recombinant DNA methods.[32]

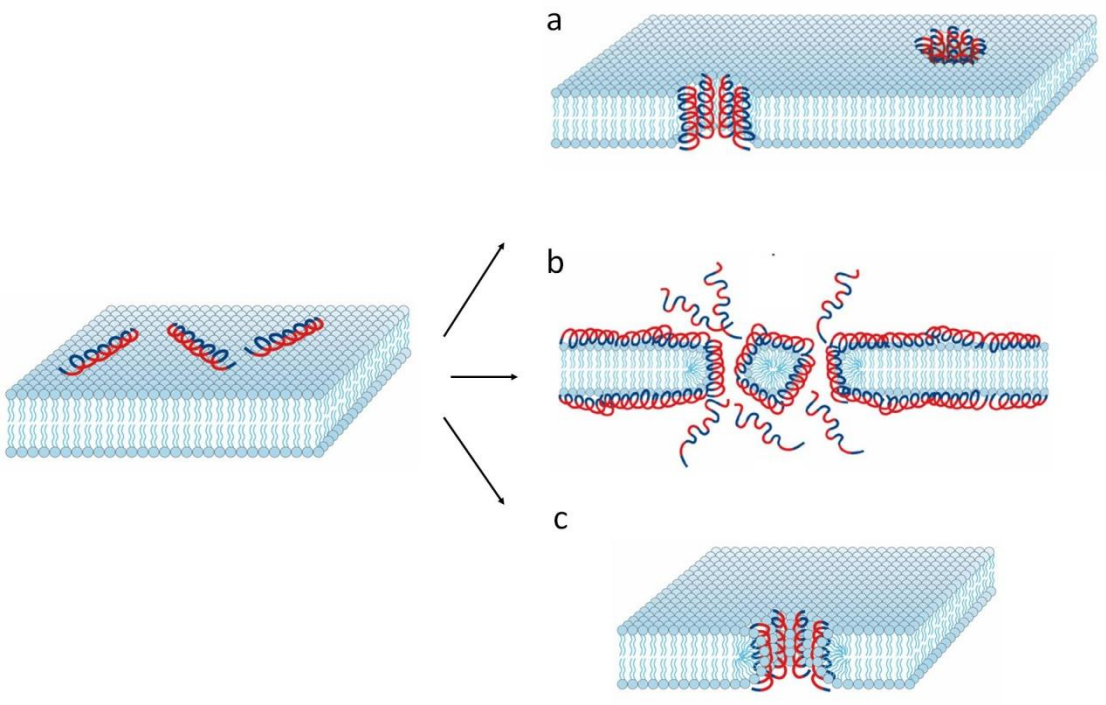

Figure 2.3 (a) Barrel stave model: the peptides aggregate on the cytoplasmic membrane then their hydrophobic part insert into the lipid bilayer interior, the hydrophilic part of peptides form pores.[13, 50] (b) Carpet model: the peptides accumulated on the membrane and forming an layer like a carpet, then act like surfactant disrupt the lipid bilayers.[13, 50] (c) Toroidal pore model: the peptides aggregate on the membrane and cause the bend of lipid monolayers form the pore.[13, 51] The red colour means hydrophilic regions, blue means hydrophobic regions.

2.1.3 Chemical Synthesis of Antimicrobial Peptides

Solid phase chemical synthesis is a widely employed method for peptide production, but this method is suitable for small scale, typically in the milligram range, making the peptide product expensive.[10] Many other chemical synthesis methods have

been attempted to produce peptides inexpensively.[52-53] Among various methods, the ring-opening polymerization of α-amino acid *N*-carboxyanhydrides (NCA) is an attractive route to synthesize antimicrobial peptides.[54-55] NCA polymerization has been studied for decades and a deficiency of the earlier products is the broad molecular weight distribution.[56-57,] Deming has recently reported the application of transition metal initiators based on cobalt and nickel which lead NCA sytnesis to a living and controlled polymerization, so that the length and composition of chain can be narrowly defined.[58-61] Hence, NCA method can be adopted to mimic the amphiphilic structure of AMPs by copolymerization of hydrophilic (Lysine, Arginine, Histidine, etc) and hydrophobic amino acids (Leucine, Phenylalanine, Alanine, etc). Monomers are made by reacting α-amino acids with triphosgene in a single step reaction to form the *N*-carboxyanhydrides (Figure 2.4). The architecture, like chain length, amino acid sequence, and composition, of the polypeptide chain can be controlled in the ensuing solution living polymerization. Functional moieties can also be modified on the chain ends or side chains. The production of peptides in large quantities with a low cost by this polymerization route is possible.[59]

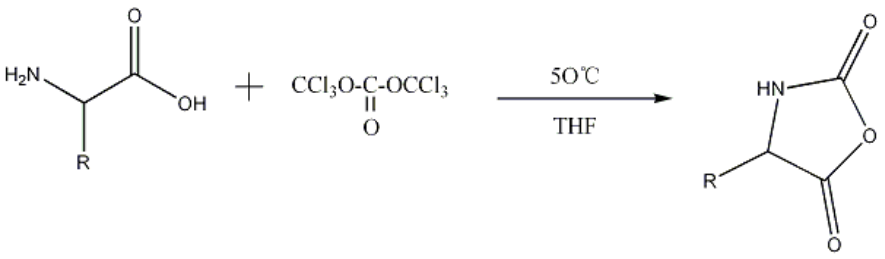

Figure 2.4 Synthesis schematic of the *N*- carboxyanhydrides monomers.[59]

2.1.4 Immobilization of Antimicrobial Peptides

The dosage needed of AMPs when they are immobilized on biomaterial surfaces is reduced compared with systemic therapy use, and immobilized AMPs tethered on the matrix or substrate is incapable of assaulting tissue cells surrounding them but able to prevent microbe colonization.[62-63] Hence, immobilization of AMPs has the potential advantages of lowering the cost and toxicity.[63]

Hydrogels have been widely used in many medical implants, but it also is an ideal place for opportunistic bacteria or other microbes.[64] Even with the help of hygienic technique during the operation, opportunistic microbes still manage to be introduced to the implant sites.[15] Host defenses are often not capable of preventing further colonization if bacterial adhesion occurs before tissue integration at the implant.[18, 65]

Antimicrobial hydrogels based on drug-release strategy have been very popular in recent years, and these may be designed to release antibiotics,[66-69] lysozyme,[70] silver ion,[71] or halogen[72] *etc.* to inhibit microbial colonization in the surrounding environments. However, the chemical/drug would eventually be depleted and sustained release could not be maintained over the long term needed for many implants. Further, prolonged exposure to these drugs/chemicals leads to resistant microbes and cumulative toxicity. Hydrogels based on AMPs cross-linked by chemical or physical force have the potential to overcome these disadvantages of previous described biocide-release hydrogels. Salick and coworkers have invented a hydrogel based on an AMP named MAX1 which shows broad-spectrum activity and is nonhemolytic

towards human red blood cells.[73] For non-hydrogel implants or biomedical devices, surface modification by immobilization of AMPs is a promising method to prevent infections. Peptide LL-37 was grafted on titanium surface with a polyethylene glycol spacer by Gabriel and coworkers, which resulted in a surface peptide layer capable of killing bacteria on contact.[74]

The proteolysis of AMPs is not a disadvantage but beneficial for implants that need biodegradable antimicrobial surfaces. The first 6 h after implantation is the "decisive period" to prevent adhesion of microbes on it, which is critical for long-term success of an implant.[75] A competition exists in this period between the implant integration to the surrounding tissue and opportunistic microbes trying to adhere to its surface. A highly effective, broad-spectrum antimicrobial surface is required during this period.[18] After this phase, the host tissue tends to integrate with the implant material, and so the degradation of immobilized AMPs by protease into nontoxic and biocompatible fragments of liquids would be aid the integration. AMPs immobilized hydrogel or biomaterial surfaces have a significant role in biomedical implant applications.

2.2 Synthetic antimicrobial oligomers

To closely mimic natural AMPs, oligomers with short specific sequences which fold into well-defined secondary structures or conformations (so-called foldamers), have been synthesized using various monomers and methods.[33, 76] Such oligomers are sequentially synthesized by coupling individual monomeric units,

and these oligomers are generally more stable and less expensive to produce than natural AMPs.[77] In the design of synthetic AMPs, the choices of cationic and hydrophobic amino acids are constrained by the total number of amino acids available, while the use of oligomers allows a broader choice of backbone and functional groups. The structures of oligomers are also easier to modify for optimisation and modulation of antimicrobial activity and toxicity.[78]

In earlier studies, efforts were mainly directed toward designing the oligomers to resemble the α-helix structure of natural AMPs. Oligomers such as oligoamides, oligoureas, and *N*-alkyl-glycines (peptoids) have been found to be able to fold into well-defined and controlled α-helix secondary structures (Figure 2.5a).[79-85] It has been generally accepted that such foldamers could be adopted as scaffolds to distribute cationic and hydrophobic groups in a predictable manner, to mimic the amphiphilic structure of host-defense peptides. Eight-residue enantiopure *N*, *N'*-linked oligoureas synthesized by fluorenylmethyloxycarbonyl (Fmoc) chemistry displayed mimetic α-helical structures as determined by CD spectroscopy.[83] These oligourea foldamers showed broad-spectrum activity against both Gram-negative and Gram-positive bacteria, and showed higher HC_{50} values (concentration that yields 50% hemolysis of red blood cells) than MICs.[83] Another class of α-helical macromolecules is the poly-*N*-substituted glycine peptoid which has a conformation that is controlled by its backbone chirality and hydrogen bonding.[84] These 'solid phase chemistry'-synthesized peptoids showed broad-spectrum antimicrobial activity against six clinically relevant pathogens,

and MICs which were comparable with natural AMPs like pexiganan. They exhibited an AMP-like membrane-disrupting mechanism, which was characterized by x-ray reflectivity measurements, and were also found to be stable against proteases due to the lack of peptide bonds.

Although early studies of synthetic AMP mimetic oligomers were initially focused on investigating the relationship between the folded α-helix structures and antimicrobial activity, the outcome of those studies showed that the well folded α-helical structure did not always correlate with antimicrobial activity, suggesting that the formation of an α-helical-derived distinct amphiphilic face was not a pre-requisite for antimicrobial activity. In a recent study on α-helix oligoamide foldamers, the best helical folding isomer showed poor antimicrobial potency coupled with high haemolytic activity, while the scrambled isomer which did not fold well, showed lower MICs and haemolytic activity.[82] Following the conclusion that there was little direct correlation between secondary structure and antimicrobial activity in synthetic oligomers, efforts were then gradually directed towards designing oligomers with amphipathic property, rather than α-helicity. DeGrado and coworkers studied the design of much simpler aromatic acrylamide oligomers which did not have a helix fold but contained facial amphipathic segments (Figure 2.5b).[77, 86-88] Tew and co-workers also developed numerous antimicrobial oligomers by aromatic acrylurea and phenylene ethynylenes.[33, 89-95] The rigid aromatic backbone of these oligomers restrains the molecule's conformation, where hydrogen bonding between the inner molecule groups further

stabilizes their facial amphipathic conformation. Many of such non-helical oligomers have demonstrated low MICs.[86, 94] Recent results strongly suggest amphiphilicity rather than helicity to be the pre-requisite for antimicrobial activity of these oligomers.[33, 77, 96]

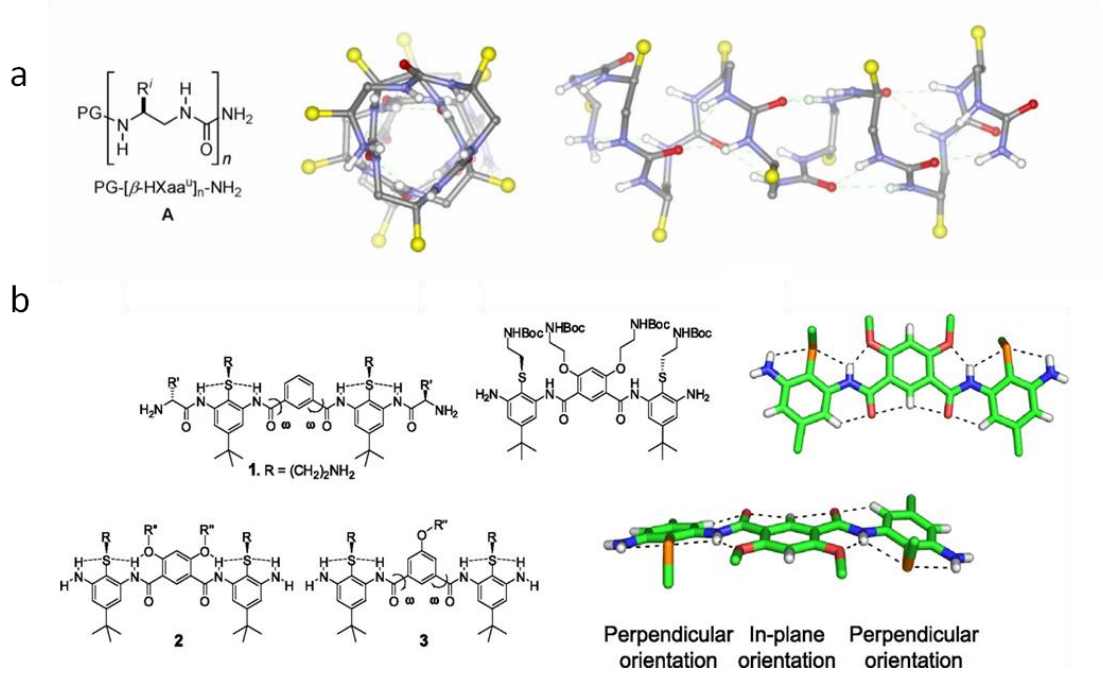

Figure 2.5 (a) Designed oligoureas fold into stable α-helix by H-bonded rings;[83] (b) Non-helical, conformationally-restrained, and facially amphiphilic antimicrobial aromatic acrylamide oligomers.[86]

2.3 Synthetic antimicrobial polymers

Compared to synthetic peptides and oligomers, polymers are generally easier to design and synthesize. The sequence or structure of peptides or oligomers require rigorous design, where the step-by-step synthesis method can be extremely tedious, even on a small scale.[97] Polymers, on the other hand, can be synthesized with significantly fewer reaction steps, and hence can be produced on a large scale relatively easily and cheaply. Antimicrobial polymers such as polynorbornenes,[98] polymethacrylates,[99] polypryidines,[100] polyvinylether,[101] *etc* are designed to mimic the cationic and amphiphilic structure of natural AMPs (Table 2.1). An amphiphilic polymer is commonly designed either a copolymer of cationic and hydrophobic monomers or homopolymeof amphiphilic monomers. Regardless of the monomer structure, cationic groups (such as protonated amine groups) and hydrophobic groups (such as alkyl chain) are usually present on the polymer chain, to confer the polymers with cationic and hydrophobic properties, which are crucial for antimicrobial activity demonstration.[102-108]

Table 2.1 Structures and properties of synthetic antimicrobial homopolymers and copolymers.

		Chemical structure	Name/description	MIC * ($\mu g\ ml^{-1}$)	HC_{50} ($\mu g\ ml^{-1}$)	Selectivity
Homopolymer		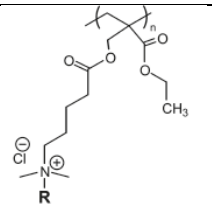	Polymethacrylate with pendant quaternary ammonium groups[109]	64 (E) 128 (S) ($R=C_{12}H_{25}$)		
		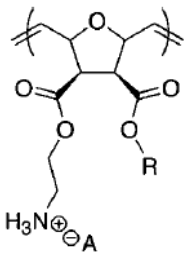	Homopolymer of facial amphiphilic oxanorbornene derived monomers[98]	<3.8 (S)	>2000	>533
		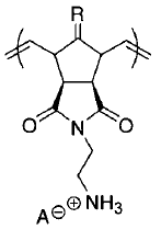	Amphiphilic polynorbornene derivatives[102]	40 (E) 40 (S)	>4000	>100
Copolymer	Random copolymer	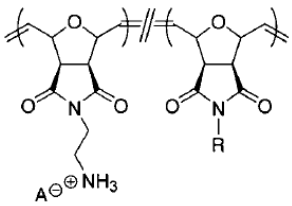	Random coplynorbornenes[110]	75 (S)	1500	20
		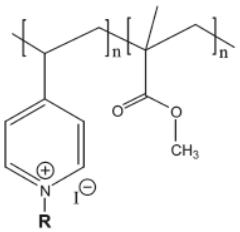	Random copolypyridinium methacrylate B_4[105]	15 (E)	0.23	0.02
		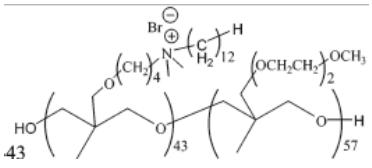	Poly[(3,3-quaternary/PEG)-copolyoxetanes][111]	6 (E) 5 (S)	>60	>10
	Block copolymer	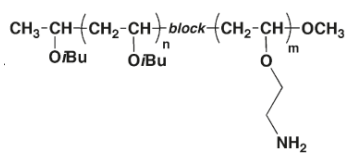	Poly(vinyl ether)[101]	62.5 (E)	>1000	>16

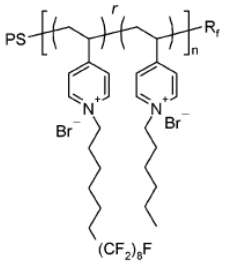	Fluorinated pyridinium block copolymers[112]	almost 100% bactericidal effect of its coating	ND	ND
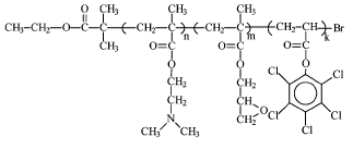	Self-quaternized P(DMAEMA-*c*-GMA)-*b*-PPCPA[113]	>99% kill after 1 hour contact with bacteria (E) of its nanofiber	ND	ND

* (E): *E. coli*; (S): *S. aureus*. ND: not detected.

2.3.1 Synthetic antimicrobial homopolymers

Amphiphilic homopolymers are synthesized either by (i) polymerization of non-amphiphilic monomers coupled with post-polymerization modification such as quaternization (Figure 2.6a),[109] or (ii) direct polymerization from amphiphilic monomers (Figure 2.6b).[114]

Dizman and co-workers synthesized methacrylate homopolymers only by using hydrophobic monomers, where cationic groups were subsequently introduced by quaternization of the functional polymethacrylate backbone. This post-polymerization modification rendered the homopolymer antimicrobial and water-soluble, where the MICs against *E. coli* and *S. aureus* were reported in the range of 32-256 μg ml^{-1}.[109] Several amphiphilic monomers which possess both hydrophobic and cationic groups within one monomer have also been designed in

the last few years, where factors like hydrophobicity and cationic charge density of the monomers were varied to investigate their effects on antimicrobial and haemolytic activity.[98, 102-103, 114-117]

Compared to facially amphiphilic homopolymers with similar random amphihpilic copolymers, Tew and co-workers reported that polynorbornene homopolymers showed distinct advantages in their selectivity for bacteria over mammalian cells.[110] These advantages are hypothesized to be attributed to the balanced distribution of cationic and hydrophobic moieties at the molecule level, which reduces the hemolytic potency induced by hydrophobic segments.[97, 110, 114] Although easier than the synthesis of well-defined oligomers, considerable efforts are still needed to design and synthesise amphiphilic monomers step by step.[97]

a

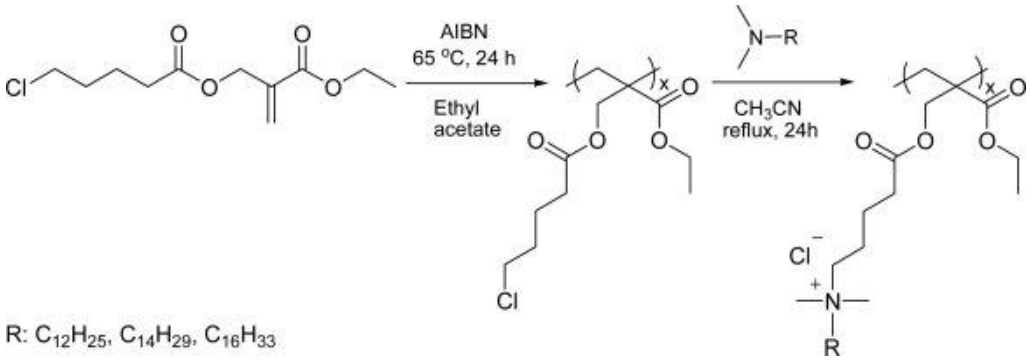

b

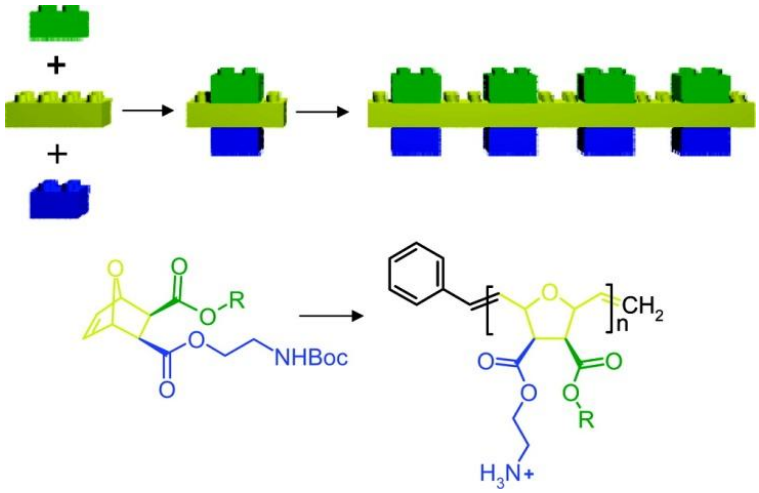

Figure 2.6 (a) Homopolymer with post-polymerization modification for its amphiphilic property.[109] (b) Homopolymer polymerized from facially amphiphilic monomer, that monomer is designed with three components: cationic (hydrophilic) part (blue), hydrophobic part (green) and polymerizable part (yellow).[114]

2.3.2 Synthetic antimicrobial copolymers

Compared to amphiphilic monomers, single functional monomers are more readily available and less expensive. The possibility to re-arrange various cationic and hydrophobic monomers allows greater flexibility in designing amphiphilic

copolymers for a specific requirement. Therefore, the use of co-polymers has been the preferred route for the development of many antimicrobial polymers, where the antimicrobial properties of these co-polymers can also be easily controlled and tuned.[99-101, 105-108, 111-113, 118-126] For example, amphiphilic factors can be easily varied just by changing the ratio of cationic and hydrophobic monomers, without necessitating chemical modification of the functional groups in the amphiphilic monomer. Antimicrobial copolymers can be further classified into two groups (i.e. (i) random or (ii) block copolymer) based on the polymer sequence (Figure 2.7). Random copolymer is a common polymer without a controlled sequence, where cationic and hydrophobic monomers are distributed randomly. Most of the reported antimicrobial copolymers are random copolymers.

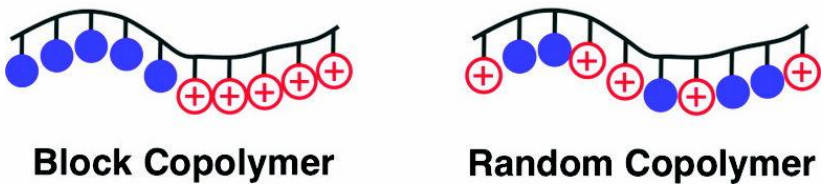

Figure 2.7 Schematic of AMP mimetic amphiphilic block copolymer and random copolymer.[101]

Sen and co-workers have developed three series of copolymers of pyridinium and methacrylate.[105] These pyridinium–methacrylate copolymers were synthesized by free radical polymerization followed by quarternization of the pyridine fragments, where

the pendant alkyl tail was introduced into the polymer chain either on the quaternized pyridine site or the methacrylate site. It was reported that placing the cationic charge and hydrophobic alkyl tail on spatially separated centers amplified mammalian cytotoxicity, where the spatially separated hydrophobic alkyl tails interacted with RBCs more strongly. If the cationic charge and hydrophobic alkyl chain were placed on the same center, improved selectivity was observed despite lowered MIC values. The polymer with the highest selectivity in these series contained a four-carbon alkyl side chain and demonstrated a MIC of 30 μg ml^{-1} and HC_{50} of 1709 μg ml^{-1}, leading to an HC_{50}/MIC of 56.[105] Gellman and co-workers also developed antimicrobial random copolymer based on nylon-3 derivatives.[107, 123] The copolymer with 60% lactam units was reported to show reduced hemolytic activity with increasing fraction of cationic monomers, leading to impressive selectivities above 200.[107] Systematic studies on copolymers of cationic and hydrophobic methacrylate derivatives were also recently reported by Kuroda and co-workers.[99, 106, 108, 119, 127] The amphiphilic polymethacrylate copolymers showed good antimicrobial activity (i.e. MIC of 16 μg ml^{-1} (*E. coli*)), but possessed HC_{50} values that were lower than MIC.[99] The selectivity bottleneck was addressed by systematic variation of the composition of the copolymers to fine-tune the cationic and hydrophobic balance, where the MIC values further decreased to 8 μg ml^{-1} for *E. coli* while the HC_{50} increase to 100 μg ml^{-1}.[106]

Block copolymers need to be synthesized by living polymerizations which require more rigorous conditions, thus not many studies were reported for their antimicrobial applications.[101, 112-113, 125, 128] In an early study of block and random

copolymers of styrene and quaternized pyridine, block copolymers (prepared as particles) were found to be more potent than random copolymers for both *P. aeruginosa* and *S. aureus*, although their hemolytic activities were unreported in this work.[128] It was ascribed that preparation of the particles resulted in the concentration of positive charge of the pyridine block at the interface facing the hydrophilic solvent, which induced a higher surface charge to kill bacteria more effectively.[128] In a more recent study, block and random polyvinylether copolymers were characterized with respect to both their antimicrobial and hemolytic activity.[101] Block polyvinylether copolymer did not show improved antimicrobial activity compared to random ones, where the MIC of the block copolymer was higher than random ones at several coplymerization ratios. Interestingly, the block copolymer showed lower cytotoxicity behaviour than random ones, due to the conformational difference between the two copolymers. Random copolymers have a random coil structure, while block copolymers can fold into a hydrophobic/hydrophilic core/shell structure, where the hydrophobic segment of the block copolymer is shielded by the hydrophilic shell when making contact with the mammalian cell membrane.[101] It has been demonstrated that the global hydrophobicity of these molecules is the dominant factor for hemolytic activity,[106, 129] thus the core/shell structure of block copolymer induced less hemolysis of RBCs.

2.4 Hybrid antimicrobial materials

Hybrid antimicrobial materials are compounds which contain two or more functional fragments combined. This synergistic merging of different functions is aimed at promoting desired properties such as biocompatibility, enhanced antimicrobial activity, and ease of applications *etc*.[130] Antimicrobial macromolecules which are hybrids of different functional segments are setting new trends in the development of efficient, multi-functional and easily usable materials.[131-135] Several classes of hybrid antimicrobial materials which have been reported to be effective in antimicrobial applications are presented in Figure 2.8, and their design strategy and synergistic effects are discussed in this section.

Multi-functional hybrid materials can be obtained by linking natural products together. For example, the natural glycopeptide vancomycin was conjugated with cyanobacterial-derived siderophore anachelin by a PEG linker using Fmoc chemistry (Figure 2.8a).[132] This hybrid material has three components, each having a different function: (i) vancomycin incurs antimicrobial activity, (ii) anachelin renders tethering functions to the system, while (iii) PEG chains with protein-resistant activity eliminates the adhesion of dead cells which will impede antimicrobial activity.[132] The synergistic combination of these three parts renders an antimicrobial and antifouling surface with superior properties compared to the single use of these three molecules.[132] In another study reported by Langer and co-workers, an antifungal agent, Amphotericin B (AmB), was chemically incorporated with dextran chain (Figure 2.8b). Dextran is a natural polysaccharide

made of branched glucose chains, commonly used as scaffolds due to its biocompatible and protein-repellent properties,[69, 136] while AmB is a FDA-approved broad-spectrum antifungal agent widely used in clinical practice.[69, 131] By conjugation with hydrophilic dextran-aldehyde polymer, the hydrophobic AmB was rendered water soluble, and the antifungal efficacy was retained.[131] The AmB-Dextran conjugation is also cross-linkable and injectable for local antifungal therapy.[131]

Self-assembly hybrid copolymers were recently designed by Yang and co-workers.[133-134, 137] Cationic cell-penetrating peptides were grafted with block cholesterol segments (assembly-driving component) to promote the ability to disintegrate microbial cell walls.[133, 137] This hybrid copolymer assembles into a nanoparticle with a core-shell structure, where cholesterol forms a hydrophobic core and the cationic peptide forms a hydrophilic shell which face the exterior (Figure 2.8c). This nanoparticle efficiently inhibited the growth of drug-resistant Gram-positive bacteria and fungi at low MICs while inducing relatively low hemolytic activity. The hydrophobic core and cationic shell nanoparticle structure increases the local density of positive charge to render higher wall- and membrane-permeabilising ability, thereby improving antimicrobial potency.[133-134, 137-138] The design of this hybrid copolymer nanoparticle was further improved by adding degradable linkages between the cationic block and self-assembly driving block, to render it biocidal and biodegradable.[134]

Nanomaterials (i.e. carbon nanotubes, graphene and graphene oxides) have

also been reported to be able to incur physical and microchemical damages to microbial cells.[139-142] A natural AMP, Nisin, was covalently linked with multi-walled carbon nanotubes (MWNTs), which yielded higher antimicrobial activity (7-fold increase) and dramatically improved anti-biofilm activity than pristine MWNTs (Figure 2.8d).[135]

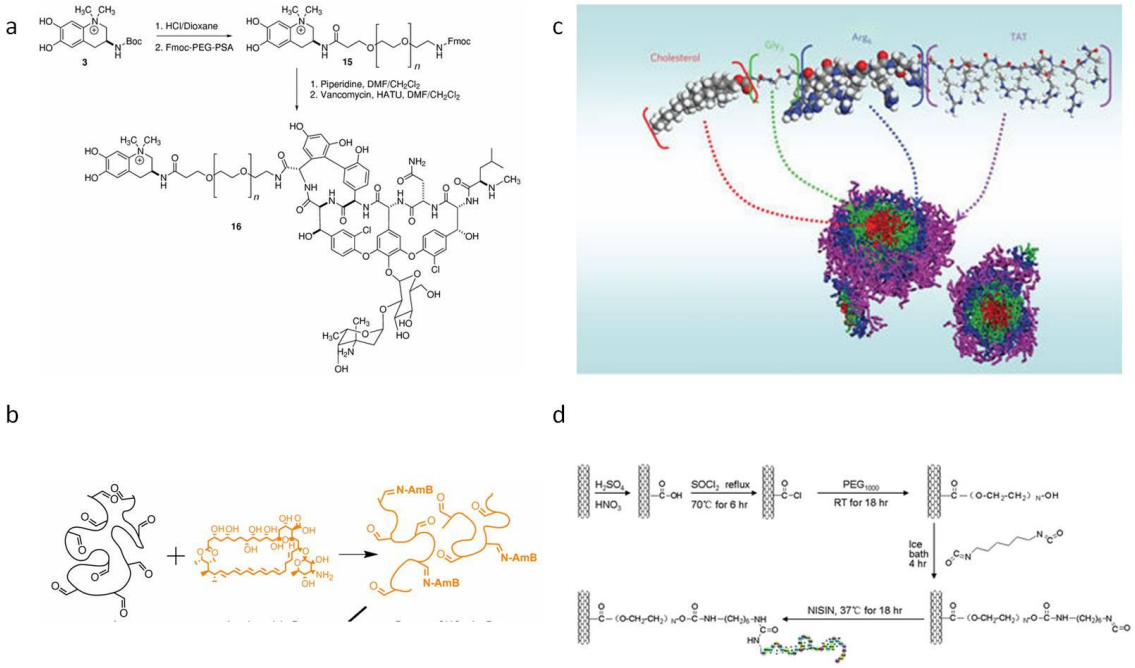

Figure 2.8 (a) Hybrids of anachelin with natural glycopeptide vancomycin;[132] (b) Conjugation of Amphotericin B to oxidized natural polysaccharides (dextran);[131] (c) Self-assembly of peptide and cholesterol hybrids;[133] (d) Conjugation of antimicrobial peptide with carbon nanotubes.[135]

2.5 Factors related to mammalian toxicity and selectivity

AMPs and their synthetic mimics are believed to carry out their biocidal activity by targeting the cell membrane in several steps: the AMPs are electrostatically attracted to the anionic cytoplasmic membrane and then penetrate into the hydrophobic lipid bilayer interior. Although some natural AMPs like magainin and human defensin show excellent selectivity for microbes over mammalian cells, some non-selective AMP like melittin are toxic both to microbes and mammalian cells. Further, the relatively low selectivity of a lot of synthetic antimicrobial molecules, resulting in cytotoxicity to mammalian cells, is an unsolved issue. In some case, the synthetic AMP mimics are even more toxic to mammalian RBCs than to bacteria. Therefore, a lot of efforts have already been done on the study to lower the hemolytic activity and improve the selectivity of synthetic antimicrobial materials. Despite the incompleteness of current studies, some basic parameters and techniques are summarized below.

2.5.1 Balance of hydrophobicity and cationic charge

Cationic charge and hydrophobicity are the most important parameters of AMP mimetic antimicrobial materials. However, the compositions of the membranes of mammalian cells and microbes are different: unlike the anionic microbial membrane, the outer leaflet of mammalian membrane are zwitterionic and has neutral net charge.[37] For this reason there is less electrostatic attraction between mammalian cell membrane and cationic molecules. Therefore it has been demonstrated that the global

hydrophobicity of these antimicrobial agents is the dominant factor critical for the hemolytic activity.[106] The hydrophobicity plays a more important role in penetrating the hydrophobic lipid bilayer interior. Although excessive hydrophobicity is able to improve the antimicrobial activity, its hydrophobic nature enables molecules to bind and be inserted into the non-charged mammalian lipid bilayer even without the aid of cationic charge.[129] Therefore the hydrophobicity/cationic charge need be varied to balance and this can be tuned by (i) varying the fraction of hydrophobic and cationic groups, (ii) varying the length of alkyl chain which affects the hydrophobocity distinctly, and (iii) reducing the total hydrophobicity by add hydrophilic moieties, *etc*.

2.5.2 PEGylation

PEG molecules are well-known biocompatible materials which are able to protect erythrocytes from cell lysis. The PEGylation of amphiphlic molecules is an effective approach to reduce the hemolytic activity. In the study of Youngblood and coworkers, PEG containing monomers was copolymerized with quaternized pyridines, and the resulting hemolytic activity was reduced while the antimicrobial activity retained or even somewhat improved.[100, 120, 126] Tew and coworkers have also modified their amphiphilic monomer with PEG moieties to achieve reduced hemolytic activity.[115]

2.5.3 Self-assembly

As hydrophobicity is more effectively related to the mammalian cytotoxicity, another way to reduce the hydrophobicity is to shield the hydrophobic part of the antimicrobial molecule by self-assembly. Yang and co-workers have demonstrated relatively low hemolysis of self-assembly antimicrobial nanoparticles and attributed the good performance to the hydrophobic core-hydrophilic shell structure.[133] The hydrophilic part of the molecules form a face-out "shell" and wrap the hydrophobic part inside it as a "core", thus reducing the disruption probability with neutral mammalian cells.[133] Kuroda and coworkers also reported similar result in the study of block amphiphilic copolymers which tends to fold into a core-shell structure, thus improving the HC_{50} dramatically.[101]

Besides the previously discussed factors, other factors such as molecular weights, chain flexibility/rigidity, microstructure of cationic and hydrophobic groups, *etc* have also been investigated. The understanding of the selectivity mechanism is still poor, and needs more systematic studies.

2.6 Antimicrobial surface coatings

There is an overwhelming demand for self-sterilizing biomaterials that do not allow microbes to attach, survive, or at least proliferate on their surfaces.[143] Moreover, biomedical devices such as contact lens with high transparency and strict geometric dimension should not experience significant change in the bulk properties with the

coating process. Therefore, surface modification of the biomaterial surfaces is of great interest to many researchers. Antimicrobial coatings have been developed that reduce the adhesion or inhibit the proliferation and survival of microbes without changing the bulk properties.[144] There are three main adopted approaches to fabricate antimicrobial surfaces: biocide-release, microbe/protein-repelling, and contact-active antimicrobial surface modifications (Figure 2.9).[145]

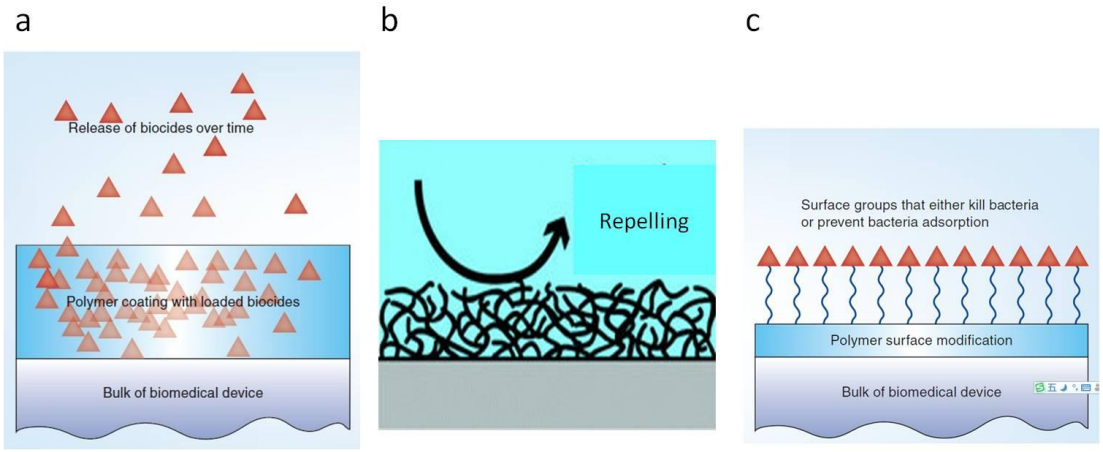

Figure 2.9 Strategies of fabricating antimicrobial surfaces: (a) biocide-release surface; (b) microbe/protein-repelling surface; (c) contact-active surface.

2.6.1 Biocide-release antimicrobial surfaces

Drug-releasing strategy is widely adopted in biomedical applications for combating infections.[18] A biocide-release coating on biomaterial surfaces can resist microbe colonization. Most commonly, the coatings are loaded with biocides such as antibiotics,[69, 146] quaternary ammonium compounds,[147] heavy metal compounds (silver

ion, tributyltin, mercury),[148-149] halogens (iodine) etc,[150] which are then slowly released into the environment to kill microbes around. Although these leaching systems are useful, their practical applications are limited by their disadvantages. Normally these technologies require much larger quantities of the antimicrobial reagent than actually needed since they are gradually released, and they therefore also pose great health hazards and contamination to the environment. Since the antimicrobial reagent is free to release from the surface, it shall be eventually exhausted and so has limited useful life. Moreover, the continuous and mostly unnecessary release of biocides promotes development of microbial resistance, which has been recognized as one of the major problems in modern public health.[151-152]

2.6.2 Microbe/Protein-repelling surfaces

Since infections begin with the adhesion of microbes on the devices surface, it is unnecessary to kill all of them in the surroundings. A microbe/protein-repelling surface which can prevent the adhesion of microbial cells should decrease the incidence of infections. This kind of surfaces can be prepared through grafting or depositing of microbe/protein repelling compounds, such as fluoropolymers,[153] diamond-like carbon,[154] and the widely-studied protein resistant poly(ethylene glycol) (PEG).[155-159] PEG grafted surfaces have been widely used in biomedical applications, such as implanted biomaterial to prevent bacterial infection or platelet adhesion, because of its high protein resistance and good biocompatibility.[160] Unfortunately,

microbes/protein-repelling surface can decrease the adhesion of microbes but never achieve zero adhesion, so that its effectiveness is limited and varies greatly depending on bacterial species.[161-162]

2.6.3 Contact-active antimicrobial surfaces

Non-leaching surfaces which kill microbes effectively by contact represent a new approach to antimicrobial surfaces.[163] Contact-active antimicrobial surfaces can be fabricated by permanent immobilization of biocides by various techniques such as depositing[164], layer by layer[165], or surface grafting[19, 166-168].

Titanium dioxide has been successfully deposited onto polydimethylsiloxane (PDMS) surface by liquid phase deposition and the adhesion of both Gram-negative and Gram-positive bacteria on the modified surfaces has been reduced.[164] Layer by layer technique is also popular in building up an antimicrobial surface. An antimicrobial peptide Chromogranin A was embedded on poly(methylmethacrylate) (PMMA) surface. Growth of *Candida albicans* has been inhibited by 65% and the proliferation was completely stopped.[165] The other approach to produce contact-active antimicrobial surfaces is binding antimicrobial reagents to the surface through covalent interactions. Antimicrobial coatings developed from covalent bonding are permanent compared with biocide-release strategies.

Radical grafting copolymerization has been widely adopted in surface modifications, and initiators are mostly immobilized on the surface or induced by ultra

violet, ozone, gas plasma, etc.[169-170] The grafting copolymerization should be initiated under heat or irradiation.[171] Novel controlled/live polymerization has also been applied in fabricating antimicrobial coatings.[172-173] Russell and co-workers developed permanent, non-leaching antimicrobial surfaces by surface-initiated atom transfer radical polymerization (ATRP).[19, 166-168] Firstly the initiator of 2-bromoisobutyryl bromide or benzophenonyl 2-bormoisobutyrate was immobilized on surfaces of filter paper[166], glass slide[167] or polypropylene[19]. 2-(dimethylaminoethyl methacrylate) (DMAEMA) was then grafted on the surface by ATRP and quaternized by ethyl bromide to build up the bactericidal surface.[167] ATRP is one kind of controlled/living radical polymerization process that provides controlled molecular weights and low polydispersities.[172] Hence the chain length of quaternary ammonium compounds which affected the antibacterial properties can be controlled.[19, 166-168]

Contact-active surfaces possess some advantages over the other two strategies. This non-leaching mode does not have environment hazard, and is effective with a small usage of biocides with a longer or even permanent durability.[163] Contact-active antimicrobial systems are also likely to reduce the incidence of resistant microbe strains. In a study of *N*-alkylated polyethylenimine immobilized antimicrobial surface, neither Gram-positive *E. coli* and Gram-negative *S. aureus* becomes resistant to this surface.[174] The problem of this mode is that it works only when the microbes contact with the surface, so that if a conditioning film was adsorbed, the surface can be masked easily and lose their effectiveness.[175]

Chapter 3 Experimental Details

This chapter describes the commonly used experimental and characterization techniques in this thesis to avoid repeating the same experimental details in later chapters. All other relevant experimental details for each study are shown in Chapter 4-6.

3.1 Culture of bacteria and fungus

The bacteria or fungus strains used in this thesis were purchased from American type culture collection (ATCC): *Escherichia coli* (*E. coli*, ATCC8739), *Pseudomonas aeruginosa* (*P. aeruginosa*, ATCC9027), *Staphylococcus aureus* (S. *aureus* ATCC6538), *Candida albicans* (*C. albicans*, ATCC10231), *Fusarium solani* (*F. solani*, ATCC36031). All broths or agar media were purchased from Becton Dickinson Company. All the bacteria and fungus are stored in 15% glycerol at – 80 ℃.

For the three bacteria (*E. coli*, *P. aeruginosa*, S. *aureus*), a single colony was inoculated in Muller Hinton (MH) broth at 37 ℃ for 4 to 8 hour, with shaking at 200 rpm. *C. albicans* was inoculated in Yeast Malt (YM) broth at 28 ℃ for 24 to 48 hour, with shaking at 200 rpm. After centrifugation (6,000 rpm) for 10 min and PBS washing, the bacterial/fungal cells were diluted to the desired concentration.

F. solani was inoculated in a slant of YM agar and grown at 28 ℃ for 3 days. Then the agar slant was washed with PBS under vortexing to harvest the spores. Spores were collected by centrifugation (6,000 rpm) of the supernatant and diluted to the desired concentration.

3.2 Antimicrobial assays

3.2.1 Minimum inhibitory concentrations (MICs)

Bacteria cells were grown overnight at 37 ℃ in LB broth (YM broth and 28 ℃ for fungus) to a mid-log phase and diluted to 10^4 to 10^5 CFU ml^{-1} in PBS. A twofold dilution series of 100 µl antimicrobial agents solution in the broth (LB broth for bacteria and YM broth for fungus) was made on 96-well microplate, followed by the addition of 100 µl bacterial/fungal suspension (10^4 to 10^5 CFU mL^{-1}). The plates were incubated at 37 ℃ for 18-24h (28 ℃, 36-48h for fungi), and the absorbance at 600nm was measured with a microplate reader (BIO-RAD Benchmark Plus, US). Positive control was without product, and negative control was without bacteria/fungi inoculum. MICs were determined as the lowest concentration that inhibited cell growth by more than 90%.

3.2.2 Antimicrobial assay for coating surfaces

The various hydrogels or surface coatings were soaked and rinsed several times in sterilized PBS for 3 days prior to the antibacterial assays. The assay for their antimicrobial activity followed a modified standard method (*ISO 14729:2001(E) Ophthalmic optics-Contact lens care products- Microbiological requirements and tests methods for products and regimens for hygienic management of contact lenses*). Briefly, 10 µl bacterial suspension (10^8 CFU ml^{-1}) in PBS was spread onto the

hydrogel/coating surfaces in a tissue culture polystyrene (TCPS) plate. The inoculated hydrogels or coatings were incubated at 37℃ for 1 h (exposure time). 1 ml of neutralizing broth was then added to the plate to recover any microbial survivors. A series of 10-fold dilutions in neutralizing broth was prepared, and plated out in LB Agar (YM Agar for fungus). The plates were incubated at 35 ℃ for 36-48 h (28 ℃ for fungus), and counted for colony forming units. A material surface without antimicrobial agents was used as a control.

The results are expressed as:

$$\text{Log reduction} = \text{Log cell count of control} - \text{Log survivor count on samples}$$

$$\%\text{kill} = \frac{\text{Cell count of control} - \text{Survivor count on testing sample}}{\text{Cell count of control}} \times 100$$

3.3 Biological assays

3.3.1 Hemolysis assay

Fresh human blood (5 ml) was collected from a healthy donor (age 25, Male). Erythrocytes were separated by centrifugation at 1000 ×g for 10 min, washed three times with Tris buffer (10 mM Tris, 150 mM NaCl, pH 7.2) and diluted to final concentration (5%, v/v). 50 µl of antimicrobial agent solution at different concentrations mixed with 50 µl erythrocytes stock were added to a 96-well microplate and incubated for 1 h at 37 ℃ with 150 rpm shaking. The microplate was centrifuged at 1000 ×g for 10 min. 80 µl aliquots of the supernatant was then transferred to a new 96-well microplate and diluted with another 80 µl of Tris buffer.

Hemolytic activity was determined at 540 nm with a 96-wells plate spectrophotometer (Benchmark Plus, BIO-RAD). Triton X-100 (0.1% in Tris buffer) which is able to lyse RBCs completely was used as positive control, while Tris buffer was used as negative control. The hemolysis percentage (*H*) was calculated from the following equation:

$$Hemolysis = [(O_p - O_b)/(O_t - O_b)] \times 100\%$$

where O_p is the absorbance for the antimicrobial agent, O_b is the absorbance for the negative control (Tris buffer), and O_t is the absorbance for the positive control of Triton X-100.

3.3.2 MTT assay

Methyl tetrazolium (MTT) assay was used to examine cell viability and proliferation. After specified cell culture time periods, MTT solution (5 mg ml^{-1}, 100 μL), formed from MTT solids pre-dissolved in PBS and filter sterilized, was introduced to each sample in the 96-well TCPS plate. The plate was then kept in an incubator at 37 °C for 4 h. After this time, DMSO (200 μL) was added. The plate was then placed in a shaking incubator for 30 min before measurement of the absorbance at wavelength 490 nm using a microplate spectrophotometer (Benchmark Plus, BIO-RAD).

3.4 Characterization techniques

3.4.1 Proton nuclear magnetic resonance (^{1}H NMR)

Proton nuclear magnetic resonance (^{1}H-NMR) spectroscopy was performed on a Bruker DMX-300 instrument. The products were first dissolved in deuterated solvents, then characterized under a resonance frequency of 300 MHz.

3.4.2 Fourier transform infrared (FTIR) spectra

Fourier transform infrared (FTIR) spectra analysis was performed on a Nicolet™ 5700 FTIR Spectrometer (Thermo Electron Corporation, US) equipped with a golden gate single reflection diamond attenuated total reflection (ATR) unit, over the wavelength range between 400-4000 cm^{-1}, at a resolution of 4 cm^{-1} and scan for 64 times.

3.4.3 Gel permeation chromatography (GPC)

The molecular weights and polydispersity of polymers were measured using a Shimadzu LC-20AD instrument equipped with a refractive index detector (RID), using a PL-aquagel-OH GPC column and sodium acetate buffer (0.2 M, pH 4.05). Samples were analysed at 40 ℃ with an eluent flowrate of 1.0 ml min^{-1}.

3.4.4 Atomic force microscopy (AFM)

The surface morphology was characterized by atomic force microscopy (Molecular Force Probe 3D system, Asylum Research Company, US), using a high resonance frequency probe (Nanoworld NCH-20, Switzerland) in tapping mode.

3.4.5 Field emission scanning electron microscopy (FESEM)

10 µl inoculum (5×10^8 CFU ml^{-1}) of each pathogen was spread onto hydrogel films and incubated for 1 h at 35 ℃ (28 ℃ for *F. solani*) and and a relative humidity of not less than 90%, then immediately fixed with glutaraldehyde (2.5%, 5 ml) solution for 4 hr. The films were dehydrated by adding aq. ethanol in a graded series (20%-100%) and then dried. The microbes on the hydrogel films were observed by FE-SEM (JEOL JSM-6700F) for morphology changes.

Chapter 4 A Contact-Active Antimicrobial and Biocompatible Hydrogel for Covalent Surface Immobilization

4.1 Introduction

Infections arising in association with medical implants and devices are a significant problem and, when these happen, surgical removal or other surgical intervention, with attendant medical risks and complications, is often inevitable. To minimize alteration of bulk properties (*e.g.* mechanical strength or transparency) of an implant, coating with an effective antimicrobial agent seems to be an attractive approach to combat infection.[18, 163, 176] Earlier generations of antimicrobial coatings based on drug/chemical elution have only short-term antimicrobial effect, and cause cumulative toxicity and/or microbe resistance.[150, 177] A contact-active coating having immobilized antimicrobial agent is generally less likely to lead to the development of microbe resistance. This class of coating disrupts the microbes' membranes without targeting their metabolic activity, which is associated with the emergence of resistance.[174]

Antimicrobial polymers have been applied as contact-active coatings.[163] Cationic polymers such as derivatives of polyethylenimine[178], poly(vinyl-*N*-hexylpyridinum)[144], polynorbornene[102], polymethacrylates[99], poly(phenylene ethynylene)[179] *etc* in solution form have been reported to disrupt the pathogen cytoplasmic membrane and some

have impressive selectivity for bacterial over mammalian cells.[37, 179-180] However, when these polymers are immobilized, their antimicrobial activities may be greatly reduced since their diffusion into cell membranes is impeded.[181-182] Polymers which retain their antimicrobial activities even after immobilization typically contain dangling hydrophobic polycations but these often have high toxicity to mammalian cells.[105, 183] At present there are few reports of coatings that are broadly antimicrobial to fungi and bacteria (both Gram-negative and Gram-positive) and that are also non-hemolytic and biocompatible.[69] Also, most reported methods of surface immobilization of polymers are multi-step and post-synthesis,[144, 161, 176] involve organic solvents,[184-185] and do not result in permanent coatings.

In this chapter, we demonstrate highly antimicrobial surfaces based on *in situ* ultraviolet (UV) immobilization of a protein-/cell-repelling and contact-active hydrogel layer made from ***q***uaternized ammonium ***c***hitosan-***g****raft*-poly(***e***thylene glycol) ***m***ethacrylate (qC-*g*-EM) (Figure 4.1). We chose chitosan, an inherently biocompatible and antimicrobial material, for further derivation to add modalities in order to (1) increase the antibacterial and antifungal activity, (2) achieve excellent biocompatibility and (3) enable easy *in situ* coating (*i.e.* surface grafting performed *concurrently* with hydrogel crosslinking). Accordingly, we have modified chitosan to add (1) hydrophobic alkyl side chain and cationic charge through quaternization of the amino group, (2) hydrophilic polyethylene glycol with six ethylene glycol repeats (PEG_6) and (3) methacrylate functionality (Figure 4.1). Others have shown that quaternized chitosan derivatives are water-soluble and more antimicrobial than

pristine chitosan.[186] PEGylation of chitosan derivatives has been shown to decrease cytotoxicity and hemolysis.[187-188] However, PEGylated quaternized chitosan derivatives have not been reported for use as antimicrobial agents.

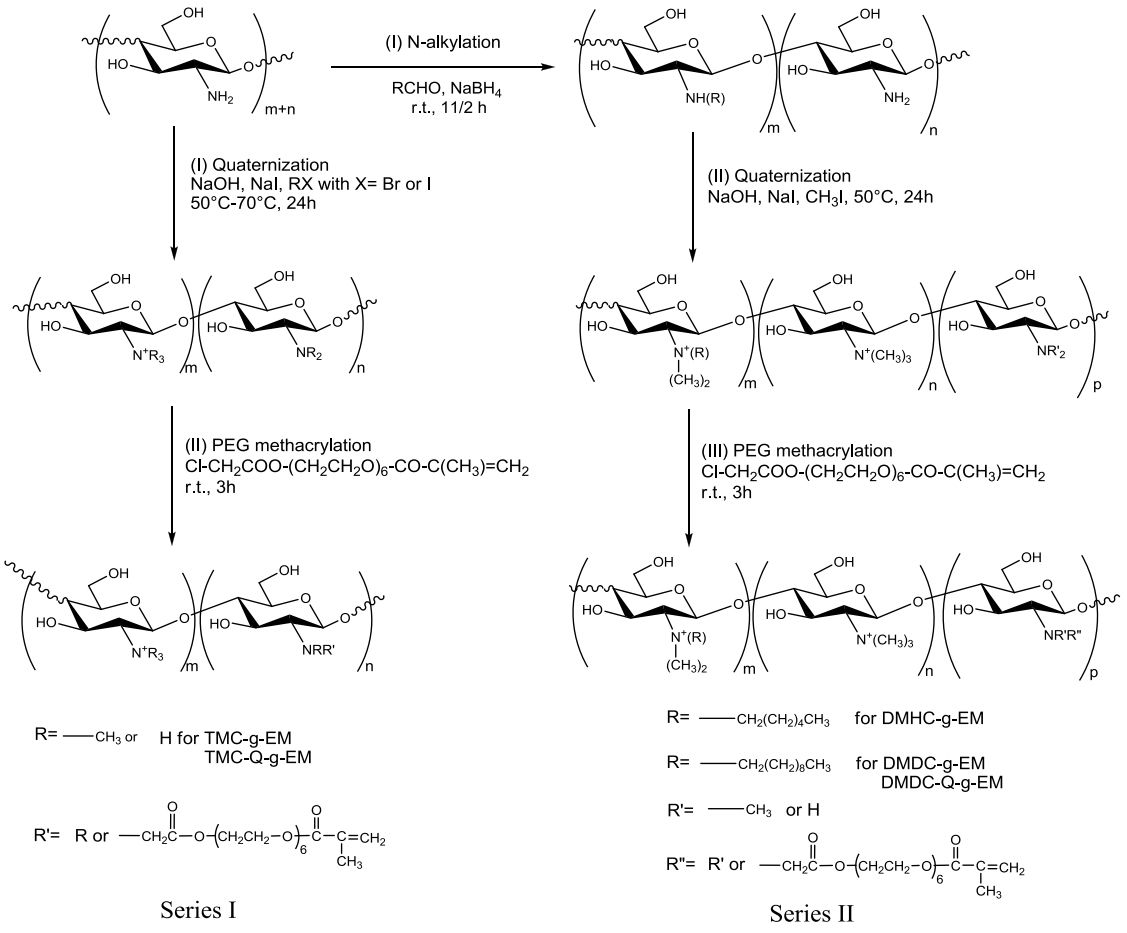

Figure 4.1 Synthetic scheme for preparation of TMC-g-EM and TMC-Q-g-EM (Series I, left side), and DMHC-g-EM, DMDC-g-EM and DMDC-Q-g-EM (Series II, right side).

Also, hydrogels based on qC-*g*-EM have not been reported or explored as antimicrobial coatings. Coulombic attraction would exist between the cationic quaternized ammonium group of qC-*g*-EM and the bacterial or fungal cell membrane, which is typically anionic.[36-37] However, unlike other coatings, hydrogels are porous so that they have interior "space" to receive parts of the microbe membrane that may be "attracted into" the hydrogel.[189-190] When the attraction between anionic membrane components and the cationic hydrogel is strong enough, energy minimization and entropy maximization will drive anionic outer microbe membrane components into the nanopores of the hydrogel, leading to membrane disruption (Figure 4.2).

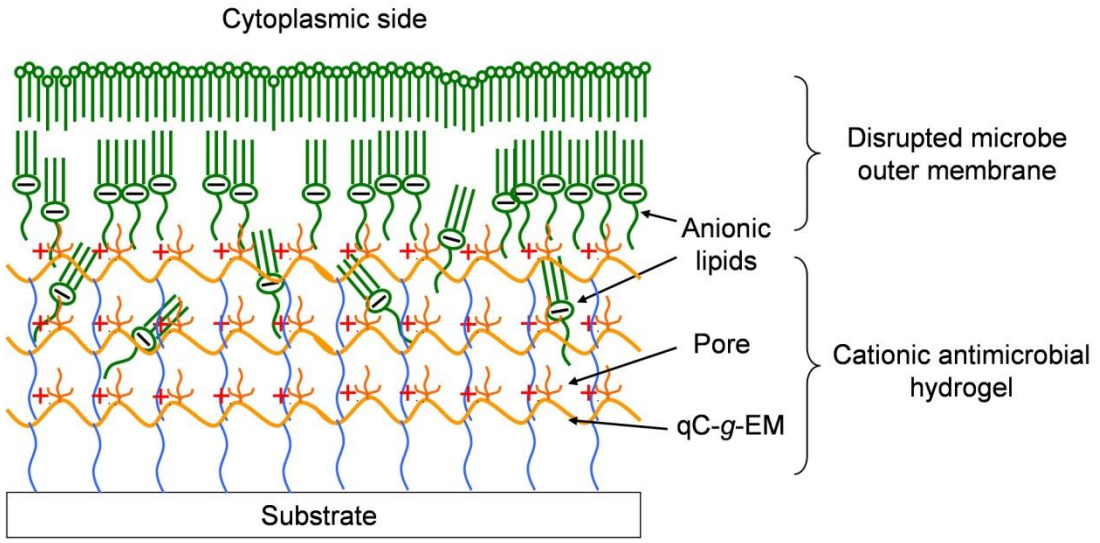

Figure 4.2 Schematic of the "anion sponge" model - parts of the negatively charged bacterial membrane are "suctioned" into the pores of qC-g-EM hydrogel.

Three qC-*g*-EMs, specifically trimethylammonium chitosan-*g*-EM (TMC-*g*-EM), dimethylhexylammonium chitosan-*g*-EM (DMHC-*g*-EM) and dimethyldecylammonium chitosan-*g*-EM (DMDC-*g*-EM), with different alkyl chains were synthesized and tested (Figure 4.1). Two different degrees of quaternization, *i.e.* 20-27% and 51-56%, were explored; "Q" is added to the polymer name *e.g.* TMC-Q-*g*-EM to denote the higher degree of quaternization. In addition, the effect of PEG_6 side chain was also explored: DMDC-M which does not have the PEG_6 side chain but is methacrylated, was also prepared by reacting DMDC with glycidyl methacrylate in the presence of triethylamine rather than with α-terminated PEG_6 methacrylate (Cl-PEG_6M).[191] The solutions and hydrogels based on the various qC-*g*-EMs were tested for efficacy in killing four clinically significant pathogens: the Gram-negative bacteria *Pseudomonas aeruginosa* (*P. aeruginosa*, ATCC9027 isolated from ear infection) and *Escherichia coli* (*E. coli*, ATCC8739 isolated from feces), the Gram-positive bacterium *Staphylococcus aureus* (*S. aureus*, ATCC6538 isolated from human lesion) and the fungus *Fusarium solani* (*F. solani*, ATCC36031 isolated from human corneal ulcer).

4.2 Experimental details

Materials

Chitosan powder, with a degree of deacetylation of 82%, was purchased from Dalian Xindie Chitin Co. The number average molecular weight was 1.05×10^5 g

mol^{-1} (measured by gel permeation chromatography (GPC)). *N*-methyl-2-pyrrolidinone (NMP), methyl iodide, sodium iodide, hexyl bromide, decyl bromide, hexanal, decanal, chloroacetyl chloride, PEG methacrylate (with six ethylene glycol repeats and M_n 360, hereafter denoted PEG_6M), PEG diacrylate (*i.e.* $PEG_{13}DA$, M_n 700), diethylene glycol diacrylate (DEG_2DA, M_n 214), potassium carbonate, sodium hydroxide (NaOH), isopropanol, hydrochloric acid (HCl), sodium borohydride, 2-mercaptoethanol, dimethyl sulfoxide (DMSO), methyl tetrazolium (MTT), iodine and starch were purchased from Sigma-Aldrich (Saint Louis, Missouri, US). Analytical grade hexane, toluene, diethyl ether, ethanol, acetone and methylene chloride were purchased from VWR Pte Ltd (Singapore) and used as received. Toluene was dried over molecular sieves. Irgacure 2959 ((2-hydroxy-1-[4-(2-hydroxyethoxy)phenyl]-2-methyl-1-propanone) was purchased from Ciba (Singapore). Antimicrobial peptides were purchased from Quality Controlled Biochemicals (Hopkinton, MA, US). Phosphate buffered saline (PBS), obtained from Sigma-Aldrich (Saint Louis, Missouri, US), was autoclaved at 121 ℃ for sterilization before use.

Synthesis of qC-g-EMs

Quaternized chitosan (qC) was first synthesized by either route I or route II (shown in Figure 4.1). For quaternized TMC (route I), chitosan (1 g, 6.21 mmol) in NMP (50 ml) was added to NaOH solution (1.5M, 15 ml). Sodium iodide (1.08 g, 7.23 mmol) and methyl iodide (11.2 g, 78.7 mmol) were then added to the chitosan/NMP/NaOH mixture and then reacted for 24 h at 50 ℃. For DMDC (route II), chitosan (1 g, 6.21

mmol) was first pre-dissolved in acetic acid (1%, 100 ml) before adding decanal (0.97 g, 6.2 mmol). After an hour of stirring at room temperature, the solution pH was increased to 4.5 followed by addition of sodium borohydride (9.32 mmol). The product was precipitated by adding NaOH solution (1 M). For TMC-Q and DMDC-Q, the reaction procedure to obtain TMC and DMDC was performed followed by 3 further repetitions of the methylation reaction.

To obtain *qC-g-EM*, NaOH solution (0.38M, 0.30 ml) was added to quaternized chitosan solution (0.2 g in 0.45 ml water), followed by addition of Cl-PEG_6M (0.50 g) pre-dissolved in isopropanol (1.50 ml). The solution was stirred at room temperature for 3 h and qC-*g*-EM was obtained through precipitation and centrifugation followed by dialysis.

Characterizations

^{1}H-NMR spectroscopy of the chitosan derivatives was performed on a Bruker Avance 300 MHz instrument. The quaternization degree of the chitosan derivative was estimated from elemental analysis and calculated from the relation:

$$\text{Quaternization degree} = \frac{\frac{\text{C}}{\text{N}} mol\%(chitosan\ derivative) - \frac{C}{N} mol\%(chitosan)}{\frac{C}{N} mol\%(chitosan)} \times 100\%$$

FTIR spectroscopy of the chitosan derivatives was carried out using a Digilab FTS 3100 instrument. The molecular weights and polydispersity were measured using a Shimadzu LC-20AD instrument equipped with a refractive index detector (RID), using a PL-aquagel-OH GPC column and sodium acetate buffer (0.2 M, pH 4.05) at 40 ℃ with an eluent flowrate of 1.0 ml min^{-1}.

The content of double bond in the qC-g-EM derivatives was determined according to the procedure given in Lim *et al.*[192] Briefly, chitosan derivative (0.3 g) in deionised water (10 ml) was added with mercaptoethanol solution (3%, 5 ml) and NaOH solution (2 M, 1 ml). After stirring for 20 min and the sequential addition of HCl (1 M, 2.5 ml) and three drops of starch indicator, the solution was then titrated with iodine solution (0.05 M) until a blue coloration was observed. The content of double bond was derived from the relation:

$$\text{Double bond amount (mmol/g)} = \frac{(V_1 - V_2) \times 0.05}{W}$$

where W refers to the weight in grams of the dried PEG_6 methacrylated chitosan derivatives, V_1 refers to the volume in ml of iodine used in titration without chitosan derivative and V_2 refers to the volume in ml of iodine used for sample titration. 0.05 refers to the iodine concentration.

Minimum inhibitory concentrations (MICs)

The experimental detail of MIC determination was shown in Chapter 3, section 3.2.1. The test was independently repeated more than twice.

Hemolysis assay

The experimental detail of hemolysis assay was shown in Chpater 3, section 3.3.1.

Preparation of hydrogel and hydrogel coating

All hydrogels except Entry 8 (DMDC-M-LS, Figure 4.6) were formulated from chitosan derivative and polyethylene glycol diacrylate ($PEG_{13}DA$ with M_n 700) in water added in the ratio 1:1:8 (w/w). For Entry 8 (DMDC-M- LS), $PEG_{13}DA$ was

replaced with diethylene glycol diacrylate (DEG_2DA) which has only 2 ethylene glycol repeats to reduce water swelling and pore size. In a typical hydrogel (using $PEG_{13}DA$), chitosan-*g*-PEG methacrylate or quaternized chitosan-*g*-PEG methacrylate (10 wt%) and $PEG_{13}DA$ (10 wt%) were blended and dissolved in deionised water (80 wt%). The mixed solution was added with the photoinitiator Irgacure 2959 (0.1 wt%) and UV-irradiated for 15 min (365 nm, 10 mW cm^{-2}) using a UV mercury lamp fitted inside a Honle UV Technology machine. The low swelling DMDC-M-LS (Entry 8, Figure 4.6) was prepared by blending DMDC-M with DEG_2DA (instead of $PEG_{13}DA$) in dimethylformamide.

Contact lens Z was provided by Menicon company and is made of a copolymer of tris(trimethylsiloxy)silylstyrene and 2,2,2-trifluoroethyl methacrylate. The contact lens were first activated with argon plasma (March PX-500^{TM}, the conditions were 50 W, 300 mTorr and 60 s) and then exposed to air for 15 min to generate surface peroxide groups. The pretreated substrates were then immersed in 1 ml precursor solution of DMDC-Q-g-EM (10 wt%) and $PEG_{13}DA$ (10 wt%) without photoinitiator, then subjected to 15 min of UV irradiation (with an intensity of 10 mW cm^{-2}), a thin layer of hydrogel was grafted onto the surface of contact lens.

After photopolymerization, the hydrogel films or coated samples were vacuum dried for 3 day and rehydrated in deionized water. The rehydrated hydrogel samples were rinsed in excess deionized water and ultrasonicated to remove ungrafted reactants and adsorbed homopolymers.

Swelling of hydrogels

After the photopolymerization process, sample hydrogels were soaked in water to remove unreacted monomers. The hydrogels were then lyophilized to obtain dried hydrogel films. The weight of each dried film was recorded before placing the film in a dish of deionised water at room temperature for 24 h. After the water swelling, the hydrogels were removed from the dish and the water on their surfaces was removed with absorbent paper, after which the weights of the swollen hydrogels were measured. The water uptake was calculated from the equation:

$$\text{Water uptake}, \% = \frac{\text{hydrogel weight - dry film weight}}{\text{dry film weight}} \times 100\%.$$

The water volume fraction was calculated as:

$$\text{Water volume fraction}, \% = \frac{\text{Volume of the uptake water}}{\text{Volume of swollen hydrogel}} \times 100\%$$

Antimicrobial assay for hydrogels

The antimicrobial efficacy of hydrogels was determined following the description in Chapter 3, section 3.2.2.

LIVE/DEAD assay to examine bacterial viability

10 μl bacteria suspension (5×10^8 CFU ml^{-1}) in PBS was spread onto the hydrogel films which were then incubated for 1 h at 37 ℃ and a relative humidity of not less than 90%. The films were then stained with LIVE/DEAD Kit (L13152, Invitrogen) for 30 minutes at room temperature. After rinsing with PBS, imaged with a Zeiss inverted optical microscope.

Microorganism morphology study

The microbes on the hydrogel films were observed by FE-SEM (JEOL JSM-6700F) for morphology changes. The experimental detail was shown in Chapter 3, section 3.4.5.

Computer simulation of microbe killing mechanism

The simulations were performed with the GROMACS package, using an all-atom GLYCAM/AMBER force field. The hydrogel coating was modeled by three layers of quaternized chitosan derivative chains in which each layer consisted of 8 quaternized chitosan derivative chains with an inter-chain separation of about 2.5 nm. Each quaternized chitosan derivative chain contained 10 monosaccharide units. Each chitosan chain in DMDC-Q hydrogel was modeled to contain 5 positive charges. Position restraints were applied to tip linkage oxygen atoms of the chitosan chains to simulate the crosslinking effect of crosslinkers in the hydrogel. The outer layer of the *P. aeruginosa* membrane was simulated to be composed of DOPC and LPS. The rough LPS structure of *P. aeruginosa* PAO1 was modeled based on experimentally sequenced data[28].

Zeta potential measurements

Zeta potential determinations for the hydrogels were made with an electrokinetic analyzer (Antor Parr) with hydrogel films cut into a rectangular shape (measuring approximately 25 mm by 20 mm with thickness of 250 μm) mounted on a clamping cell using KCl solution (0.1 mM, pH 5.5) as background electrolyte and PMMA as reference plate.

Determination of pore sizes

The hydrogel pore size was calculated based on the Peppas-Merrill model.[64] Flory and Rehner developed the rubber elasticity theory for cross-linked polymer networks in the 1940s,[193] and Peppas and Merrill extended this theory to make it applicable for hydrogels[194]. The pore size is normally described using the linear distance between two neighbouring crosslinks (ξ), which is related to the polymer volume fraction in swollen state ($\nu_{2,s}$) and the number average molecular weight of the polymer chain between crosslinks ($\overline{M_c}$). (Eq. (1)):

$$\frac{1}{\overline{M_c}} = \frac{2}{\overline{M_n}} - \frac{(\frac{\bar{\nu}}{V_1})[\ln(1-\nu_{2,s}) + \nu_{2,s} + \chi \nu_{2,s}{}^2]}{\nu_{2,r}\left[\left(\frac{\nu_{2,s}}{\nu_{2,r}}\right)^{1/3} - \left(\frac{\nu_{2,s}}{2\nu_{2,r}}\right)\right]} \quad (1)$$

Here, $\overline{M_c}$ is the number of repeat units between crosslinks, $\overline{M_n}$ is the number average molecular weight, V_1 is the molar volume of water (18 cm^3 mol^{-1}), $\bar{\nu}$ is the polymer's specific volume (0.463 cm^3 g^{-1} for chitosan[195]), χ is the Flory-Huggins interaction parameter (-0.21 for quaternized chitosan derivatives[196]), $\nu_{2,s}$ is the polymer's volume fraction after swelling, $\nu_{2,r}$ is the polymer's volume fraction in the relaxed state.

From $\overline{M_c}$ the number of repeat units between neighbouring crosslinks, N can be calculated as below:

$$N = \frac{2\overline{M_c}}{M_r} \quad (2)$$

Here M_r is the average molecular weight of the repeating unit.The pore size (ξ)

in Peppas-Merrill theory can be calculated by Eq. (3):

$$\xi = \nu_{2,s}^{-1/3}(\overline{r_o^2})^{1/2} \quad (3)$$

Where, $(\overline{r_o^2})^{1/2}$ is the polymer unperturbed root mean square of the distance between two ends and can be expressed by Eq. (4):

$$(\overline{r_o^2})^{1/2} = (C_n N)^{1/2} L = (C_n \frac{2\overline{M_c}}{M_r})^{1/2} L \quad (4)$$

Where L is the length of the repeat unit (5.5 Å for chitosan), and C_n is the polymer Flory characteristic ratio.[197] Therefore the pore size ξ can be calculated by Eq. (4):

$$\xi = \nu_{2,s}^{-1/3}(\overline{r_o^2})^{1/2} = \nu_{2,s}^{-1/3}(C_n \frac{2\overline{M_c}}{M_r})^{1/2} L \quad (5)$$

***In vitro* biocompatibility study**

The primary epidermal keratinocytes used were from human neonatal foreskin (ATCC). Cells, kept in complete growth medium (ATCC), were first trypsinized by 0.25% (w/ v) trypsin and 0.03% (w/ v) ethylenediaminetetraacetic acid. The DMDC-Q-*g*-EM hydrogel (DMDC-Q-g-EM + $PEG_{13}DA$) films were pretreated before cell seeding: hydrogel films were cut into 5 mm diameter disks and placed in 70% ethanol for 24 h for sterilization. The sterilized disks were then equilibrated with PBS for one night. Cells (density 0.5×10^5 cells cm^{-2}) and some culture medium were added to the 96-well culture plates. When cells had adhered to the plate (about 4-5 h), the hydrogel samples were placed into the wells over the cell cultures. The hydrogels were directly contacted with the tested cells to exert a potentially toxic effect. The culture medium was changed every 2 days. Cells were analyzed with MTT assay and

Live/Dead assay on specified days. Cells in TCPS wells without hydrogels were used as control.

Methyl tetrazolium (MTT) assay was used to examine cell viability and proliferation. The experimental detail of MTT assay was shown in Chapter 3, section 3.3.2.

The viability of primary epidermal keratinocytes was examined with the LIVE/DEAD Assay. After specified cell culture time periods, the hydrogels were removed and placed in a new 96-well TCPS plate containing the LIVE/DEAD Assay reagent (Invitrogen). The plate was then kept in an incubator at room temperature for 45 min. After solution removal and PBS rinsing, the morphology of the cells was observed with a Zeiss inverted optical microscope.

***In vivo* biocompatibility study**

The DMDC-Q-*g*-EM hydrogel coated and uncoated contact lenses were inserted in a manually created sub-conjunctival pocket in the upper bulbar region of the eye (Female white New Zealand rabbits, n=3, 3.0-3.5 kg). *In vivo* confocal microscopy (Heidelberg HRT3, Heidelberg Engineering GmbH, Germany) was carried out on PO days 3 and 5 to evaluate the appearance of the surface conjunctival epithelial cells overlying the pocket. Conjunctiva overlying the pocket were collected on PO day 5 and embedded in Optimal Cutting Temperature compound (Leica, Nussloch, Germany). Cryosections (Microm, Walldorf, Germany) of 10 μm thickness from each animal were stained with hematoxylin and eosin (Sigma-Aldrich Corp., MO, USA), then imaged with a Zeiss Axioplan microscope (Zeiss, Oberkochen, Germany).

4.3 Results and discussion

4.3.1 Characterization of the derivatives

NMR analyses confirm the successful syntheses of these polymers, Figure 4.3 shows the ^{1}H-NMR spectra of the quaternized chitosan intermediates and the products. The signal at δ 3.2 ppm in Figure 4.3a, assigned to the ammonium protons of the quaternized chitosan, confirms the formation of TMC. Significant *N*-dimethylation (46%), which has also been observed by others, was also present in the product.[198] Figure 4.3b shows the spectrum for TMC-*g*-EM, with the protons of the methyl groups (*c*) in the methacrylate observed at δ 1.9 ppm while the protons of the double bond (*d*) are observed at δ 5.6 and 6.1 ppm. The methylene signal of the grafted PEG_6M (*a*) is observed at δ 3.7 ppm. Some signals present in TMC (notably signals from $-N^{+}(C\underline{H}_3)_3$ and $-N(C\underline{H}_3)_2$) are also observed in Figure 4.3b. This result confirms that PEG_6M had been grafted to the quaternized chitosan. Figure 4.3c shows signals of Cl-PEG_6M at δ 3.7 ppm ($-C\underline{H}_2-C\underline{H}_2-O$) (*a*), 4.1 ppm ($Cl-C\underline{H}_2-COO-$) (*b*), 1.9 ppm ($-C(C\underline{H}_3)=CH_2$) (*c*), 5.6 and 6.1 ppm ($-C=C\underline{H}_2$) (*d*).

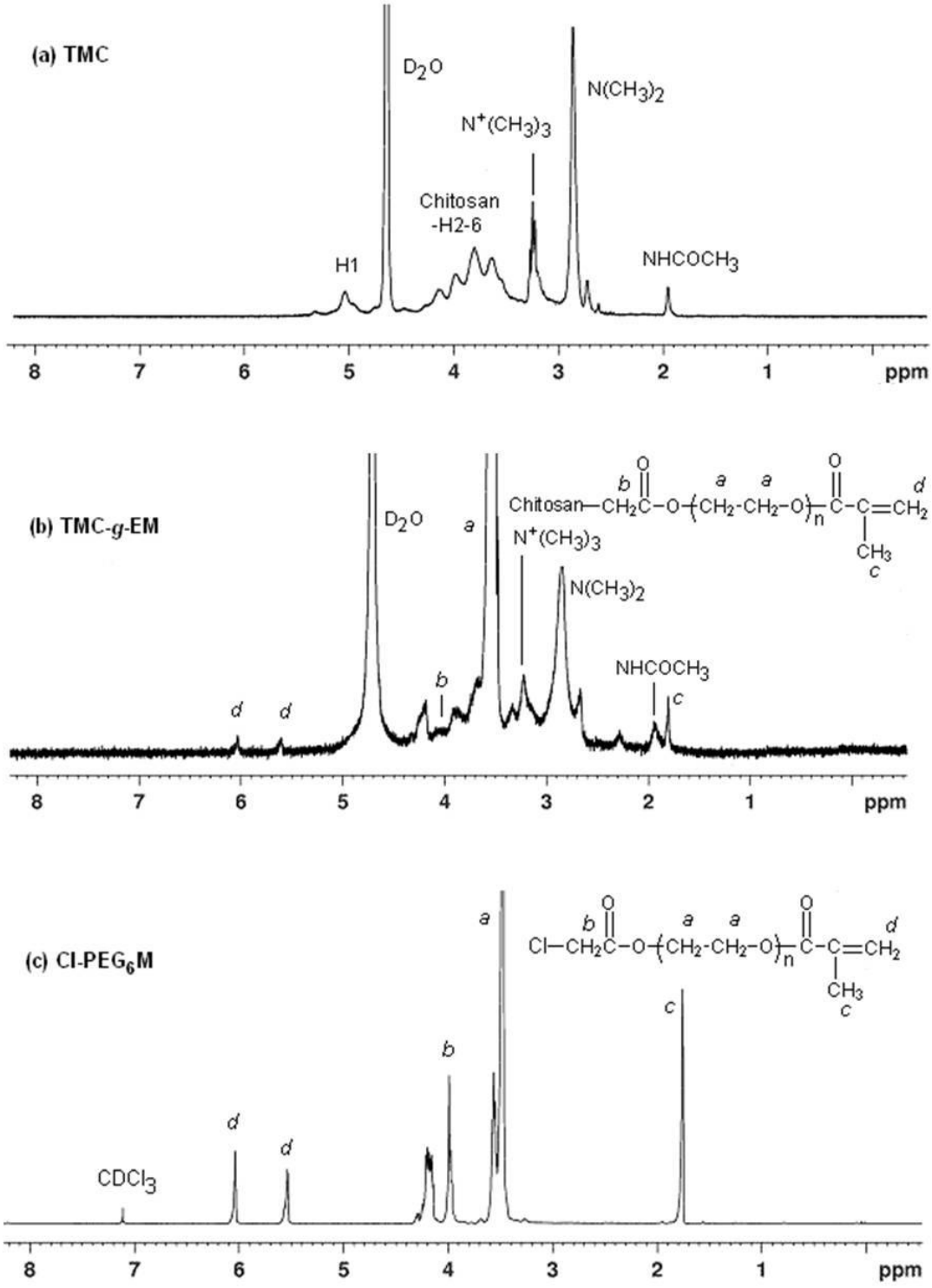

Figure 4.3 NMR characterization of quaternized chitosan derivatives. ^{1}H-NMR spectra of (a) TMC (in D_2O), (b) TMC-*g*-EM (in D_2O) and (c) Cl-PEG_6M (in $CDCl_3$), 300 MHz.

The FTIR spectra confirm the formation of the quaternized chitosan derivatives were shown in Figure 4.4: the OH stretch of chitosan was observed at 3442 cm^{-1}, the amide I band and NH bending were found at 1662 cm^{-1} and 1601 cm^{-1} respectively, while the C-O stretch occurred at 1081 cm^{-1} (Figure 4.4a). After quaternization, the N-H band at 1601 cm^{-1} was nearly gone while a new band at 1507 cm^{-1}, due to the quaternary ammonium group in chitosan, was observed (Figure 4.4b). The peaks between 1151 and 1032 cm^{-1}, attributed to the C3 and C6 alcohol groups in chitosan, were unaffected, indicating that the C3 and C6 position of chitosan were not alkylated during quaternization. For the PEG_6 methacrylated quaternized chitosan, the strong peak at 1104 cm^{-1} attributed to the C-O stretch (Figure 4.4c) confirms that PEG_6 is present in TMC-*g*-EM. The intense peak at 2878 cm^{-1} due to the sp^3 C-H structure indicates the presence of grafted alkyl group on the chitosan. The peaks for the vinyl group and C=O stretch of the PEG_6 methacrylate structure were observed at 818 cm^{-1} and 1717 cm^{-1}, respectively (Figure 4.4c). These peaks were assigned by comparing with the spectrum of Cl-PEG_6M (Figure 4.4d), which also showed these peaks at about the same wavenumbers.

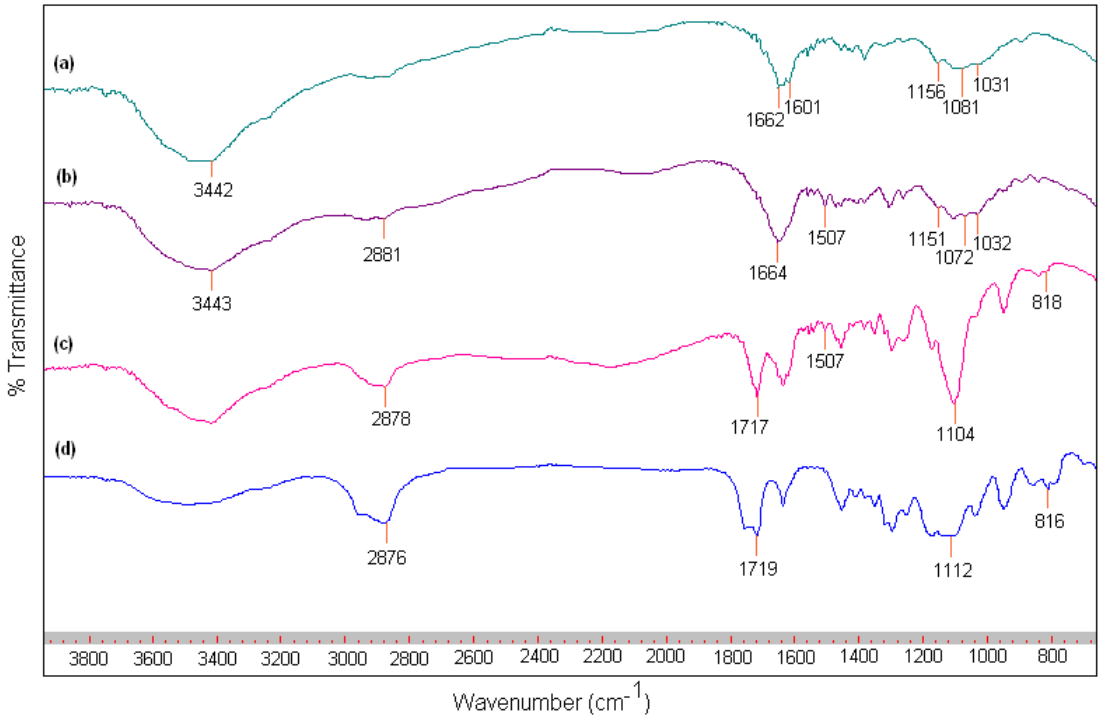

Figure 4.4 FTIR spectra of (a) chitosan, (b) TMC, (c) TMC-*g*-EM and (d) Cl-PEG$_6$M.

Table 4.1 Characteristics of the qC-*g*-EM polymers.

No.	Name	Series	Degree of quaternization (%)	Double bond content (mmol g^{-1})	M_n (g mol^{-1}) *10^5	M_w (g mol^{-1}) *10^5	PID
1	C-*g*-EM		-	0.76	0.74	0.86	1.15
2	TMC-*g*-EM	I	24	0.84	0.75	1.22	1.63
3	DMHC-*g*-EM	II	27	1.02	0.49	0.67	1.38
4	DMDC-*g*-EM	II	20	1.00	0.36	0.52	1.46
5	TMC-Q-*g*-EM	I	51	0.80	0.35	0.41	1.17
6	DMDC-Q-*g*-EM	II	56	0.80	0.24	0.38	1.56
7	DMDC-M	II	20	1.13	0.33	0.36	1.06

M_n: number-average molecular weight; M_w: weight-average molecular weight; PID: polydispersity index.

4.3.2 Biological properties of qC-*g*-EM solutions

After quaternization and PEG_6 methacrylate (PEG_6M) grafting, all chitosan derivatives are soluble in water at neutral pH. Minimum inhibitory concentration (MIC) determination was carried out with the chitosan derivative solutions to evaluate their antimicrobial activities. The results (Table 4.2) confirm that the quaternized chitosan derivatives (Entries 2-7) have better antimicrobial activities than unquaternized chitosan (Entry 1). The MICs of qC-*g*-EMs against fungi are generally low (≤ 200 μg ml^{-1}). Increasing the alkyl chain length from TMC-*g*-EM to DMDC-*g*-EM (Entries 2-4, Table 4.2) alone decreases the MICs against Gram-positive *S. aureus* but not against the Gram-negative *E. coli* and *P. aeruginosa*. However, the more highly quaternized TMC-Q-*g*-EM and DMDC-Q-*g*-EM (Entries 5 and 6, Table 4.2) have dramatically lower MICs against both bacteria and fungi (24 – 200 μg ml^{-1}), which are comparable to those of common antimicrobial peptides which we also tested (Table 4.2).

Figure 4.5 shows that all the chitosan derivatives have relatively low hemolysis. All the derivatives, except DMDC-M, exhibited less than 10% hemolytic activity up to 12,500 μg ml^{-1}. The highly quaternized TMC-Q-g-EM and DMDC-Q-g-EM have 0% and 2.1% hemolytic activity respectively even at 3,100 μg ml^{-1}, which is more than 15× their minimum inhibitory concentrations (MICs) of 24 to 200 μg ml^{-1} for all four pathogens tested (Table 4.2). Comparing DMDC-M with DMDC-g-EM, grafting with PEG6M reduces the hemolytic activity.

Table 4.2 MICs of the qC-*g*-EM solutions against various pathogens

No.	Name	MIC* (μg ml^{-1})			
		Gram-negative		*Gram-positive*	*Fungi*
		P. aeruginosa	*E. coli*	*S. aureus*	*F. solani*
1	C-*g*-EM	13,000	13,000	6,300	3,100
2	TMC-*g*-EM	780	780	1,600	200
3	DMHC-*g*-EM	780	3,100	200	200
4	DMDC-*g*-EM	780	1,600	200	200
5	TMC-Q-*g*-EM	98	200	98	24
6	DMDC-Q-*g*-EM	98	98	49	24
7	DMDC-M	1,600	1,600	390	200
	Melittin	63	63	8	--
	LL-37	>250	>250	>250	--
	Indolicidin	130	>250	130	--
	Magainin I	>250	130	130	--
	Defensin (HNP-1)	>130	>130	>130	--

*MIC is defined as the minimum inhibitory concentration inhibiting more than 90% of microbial growth.

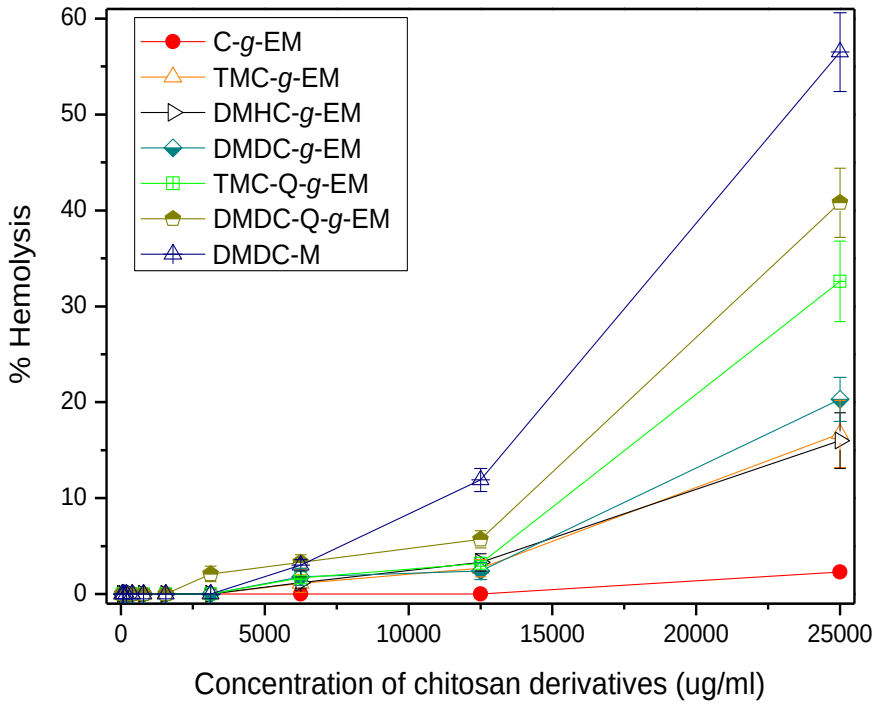

Figure 4.5 Hemolysis (%) of human red blood cells by various quaternized chitosan derivatives

4.3.3 Antimicrobial activity of qC-*g*-EM hydrogels

To form free-standing hydrogel films, the chitosan derivatives, poly(ethylene glycol) diacrylate (with 13 ethylene glycol repeats, denoted hereafter as $PEG_{13}DA$) and water were mixed in the ratio of 1:1:8 (w/w), together with 0.1 wt% photoinitiator (Irgacure 2959), and then UV irradiated. The hydrogels were challenged with the four pathogens at a concentration of about 2.5×10^6 CFU cm^{-2} and the cell count reductions after one hour were recorded. Figure 4.6 shows the antimicrobial activity of the hydrogel films. The hydrogel based on the non-quaternized C-*g*-EM (Entry 1, Figure 4.6a) exhibited low activity against these microbes. All the qC-*g*-EM hydrogels (Entries 2-6, Figure 4.6a) show outstanding antifungal activity against *F. solani* but differing antibacterial activities. Increasing the alkyl side chain length from TMC to DMHC to DMDC (Entries 2-4, Figure 4.6a) increases the killing efficacy against Gram-positive *S. aureus*. More interestingly, the two highly quaternized TMC-Q-*g*-EM and DMDC-Q-*g*-EM hydrogels (Entries 5 and 6, Figure 4.6a) have excellent log reductions of above 2.0 (>99% kill) for all four microbes, which are superior to their counterparts with lower degrees of quaternization (Entries 2 and 4, Figure 4.6a).

The DMDC-Q-*g*-EM hydrogel was repeatedly challenged with *S. aureus* up to four times. The tested hydrogel films were washed with phosphate buffer saline (PBS) and vortexed before the next use. Figure 4.6b shows that even after three prior challenges with high concentrations of microbes, the dead cells easily washed from the hydrogel, preserving its antimicrobial activity in the next (fourth) challenge.

a

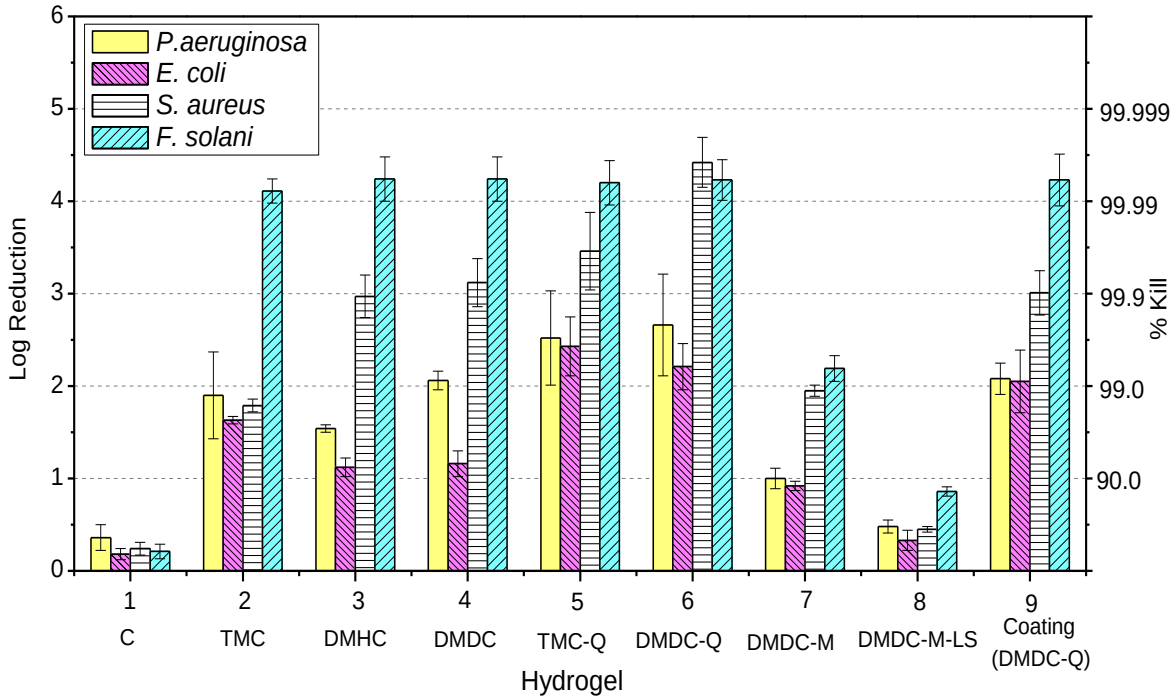

b

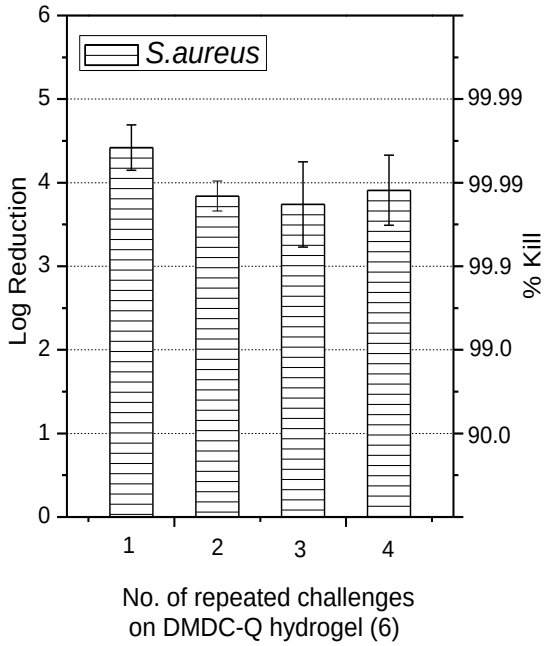

Figure 4.6 Antimicrobial activities of qC-*g*-EM hydrogels against various bacteria and fungi. (a) Log reduction and %kill of four pathogens on various qC-*g*-EM hydrogels; (b) Multiple use antimicrobial activities of DMDC-Q-*g*-EM hydrogel (Entry 6) against *S. aureus*. Error bars represent mean ± standard deviation of mean for n=3.

The LIVE/DEAD bacterial viability assay was carried out on DMDC-Q-*g*-EM hydrogel with *S. aureus*, using $PEG_{13}DA$ hydrogel as control (Figure 4.7). Using this assay, bacterial cells that appear green are live cells with intact membranes while bacterial cells that stain red are dead cells that have damaged membranes. Figure 4.7 shows that *S. aureus* cells are alive on the $PEG_{13}DA$ control but dead on the DMDC-Q-*g*-EM hydrogel.

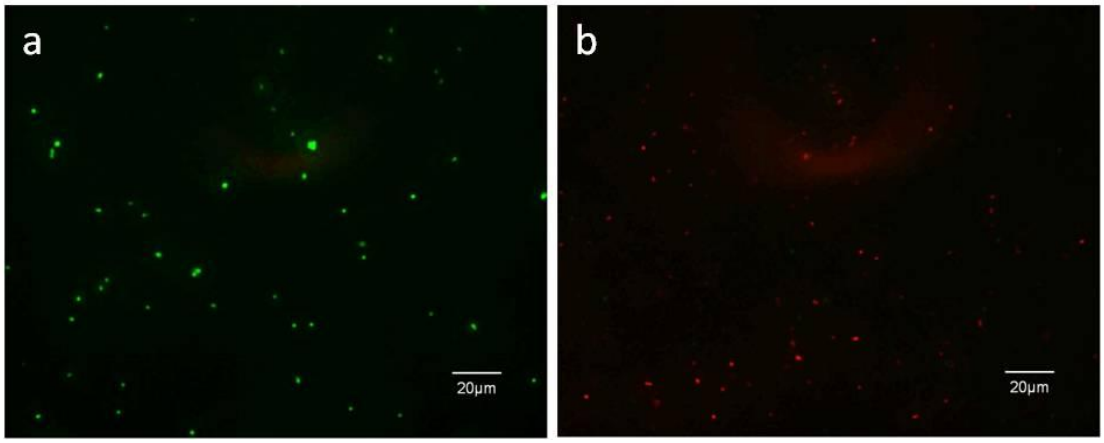

Figure 4.7 LIVE/DEAD bacterial viability assay of *S. aureus* on (i) $PEG_{13}DA$ control and (ii) DMDC-Q-*g*-EM hydrogel (Entry 6) after 1h incubation at 37 ℃ and washing (Scale bar = 20 μm)**.**

FE-SEM was also carried out to observe the morphology of the various microbes on DMDC-Q-*g*-EM hydrogel after 1 h contact (Figure 4.8). Distorted and wrinkled membranes were observed in *E. coli* and *F. solani* on the hydrogel surfaces (Figure 4.8(ii) and (iv)). Lesions and holes were observed in *P. aeruginosa* and *S. aureus* (Figure 4.8(i) and (iii)) after contact with the hydrogel. Many of the small pores in *P. aeruginosa* cells (arrows in Figure 4.8(i)), were near the edge where the microbe membrane contacted the hydrogel.

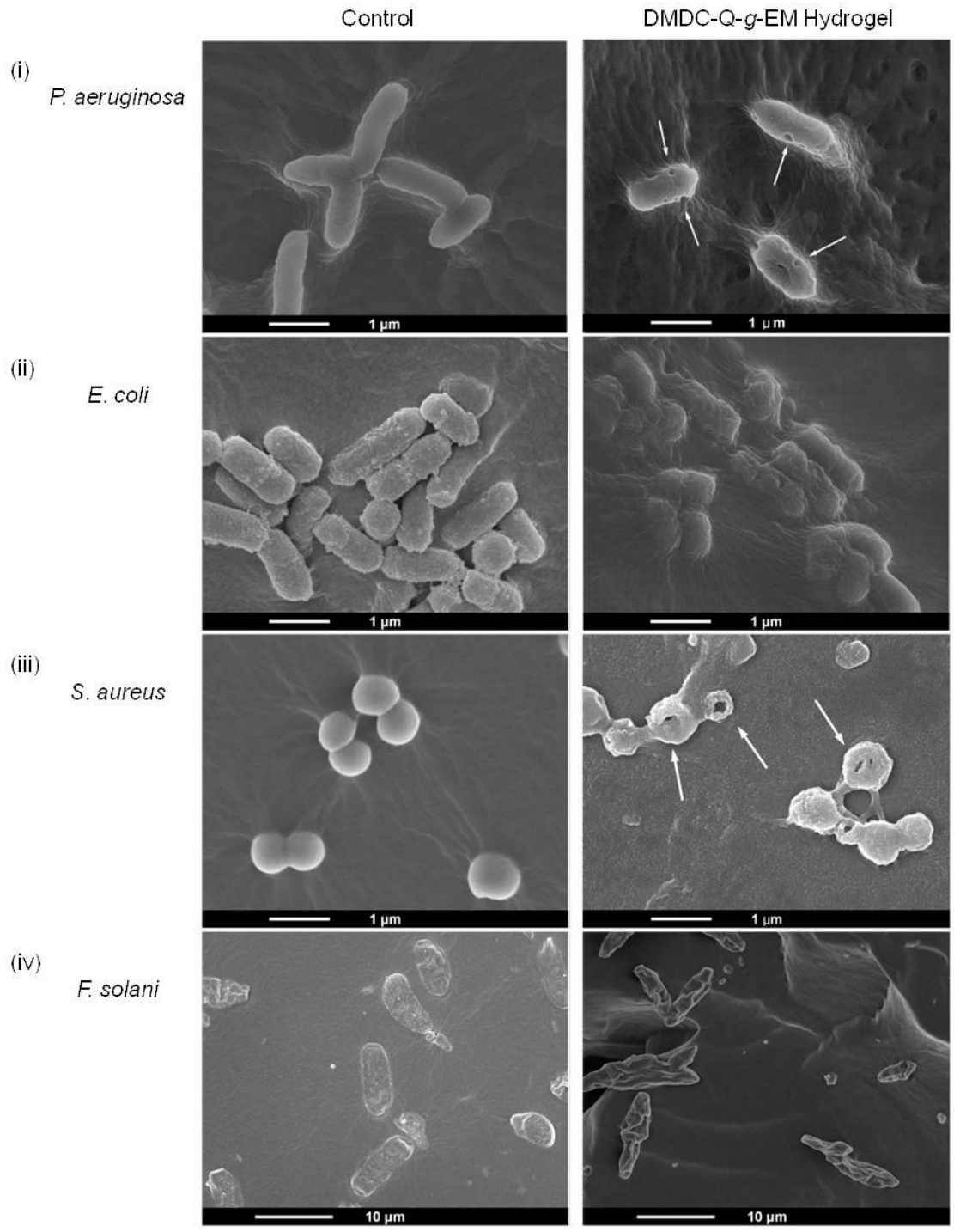

Figure 4.8 Morphology of various pathogens in contact with DMDC-Q-*g*-EM hydrogel (RIGHT, Entry 6) and control (LEFT) (Scale bar = 1 µm for (i)-(iii), scale bar = 10 µm for (iv)). Arrows indicate lesions and holes on the cell membrane after contact with DMDC-Q-*g*-EM hydrogel.

4.3.4 Mechanism studies

We postulate that our cationic nanoporous hydrogels act like a molecular "anion sponge" suctioning out parts of the anionic microbe membrane into the gel interior voids to cause microbe membrane disruption (Figure 4.2). This interpretation is suggested by computer molecular dynamics simulations conducted to probe the interaction between DMDC-Q hydrogel and bacterial membranes. Figure 4.9a shows a model of Gram-negative *P. aeruginosa* membrane, consisting of 243 zwitterionic 1,2-dioleoyl-sn-glycero-3-phosphocholine (DOPC) and 9 anionic lipopolysaccharide (LPS) molecules. The molecular model of LPS of *P. aeruginosa* PAO1 was generated based on experimentally sequenced data.[199] When the bacterial lipid bilayer was placed near the DMDC-Q chains for 50 ns, it was significantly disturbed; some of the anionic LPSs were even completely pulled out of the bilayer and drawn into the pores between the DMDC-Q chains (Figure 4.9a). The negative-charged regions of the remaining LPS molecules moved into close proximity to the hydrogel surface. The suctioning of cell membrane components into the porous hydrogel distorts and wrinkles the membrane, or even produces holes in it, corroborating our FE-SEM results (Figure 4.8). This membrane disruption eventually kills the microbe. Similar results were also found in the simulation of the interaction between a Gram-positive bacterial membrane model and DMDC-Q hydrogel (Figure 4.9b).

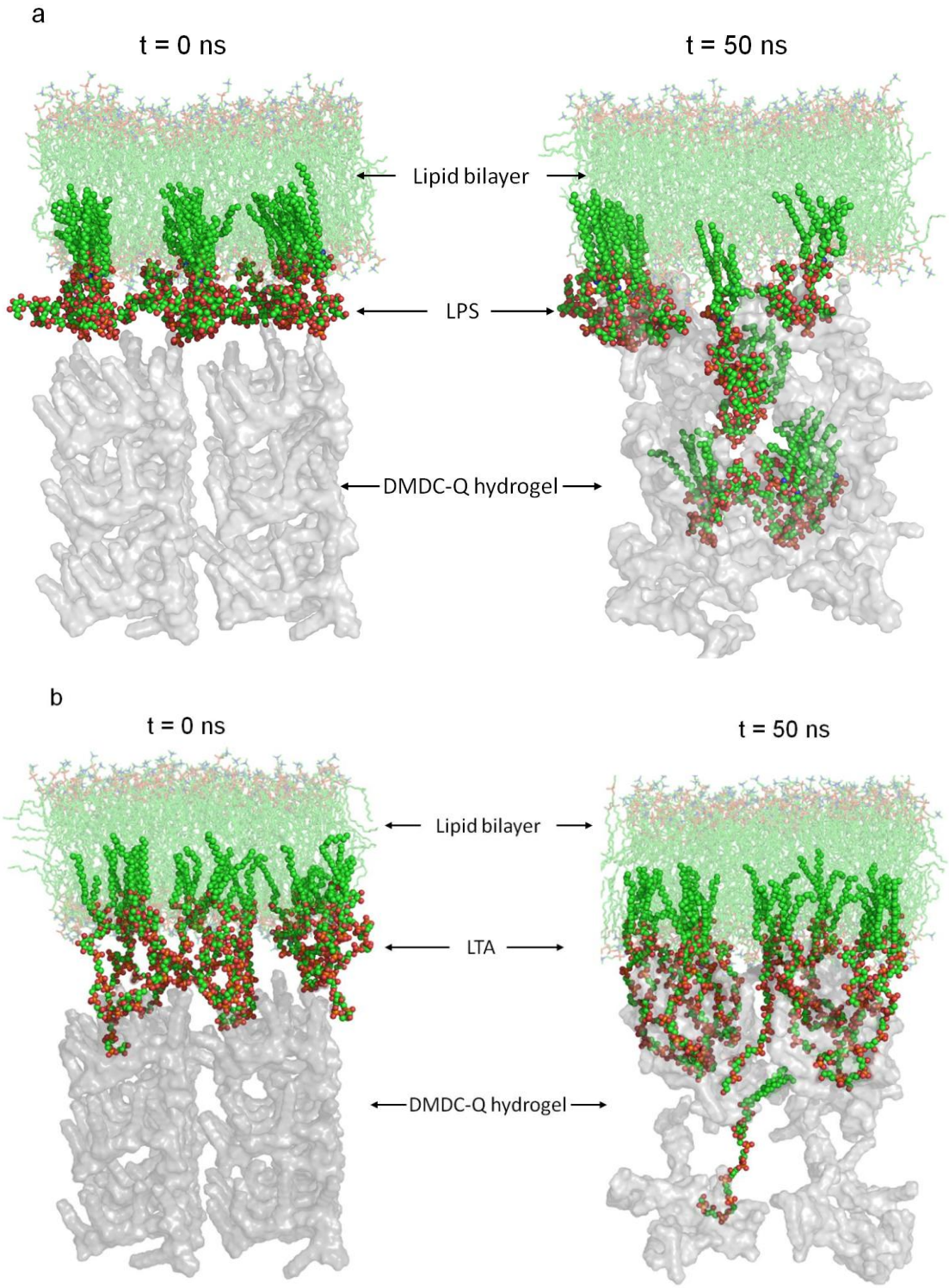

Figure 4.9 Computer simulation of the killing mechanism showing the "suctioning" of (a) Gram-negative (*P. aeruginosa*) bacterial membrane lipopolysaccharide (LPS) molecules, (b) Gram-positive bacterial membrane lipoteichoic acids (LTA) into the DMDC-Q hydrogel after 50 ns.

Our "anion sponge" model of these cationic nanoporous hydrogels differs from previous models of cell membrane disruption based on the penetration of antimicrobial polymer into the microbe membrane or ion exchange between the cell membrane and antimicrobial polymer.[144, 174] Previous antimicrobial surfaces have typically been based on brushes or pendant chains of hydrophobic cationic polymers emanating from a monolayer or thin coating. These coatings do not contain pores needed to "receive" disrupted membrane parts and the antimicrobial polymers may show greatly reduced microbe activities after immobilization.[181-182] Our qC-g-EM hydrogel, however, retains its antimicrobial efficacy after UV immobilization because of the presence of the pores. The high antifungal activity of all the highly hydrated hydrogels (Entries 2 – 6, Figure 4.6a) may possibly be due to the compatibility of the chitosan derivatives with fungal cell wall which contains a significant amount of chitin, allowing close approach of the hydrogel to the cell membrane.

Increasing the positive charge density and pore size of our cationic hydrogels would significantly increase their killing efficacy. The measured surface zeta potentials (Table 4.3) confirm that the highly quaternized TMC-Q-*g*-EM and DMDC-Q-*g*-EM hydrogels have higher charge densities: Entries 5 and 6 have zeta potentials of 11.9 ± 0.4 mV and 13.7 ± 0.9 mV respectively, higher than the values (10.4 ± 0.3 mV and 11.4 ± 0.2 mV) for their counterparts with lower degrees of quaternization (Entries 2 and 4). The higher antibacterial efficacies of TMC-Q-*g*-EM and DMDC-Q-*g*-EM hydrogels compared with TMC-*g*-EM and DMDC-*g*-EM (Figure 4.6a) illustrates the significance of hydrogel charge density in effective microbe killing by these

materials.

Table 4.3 Zeta potentials of hydrogels

Entry	1	2	3	4	5	6	7	8	10	11
Hydrogel	C	TMC	DMHC	DMDC	TMC-Q	DMDC-Q	DMDC-M	DMDC-M-LS	THC	TDC
Zeta Potential (mV)	3.9 ± 0.1	10.4 ± 0.3	9.4 ± 0.1	11.4 ± 0.2	11.9 ± 0.4	13.7 ± 0.9	10.9 ± 0.4	11.9 ± 0.1	10.3 ± 0.3	9.1 ± 0.1

(Hydrogels 1-6 and 10-11 have been abbreviated by the type of quaternized chitosan used in their formulations and consist of qC-*g*-EM + $PEG_{13}DA$. Hydrogel 7 is DMDC-M + $PEG_{13}DA$. Hydrogel 8 is DMDC-M + DEG_2DA.)

To demonstrate the importance of the pores of the cationic networks for achieving effective microbe killing, we compared DMDC-*g*-EM hydrogel (Entry 4) with two other smaller pore size hydrogels formulated using DMDC-M (Entries 7-8, Figure 4.6a). Specifically, we replaced (*I*) DMDC-*g*-EM with DMDC-M (without the PEG_6 side chain) in Entry 7 (Figure 4.6a) and (*II*) $PEG_{13}DA$ crosslinker with a shorter diethylene glycol diacrylate (DEG_2DA) in DMDC-M-LS (Low swelling) (Entry 8 in Figure 4.6a). The killing efficacies of DMDC-M (Entry 7) and, especially, DMDC-M-LS (Entry 8) are lower than that of DMDC-*g*-EM hydrogel (Entry 4). The water uptakes of Hydrogels 4, 7 and 8 were measured to be 1040 ± 30%, 830 ± 8% and 110 ± 3% respectively (Figure 4.10).

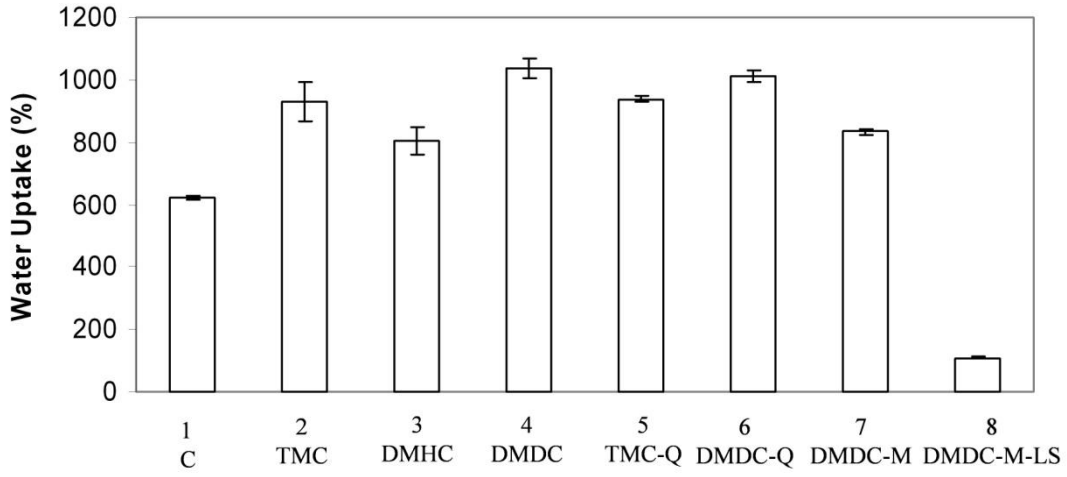

Figure 4.10 Water uptake of the various hydrogels. Data presented are mean s.d. mean for n=3 experiments. (Hydrogels 1-6 have been abbreviated by the type of quaternized chitosan used in their formulations and consist of qC-*g*-EM + $PEG_{13}DA$. Hydrogel 7 is DMDC-M + $PEG_{13}DA$. Hydrogel 8 is DMDC-M + DEG_2DA.)

Based on the Peppas-Merill theory, we calculated the pore sizes of Hydrogels 4, 7 and 8 to be 16.5 nm, 10.4 nm and 1.6 nm respectively (Table 4.4).[194, 200] The zeta potentials of Hydrogels 7 and 8 (10.9 ± 0.4 mV and 11.9 ± 0.1 mV, Table 4.3) are similar to that of Hydrogel 4 (11.4 ± 0.2 mV), ruling out the effect of differences in charge density in this series. Decreasing the water swelling and hence pore size in Hydrogel 8 significantly decreases its killing efficacy (Figure 4.6a). Conversely, Hydrogel 4 has the best killing efficacy because of its largest pore size of about 16.5 nm. Each folded LPS molecule is estimated to be about 3.5 nm - 4.5 nm in size and so it appears that Hydrogel 8 does not have large enough pores to receive these molecules.

Table 4.4 Pore size of DMDC hydrogel, DMDC-M hydrogel and DMDC-M-LS (low swelling) hydrogels.

Entry	Hydrogel*	$\overline{M_c}$	Pore size ξ (nm)
4	DMDC	1150	16.5
7	DMDC-M	780	10.4
8	DMDC-M-LS	153	1.6

*DMDC hydrogel is DMDC-*g*-EM + $PEG_{13}DA$, DMDC-M hydrogel is DMDC-M + $PEG_{13}DA$, and DMDC-M-LS (low swelling) hydrogel is DMDC-M + DEG_2DA

One problem of present contact-active antimicrobial surfaces in application is that they can easily be masked by adsorbed conditioning films from organic compounds such as proteins or remnants of dead cells, resulting in loss of effectiveness.[175] This conditioning film undoubtedly blocks contact-active antimicrobial surfaces from contact with microbes, causing loss of antimicrobial activity. In contrast, hydrated PEGylated hydrogels are known to be inherently cell-/protein-resistant, accounting partly for the observed durable antimicrobial activity.[201] Further, diffusion of disrupted membrane molecules into the interior of the gel layer is expected to prevent the gel surface from becoming fouled after repeated challenges. Big pores are needed to admit the microbe membrane fragments. Also, a high total pore volume fraction guarantees plenty of interior volume for membrane fragments to diffuse into, so that the contact-active surface possibly *cleans itself* if it becomes momentarily fouled by absorbed membrane components after contact with a microbe. Our hydrogels (Entries 1-7, not Entry 8) have high pore volume as can be inferred from their high water volume fractions of greater than 90% (Figure 4.11).

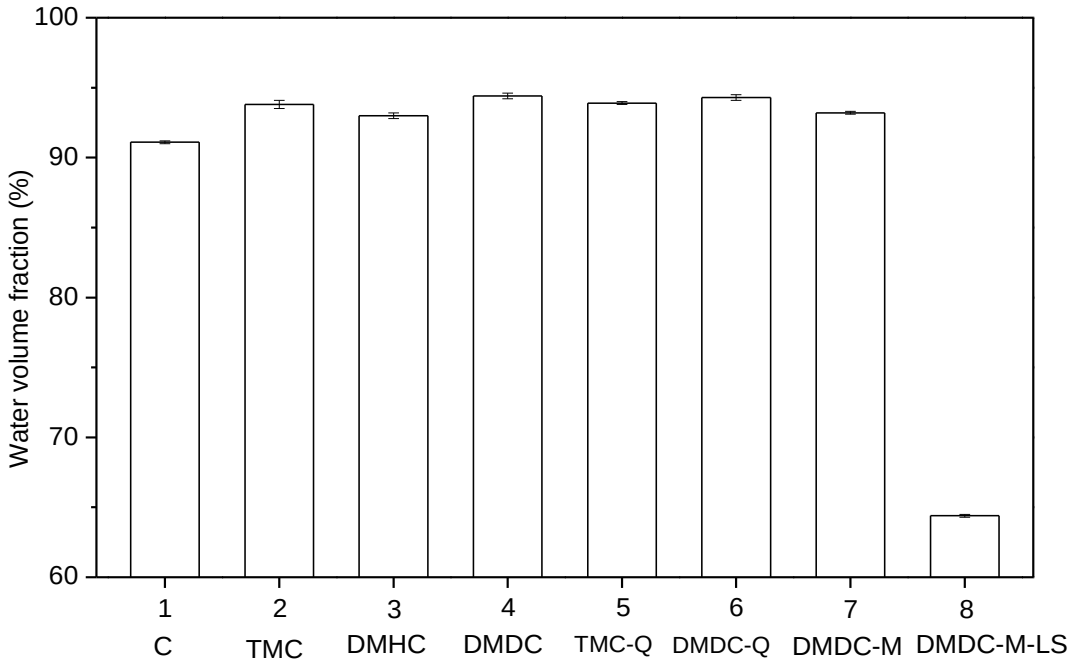

Figure 4.11 Water volume fraction of various hydrogels, data presented are mean ± s.d. mean for n=3 experiments. (Hydrogels 1-6 have been abbreviated by the type of quaternized chitosan used in their formulations and consist of qC-*g*-EM + $PEG_{13}DA$. Hydrogel 7 is DMDC-M + $PEG_{13}DA$. Hydrogel 8 is DMDC-M + DEG_2DA.)

4.3.5 Surface immobilization of antimicrobial hydrogel

As a demonstration of application of our material and coating, a hydrogel layer of DMDC-Q-*g*-EM was *in situ* immobilized on a fluoropolymer substrate (contact lens Z from Menicon). The surface to be coated was first surface-activated with peroxides using argon plasma followed by air ageing and the substrate was then placed in the hydrogel precursor solution and photopolymerized without a mold. Under UV irradiation, a crosslinked hydrogel layer emanates from the surface as the

acrylate/methacrylate functionality of the precursor solution reacts with the peroxide-decorated surface and with itself. The coating is concurrently covalently attached to the surface as the hydrogel is crosslinked from the precursor solution. Our method is simpler than typical procedures for forming antimicrobial coatings.

Figure 4.12 shows photographs and scanning electron microscopy (SEM) images of the hydrogel coated fluoropolymer substrate, together with the control uncoated disc. Fluorescein, a dye that binds to the N^+ present on the quaternized chitosan, was used to stain the hydrogel coating. Figure 4.12 a(i) and a(ii) show the gross visual appearance of the uncoated and fluorescein-stained hydrogel-coated surfaces. Figure 4.12a(ii) shows that the hydrogel layer was rather uniformly coated on the substrate. Figure 4.12b(ii) shows that the freeze-dried hydrogel layer was a few microns thick and had good adhesion to the fluoropolymer substrate though the hydrogel has very high water content. The thin layer of hydrogel grafted on the surface showed good antimicrobial action with log reductions of 2.1 to 4.2, which is comparable to free DMDC-Q-*g*-EM hydrogel films (Figure 4.6a).

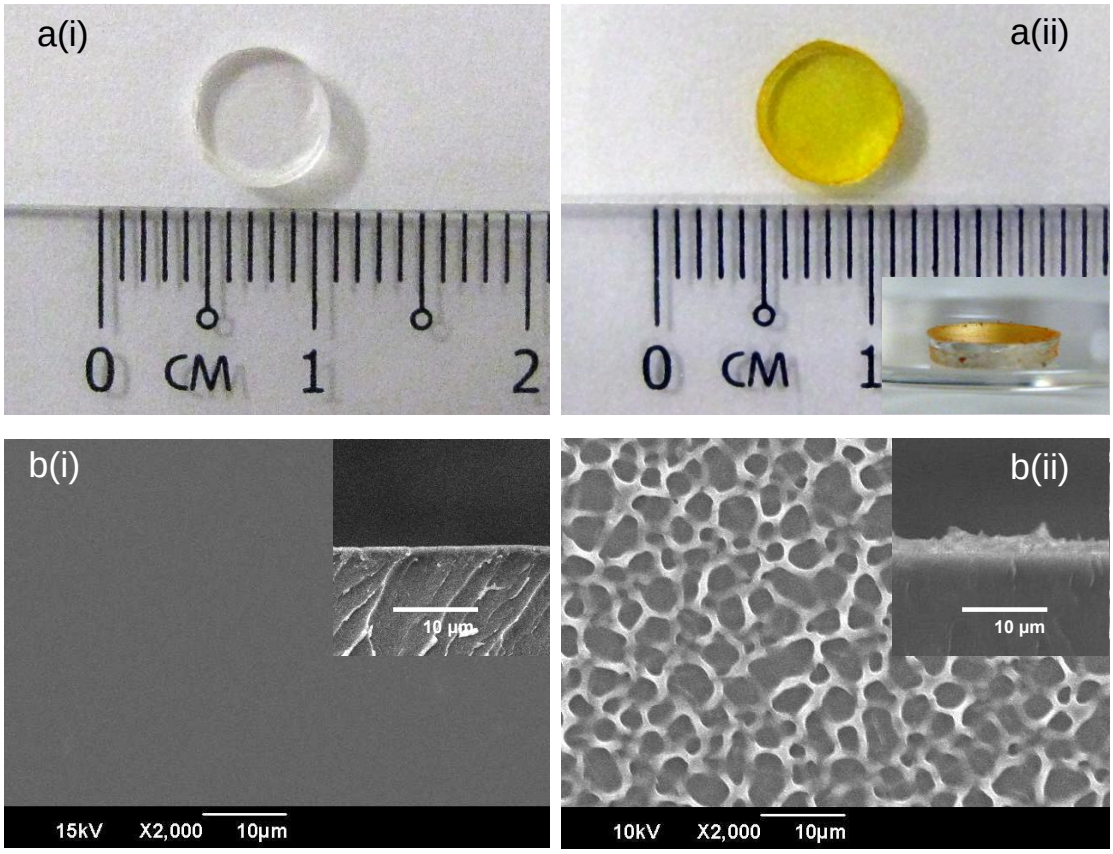

Figure 4.12 Coating of DMDC-Q-*g*-EM hydrogel on flouropolymer substrate: a, Photographic image of (i) uncoated and (ii) fluorescein-stained DMDC-Q-*g*-EM hydrogel coated substrate. b, SEM images of top view and cross-section (inset) of (i) uncoated and (ii) freeze-dried DMDC-Q-*g*-EM hydrogel (Entry 6) coated substrate surface (Scale bar = 10 µm).

4.3.6 *In vitro* and in *vivo* biocompatibility studies

The biocompatibility of DMDC-Q-*g*-EM hydrogel was demonstrated by both *in vitro* and *in vivo* tests. The *in vitro* test contacted human primary epidermal keratinocytes with DMDC-Q-*g*-EM hydrogel films for 7 days, with tissue culture polystyrene dish (TCPS) as control. Methyl tetrazolium (MTT) and LIVE/DEAD cell

viability assays (Figure 4.13) show that the human keratinocytes proliferate well in contact with DMDC-Q-*g*-EM hydrogel. MTT assay measures mitochondrial activity and cell viability and proliferation. Figure 4.13a shows that the MTT absorbance increases with culture time, indicating that the cells proliferate even in the presence of the hydrogel. In Figure 4.13b, the keratinocytes are mostly stained green indicating that they are alive on the hydrogels, suggesting that our hydrogel is *in vitro* biocompatible.

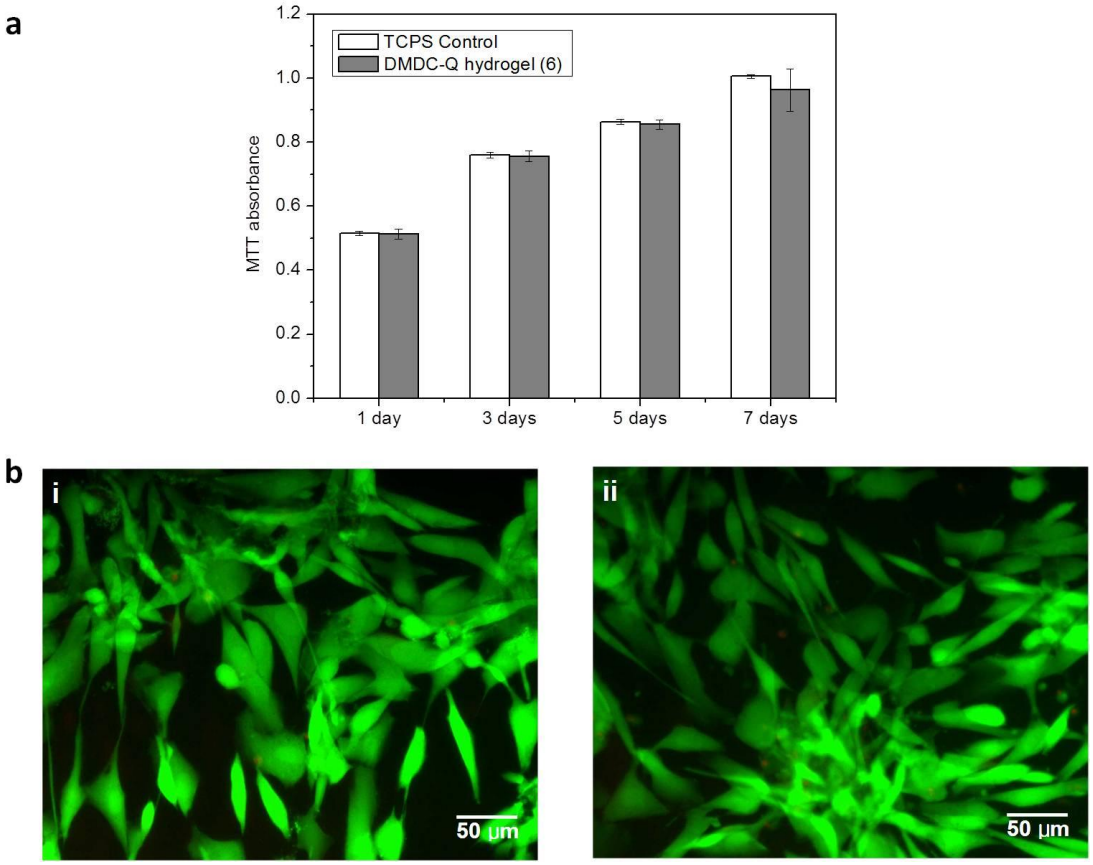

Figure 4.13 *In vitro* biocompatibility studies. (a) MTT activities (absorbance at 490 nm) of primary epidermal keratinocytes on TCPS control and DMDC-Q-*g*-EM hydrogel (Entry 6). Error bars represent mean ± standard deviation of mean for n=3. (b) LIVE/DEAD analysis of primary epidermal keratinocytes on (i) TCPS control and (ii) DMDC-Q-*g*-EM hydrogel (Entry 6) after 7 days of culture (Scale bar = 50 µm).

The *in vivo* biocompatibility of DMDC-Q-*g*-EM hydrogel coating with the epithelial cells of the rabbit ocular surface was examined. Uncoated and coated lenses were each implanted into a pocket underneath the rabbit conjunctival epithelium. The response of the conjunctival tissue was examined clinically by slit-lamp and *in vivo* confocal microscopy over 5 days. The bulbar conjunctiva overlying the control and DMDC-Q-*g*-EM hydrogel coated lenses remained healthy as determined by examination with *in vivo* confocal microscopy at post-operative (PO) days 3 and 5. Representative histological images of rabbit conjunctiva collected at PO day 5 and stained by hematoxylin and eosin (H&E) are shown in Figure 4.14. Importantly, there was no indication of epithelial erosion, or of unusual neutrophil infiltration other than what may be expected after surgery. A few neutrophils appeared in the conjunctival tissue associated with the lens (Figure 4.14c, d). No erosions of the epithelium, or vascular changes were found to be associated with the presence of the lens. The *in vivo* results show that the coating has no effect on the epithelial cells and does not lead to any pathological changes. The coated lens is compatible with conjunctiva and the hydrogel coating has no toxicity to the epithelial cells or the underlying stroma.

Our hydrogel has good *in vitro* and *in vivo* biocompatibility. Unlike microbial membranes, the outer leaflet of the mammalian cell membrane lacks anionic lipids.[36-37] So there is much less Coulombic attractive “suctioning” force to disrupt mammalian cells when they are in contact with the “anion sponge”, which accounts for its excellent biocompatibility.

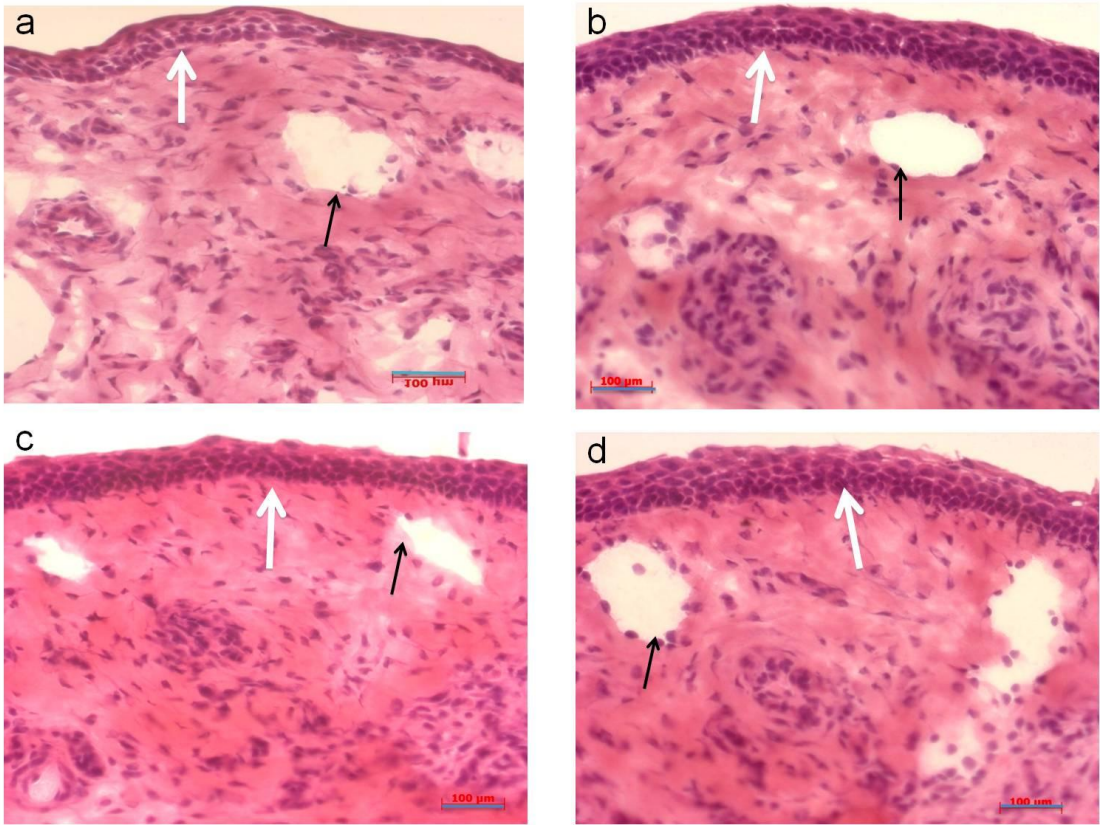

Figure 4.14 Microscopic observations of hematoxylin and eosin (H&E)-stained frozen sections of conjunctiva. (a) Normal conjunctiva epithelium showing normal epithelium and stromal blood vessels. (b) PO day 5 positive control, tissue overlying the surgically created pocket without a lens implant. (c) PO day 5, tissue overlying the pocket with an uncoated lens. (d) PO 5 day, tissue overlying the pocket containing a DMDC-Q-*g*-EM hydrogel coated lens (Entry 9). White arrows indicate the conjunctival epithelium and black arrows indicate blood vessels. (Scale bar = 100 µm)

4.4 Conclusion

In summary, we have demonstrated simultaneous polymerization and covalent grafting of a qC-*g*-EM based hydrogel onto a fluoropolymer substrate surface via a

simple two-step process to create a uniform covalent adherent thin coating that effectively reduces the viability of four tested pathogens by 2 to >4 orders of magnitude. Specifically, DMDC-Q-*g*-EM hydrogel exhibits superior antimicrobial activity with an inhibition above 99% for all four clinically significant pathogens tested, including Gram-negative and Gram-positive bacteria and fungi. Our hydrogel is contact-active antimicrobial and also *in vitro* and *in vivo* biocompatible. And the coating has very good adhesion. We propose that the polycationic hydrogel acts like an "anion sponge" to draw anionic phospholipids out of the bacterial cell membrane into the gel pores and that the hydrogel positive charge density and pore size determine the killing efficacy of the coating. We believe that this PEGylated quaternized chitosan-based hydrogel coating, which is easily UV immobilized on any surface, will be widely applicable for combating infection in many classes of implant/prosthesis and in other medical devices.

4.5 Acknowledgements

Part of the work presented in this chapter has been published in *Nature Materials* (DOI:10.1038/NMAT2915). Dr. Mu Yuguang and his group at the School of Biological Sciences, Nanyang Technological University, did the computing simulation of Figure 4.9. Dr Zhu Hong-yuan at Singapore Eye Research Institute did the animal study of Figure 4.14.

Chapter 5 Cationic peptidopolysaccharides show excellent broad-spectrum antimicrobial activities and high selectivity

5.1 Introduction

In this chapter, we attempt to further improve the selectivity of polysaccharide-based antimicrobial molecules. The emergence of microbial resistance to conventional antibiotics in recent decades is a serious challenge and has led to an overwhelming demand for new antimicrobial agents.[202] Unlike conventional antibiotics which target microbe metabolism, natural antimicrobial peptides (AMPs) exert their antimicrobial activity by disrupting the cytoplasmic membrane.[11, 32] This mode of antimicrobial activity is believed to be less susceptible than metabolic targeting to the development of resistance.[11] Although natural AMPs are highly effective, their application is limited by high toxicity, poor proteolytic stability and pharmacokinetics and high manufacturing cost.[32] Therefore, unremitting efforts have been made on the design, synthesis and testing of new microbial membrane-acting peptides and their analogues which are nontoxic or biocompatible and inexpensive to produce.[77, 84, 203]

To date, common characteristics of AMPs are a facially amphiphilic nature and cationic charge.[47, 114] These two characteristics allow the AMP to be first electrostatically attracted to the anionic cytoplasmic membrane and then to penetrate into the hydrophobic lipid bilayer interior. Numerous chemical structures have been

designed and synthesized to mimic the cationic and amphiphilic structure of natural AMPs; these include synthetic peptides,[54-55, 203] peptoids,[84] polymethacrylates,[204] polypryidines,[122] polynorbornenes,[98] polysaccharides,[205] *etc*. Many synthesis efforts have considered the interaction of the antimicrobial peptides/polymers with the microbe cytoplasmic membrane but have largely ignored their compatibility with the complex cell wall structure. Outside the cytoplasmic membrane of both Gram-negative and Gram-positive bacteria, there is a peptidoglycan layer.[37] To date, peptidopolysaccharides that have peptidoglycan-mimetic chemical structure facilitating penetration into the bacterial cell wall have not been applied as antimicrobial biomacromolecules. Further, the relatively low selectivity of synthetic antimicrobial molecules, resulting in cytotoxicity to mammalian cells (more specifically, hemolysis of red blood cells), is an unsolved issue.[204] We postulate that antimicrobial molecules designed to resemble bacterial cell wall constituents may be less hemolytic than present AMPs and AMP analogues due to their dissimilarity to mammalian outer membrane constituents.

In this chapter we demonstrate a new class of antimicrobial polymer based on cationic peptidopolysaccharide, specifically a copolymer of chitosan and polylysine, which is a bacterial cell wall peptidoglycan mimetic (Figure 5.1). The cationic chitosan-*graft*-polylysine has excellent broad-spectrum antimicrobial properties against clinically significant Gram-negative (*Escherichia coli* (ATCC8739), *Pseudomonas aeruginosa* (ATCC9027)) and Gram-positive (*Staphylococcus aureus* (ATCC6538)) bacteria and fungi (*Candida albicans* (ATCC10231) and *Fusarium*

solani (ATCC36031)) as demonstrated by its low minimum inhibitory concentrations (5 - 20 μg ml^{-1}). The optimized composition also has high selectivity for these pathogens over human red blood cells (> 5,000 - 10,000), low toxicity to mammalian cells and does not significantly stimulate tumor necrosis factor-α (TNF-α) secretion from murine macrophages.

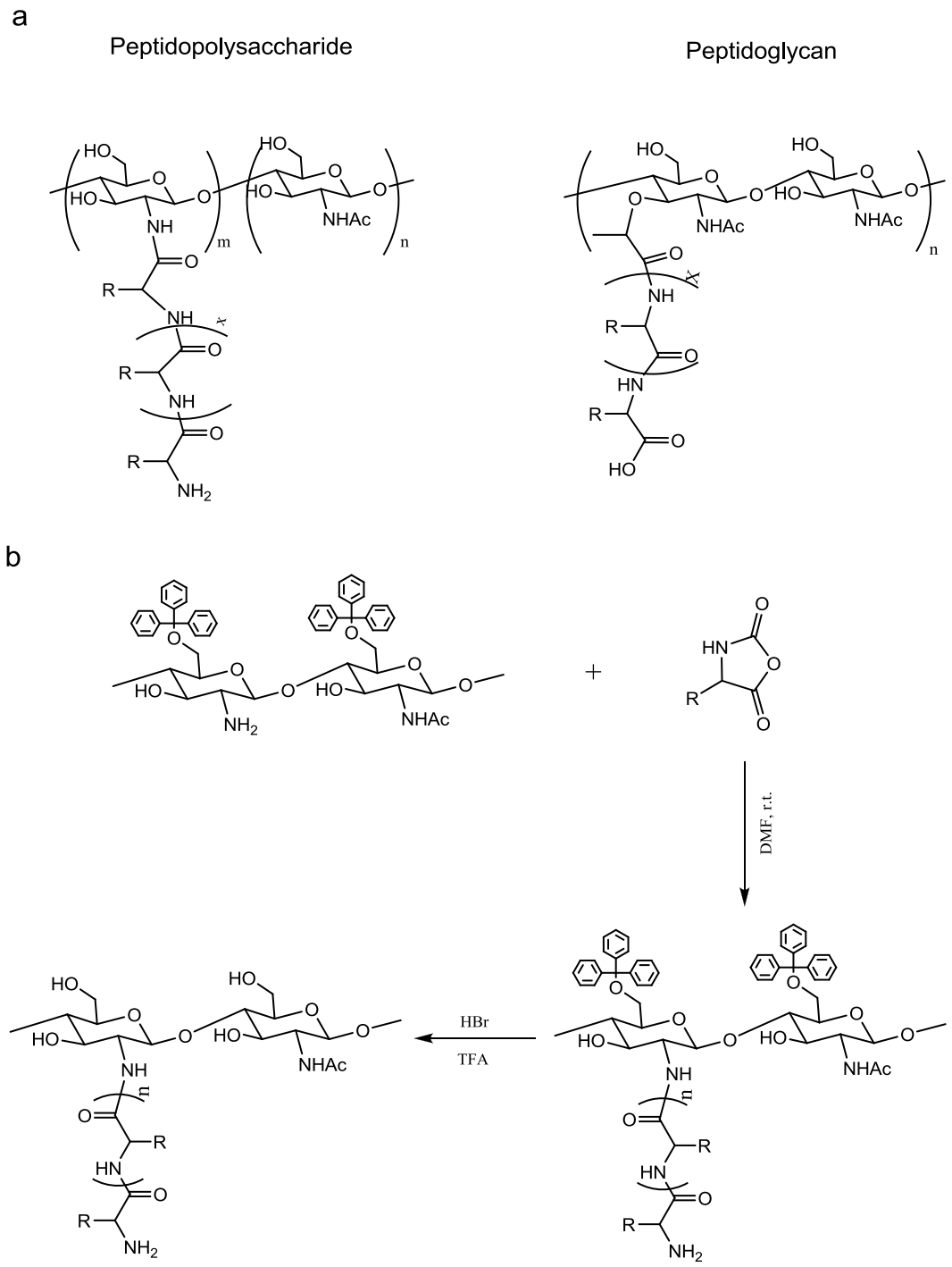

Figure 5.1 (a) Chemical structure of cationic peptidopolysaccharide (chitosan-*graft*-polypeptide) (R = Lys or Phe), and bacterial cell wall peptidoglycan (R = Ala, Glu, Lys, etc.[206]). (b) Synthetic scheme for preparation of Chitosan-*g*raft-polypeptide.

5.2 Experimental Details

Materials

Chitosan, low molecular weight (4.5×10^4 g mol^{-1}, 90% deacetylated) and high molecular weight (1.1×10^6 g mol^{-1}, 80% deacetylated), Nε-benzyloxycarbonyl-L-lysine, L-phenylalanine, triphosgene, tetrahydrofuran (THF), Phthalic anhydride, triphenylchloromethane, hydrazine solution, hydrogen bromide (33% in acetic acid), *N*, *N*-dimethylformamide (DMF), pyridine, trifluoracetic acid (TFA), sodium hydroxide (NaOH), sodium phosphate dibasic, sodium phosphate monobasic, phosphate buffered saline (PBS), 2-mercaptoethanol, fluorescein isothiocyanate-dextran (FITC-Dextran), 3-(4,5-dimethylthiazol-2-yl)-2,5-diphenyl tetrazolium bromide (MTT), dimethyl sulfoxide (DMSO), gramicidin D, glutaraldehyde, and osmium tetroxide were purchased from Sigma-Aldrich Corp. (St Louis, US). Tris buffer was purchased from Vivantis Biochemical Company (Subang Jaya, Malaysia). LIVE/DEAD BacLight bacterial viability kit L13152 was purchased from Invitrogen (Carlsbad, US). All bacteria and fungi strains were obtained from ATCC: *Escherichia coli* (ATCC8739), *Pseudomonas aeruginosa* (ATCC9027), *Staphylococcus aureus* (ATCC6538), *Candida albicans* (ATCC10231), and *Fusarium solani* (ATCC36031). All broth and agar were purchased from Becton Dickinson Company (Franklin Lakes, US).

Synthesis of *N*-carboxyanhydride (NCA) monomers

The *N*-carboxyanhydride (NCA) monomers were synthesized by the method described in our previous work.[55] Briefly, 10 g of the amino acid was suspended in 100 mL of anhydrous THF and the mixture was heated to 50 ℃, followed by addition of one-third equivalent amount of triphosgene and stirring for 3h. The reaction mixture was then filtered and the filtrate was poured into 300 mL hexane and stored at -20 ℃ for 24 h to fully precipitate the product. The recrystallized NCA monomer was then filtered and washed with hexane, then vacuum dried at 50 ℃ overnight.

Synthesis of 6-O-triphenylmethyl chitosan

6-O-triphenylmethyl chitosan was prepared by a method similar to that reported by Yu *et al*.[207]

N-Phthaloyl Chitosan: 5g Chitosan was dispersed in 100ml anhydrous DMF and stirred at 80 ℃ for 1h in order to completely dissolve it. The solution was reacted with 13.8 g phthalic anhydride (93 mmol) at 130 ℃ for 12h under Ar protection. After this reaction the product was precipitated in 500 ml ethanol and filtered. The product was washed with diethyl ether and water consecutively, and then vacuum dried.

N-Phthaloyl-6-O-triphenylmethyl chitosan: 5g *N*-phthaloyl chitosan was dissolved in 100ml anhydrous pyridine then added with 15 g (55 mmol) triphenylchloromethane. The mixture was stirred at 90 ℃ for 24 h under Ar protection, after which the solvent was evaporated under vacuum and the product was washed with diethyl ether and ethanol consecutively.

6-O-triphenylmethyl chitosan: 5 g *N*-Phthaloyl-6-O-triphenylmethyl chitosan was

added in 100 ml 50%wt hydrazine solution and stirred at 100 ℃ for 18 h under Ar protection. Then the suspension was filtered and the residue was washed with water, ethanol and diethyl ether consecutively.

Synthesis of Chitosan-g-NCA copolymers

Chitosan-*g*-NCA copolymers was prepared by a method similar to that reported by Yu *et al*.[208] 6-O-triphenylmethyl chitosan was dispersed in and NCA monomer was dissolved in 50 ml anhydrous DMF and stirred at room temperature for 5 d, after which the product was precipitated into acetone and dried in vacuum. To obtain the final copolymers, 6-O-triphenylmethyl chitosan-*g*-NCA copolymers were deprotected with HBr. Typically, 1.0g of the copolymer was dissolved in 15 ml TFA, 10 ml of HBr (33% in acetic acid) was added and the mixture was stirred for 4 h in an ice bath. The product was precipitated with acetone, then filtered and dissolved in distilled water, and the pH was adjusted to 7 with NaOH (1M). After neutralization the product was dialyzed with cellulose membrane (Sigma, M. W. 10334) and then freeze-dried.

Characterization of polymers

NMR spectra of the synthesized products were obtained with a Bruker Avance DPX 300 instrument. The molecular weights and polydispersities were measured using a Shimadzu LC-20AD instrument equipped with a refractive index detector (RID), using a PL-aquagel-OH GPC column and sodium acetate buffer (0.2 M, pH 4.05). Samples were analysed at 40 ℃ with an eluent flow rate of 1.0 ml min^{-1}.

Minimum inhibitory concentrations (MICs)

The experimental detail of MIC determination was shown in Chapter 3, section 3.2.1, the test was independently repeated more than twice.

Morphology study of microorganisms

The morphology changes of microorganisms induced by CS-*g*-K_{16} were examined with FE-SEM after 30 min-treatment with CS-*g*-K_{16} at MIC, the experimental detail was shown in Chapter 3, section 3.4.5.

LIVE/DEAD Assay to examine bacterial viability

LIVE/DEAD assay was carried out using CS-*g*-K_{16} with *E. coli*. A suspension of *E. coli* (10^8 CFU ml^{-1}) in PBS was prepared followed by addition of CS-*g*-K_{16} at MIC, after which the mixture was incubated at 37 ℃ for 30 min. After incubation the cells were collected by centrifugation and stained with BacLight bacterial viability kit L13152 (Invitrogen) for 30 min at room temperature. The green color SYTO 9 dye enters both intact and membrane-compromised cells, while the red color propidium iodide dye can only enter membrane-damaged cells, within which it reduces the green SYTO dye. The cells were then imaged with fluorescence microscopy (Carl Zeiss, Germany).

Membrane permeabilization assay

The permeabilization of bacterial membranes by the optimized cationic peptidopolysaccharide was characterized by SYTOX Green (Invitrogen) uptake assay. CS-*g*-K_{16} was added into a 10^8 CFU ml^{-1} bacteria suspension (*E. coli*.) at a concentration of 10 μg ml^{-1}, and incubated at 37 ℃ for 30 min. After incubation, the

cells were collected by centrifugation and stained with 5 μM SYTOX Green dye for 30 min at room temperature. The cells were then imaged with fluorescence microscopy (Carl Zeiss, Germany).

Determination of peptidopolysaccharide-induced pore size

FITC-dextran with different molecular weights (40, 70, 500 kDa) were used to determine the size of the pores induced by the optimized peptidopolysaccharide. Briefly, bacteria were collected at mid-log phase and washed three times with isotonic saline solution to remove the broth component. CS-*g*-K_{16} (10 μg ml^{-1}) and FITC-dextran (500 μg ml^{-1}) were added into the suspension and incubated at 37 ℃ for 30 min. After incubation, the cells were collected by centrifugation and washed to remove free dyes. The cells were then imaged with fluorescence microscopy (Carl Zeiss, Germany).

Membrane depolarization

Bacteria were harvested at mid-log phase, washed three times with a buffer solution of 20 mM glucose and 5 mM HEPES (pH 7.4). The bacteria was resuspended in the washing buffer with additional 0.1 M KCl, then incubated with $DiSC_3(5)$ (20 nM) until it was incorporated into the cell membranes. CS-*g*-K_{16} was added at a concentration of 100 μg ml^{-1}, and the fluorescence was monitored with a fluorescence spectrometer (PerkinElmer LS55, U.S.) at λ_{ex}=620 nm and λ_{em}=670 nm. Finally, 0.2 nM Gramicidin D was added to obtain full release of the dye.

Circular dichroism (CD)

POPC:POPG (molar ratio, 4:1) small unilamellar liposomes were prepared using a mini-extruder (Avanti Polar Lipids-Mini Extruder, U.S.). 50 μg ml^{-1} CS-*g*-K_{16} was dissolved in 20 mM sodium phosphate buffer (pH 7.4) and CD spectra were measured with the addition of 0, 5 and 500 μM liposomes at room temperature, using a circular dichroism spectrometer (Chirascan^{TM}, Applied Photophysics, UK).

Hemolysis assay

The hemolytic activity of peptidopolysaccharides was determined following the experimental detail of Chapter 3, section 3.3.1.

In vitro biocompatibility studies

The biocompatibility study was carried out with human aorta smooth muscle cells (SMCs, CC-2571, Lonza). SMCs were cultured in 96-well plates from initial inocula of 1×10^5 cells in each well. A graded concentration series of CS-*g*-K_{16} solutions in culture medium was prepared, 200 μl of which was added to the SMC cultures. The cells were incubated at 37 ℃ for the desired time, then the cell viability was determined following the description in Chapter 3, section 3.3.2.

Co-culture of bacteria and mammalian cells

SMCs were cultured in 96-well plates from inocula of 1×10^5 cells in each well and incubated at 37 ℃ for 24 h in a culture medium free of any antibiotics. 1×10^5 cells of *E. coli* were seeded in each of the SMC culture wells. Then CS-*g*-K_{16} was added in the SMC and *E. coli* co-culture wells at a concentration of 100 μg ml^{-1}. Wells

without CS-*g*-K_{16} were used as a control. The co-culture was imaged using an inverted optical microscope (Carl Zeiss, Germany).

Pro-inflammatory cytokine analysis

To gauge the host immune response of the optimized peptidopolysaccharide, the TNF-α secretion of macrophages when challenged with CS-*g*-K_{16} was measured. Murine macrophage cell line (Raw 264.7) was seeded in 96-wells plate at a density of 1×10^5 cells per well, and cultured at 37 ℃ for 24 h. CS-*g*-K_{16} was then added in the cell culture medium at different concentration (2.5–120 μg ml^{-1}) and incubated at 37 ℃ for 6 h. LPS (1 μg ml^{-1}) which is able to trigger TNF-α secretion, was used as a positive control. After the 6 h exposure to peptidopolysaccharides or controls, the culture medium was changed and the cells were cultured at 37 ℃ for 24 for the secretion of cytokines. The secreted level of TNF-α was determined by enzyme-linked immunosorbent assay (ELISA) with TNF-α ELISA kit (Raybiotech, US).

Animal toxicity studies

18 female BALB/c mice (6-8 weeks, 18-22g) were used in animal toxicity studies and divided into 2 groups for drug administration and 1 group for control. The blood of the mice constituted about 6% of their weight, or ~1.2 ml volume per mouse. 100 μl CS-*g*-K_{16} solution in sterilized PBS (pH = 7.4) was administrated by tail vein injection. 2 groups of 6 mice each were intravenously injected with 5.5 mg kg^{-1} (4-18 × MICs) or 17.5 mg kg^{-1} (14-58 × MICs) and observed 7 days post-injection. All handling of animals was performed according to Nanyang Technological Univerisity's Institutional Animal Care and Use Committees approved protocol.

5.3 Results and Discussion

5.3.1 Characterizations

In order to study the effect of lysine (K) and phenylalanine (F), which are respectively cationic hydrophilic and hydrophobic amino acid residues, two series of peptidopolysaccharides were synthesized: (1) chitosan-*graft*-polylysine series (denoted CS-*g*-K_n) and (2) chitosan-*graft*-poly(lysine-*ran*-phenylalanine) series (denoted CS-*g*-K_nF_n). Peptide side chains made from lysine and phenylalanine were grafted onto the chitosan backbone by α-amino acid *N*-carboxyanhydride (NCA) ring-opening polymerization (ROP) (Figure 5.1b) initiated from the amine groups.[208] NCA ROP is a facile, inexpensive and easily scalable synthesis technique.[59] For most samples, the chitosan backbone used had a relatively low molecular weight (4.5×10^4 g mol^{-1}, unless otherwise stated). A higher molecular weight (1.1×10^6 g mol^{-1}) sample was also used to study the effect of molecular weight. By protection of the the 6-CH_2OH groups on chitosan by triphenylmethyl groups, the α-amino acid NCA monomers reacted with the amine groups at the C-2 position of chitosan, so that the polypeptide side chains were grown from the chitosan main chain. The grafting ratio (*i.e.* the molar ratio of the grafted amino acid to chitosan) was varied to explore its effect on antimicrobial activity. The synthesis of chitosan-*graft*-polypeptide copolymer was confirmed by ^{1}H NMR analyses (Figure 5.2). The grafting ratio was determined by the integrals of polypeptide and saccharide ^{1}H NMR signals and the copolymers were named by the grafting ratio (Table 5.1). The number-average

degree of polymerization (DP_n), which represents the average length of the polypeptide side chain, can be calculated using the grafting ratio divided by the deacetylation degree of chitosan (Table 5.1).[208] The molecular weights and polydispersities determined by GPC are also summarized in Table 5.1.

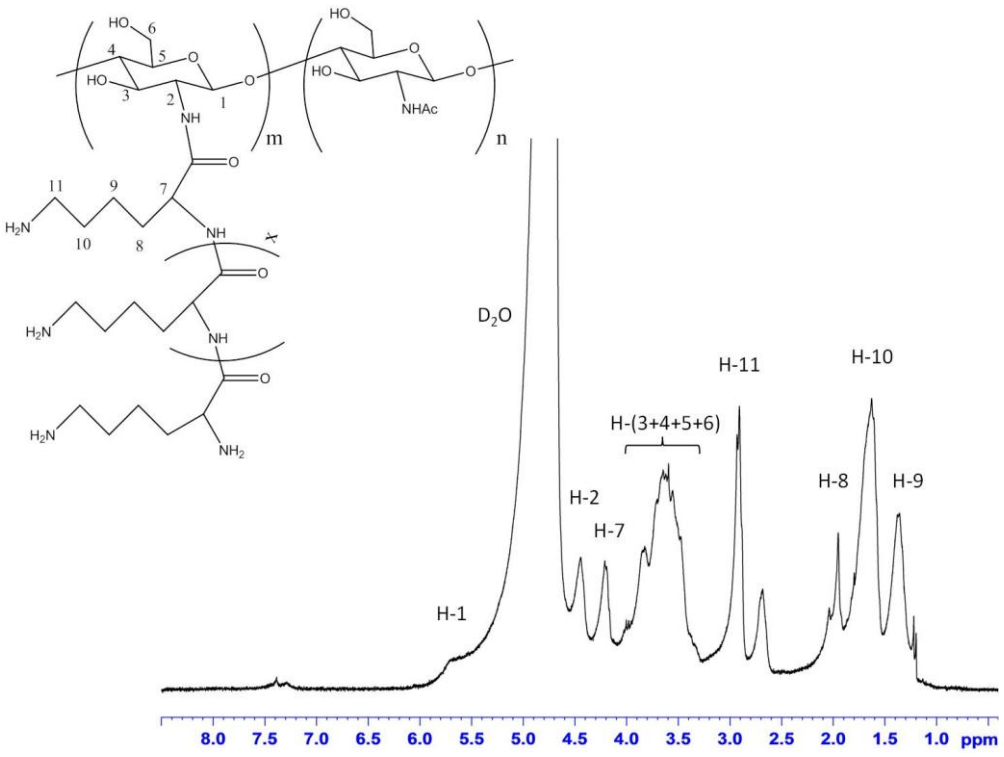

Figure 5.2 Typical ^{1}H NMR spectra of chitosan-*g*-polylysine copolymers.

Table 5.1 Characteristics of the chitosan-*g*-polypeptide copolymers.

Copolymers	Grafting ratio	DP_n	*Mn* (× 10^4 g mol^{-1})	*Mw* (× 10^4 g mol^{-1})	PDI
CS-*g*-K_1	1.1	1.2	1.26	1.53	1.22
CS-*g*-K_3	3.4	3.8	1.35	1.57	1.16
CS-*g*-K_9	9.0	10	2.04	2.32	1.14
CS-*g*-K_{16}	16.9	18.8	2.17	2.46	1.13
CS-*g*-K_{25}	23.7	26.3	3.13	3.38	1.08
CS-*g*-K_3-HMW	3.1	3.9	29.2	33.9	1.16

DP_n (number-average degree of polymerization) = grafting ratio/deacetylation degree. M_n: number-average molecular weight. M_w: weight-average molecular weight. PDI: polydispersity index.

5.3.2 Antimicrobial activities

The antimicrobial activity of synthetic polymers which mimic natural AMPs is known to be affected by two major factors: cationic charge and hydrophobicity.[102-108] Two series of chitosan-*graft*-polypeptide with varying degrees of cationic charge and hydrophobicity were synthesized and tested. Series 1 (#1A-1E, Table 5.2) has grafted polylysine with varying grafting ratio from 1 to 25 and consequent varying cationic charge. Series 2 (#2A-2B, Table 5.2) has grafted poly(lysine-*ran*-phenylalanine) containing equimolar hydrophobic phenylalanine and cationic lysine residues with grafting ratio of 16 (#2A) and 25 (#2B). Both series were water soluble at neutral pH. For the first CS-*g*-K_n series (#1A-1E, Table 5.2) with polylysine grafts of varying average lengths, the antimicrobial activities improved significantly as the polylysine ratio increased from 1 to 9 (#1A-1C), with MICs of 5 - 20 μg ml^{-1} for #1C for all pathogens tested. The MICs vary only slightly between n = 9, 16, and 25 (#1C-1E), with the minimum MICs of the CS-*g*-K_n series exhibited by CS-*g*-K_{16} (#1D). The optimum CS-*g*-K_{16} (#1D) MICs are better than those of known highly effective AMPs such as magainin and mellitin (#4A, #4B, Table 5.2). The CS-*g*-K_n series (#1) has much lower MICs than the corresponding cationic homopolymer made by the same NCA polymerization method but without the chitosan backbone; for example, P(K_{16}) and P(K_{25}) (#5A-5B) did not show significant antimicrobial activity whilst CS-*g*-K_{16} and CS-*g*-K_{25} (#1D-1E) has low MICs. The chitosan backbone without the the polylysine graft is also expected to show relatively poor antimicrobial effect; the MICs of water soluble chitosan-*graft*-poly(ethylene glycol) (CS-g-PEG) derivative were 630 to

higher than 2500 μg ml^{-1} (Table 5.2, #3A). (Without the PEGylation, the chitosan is not able to dissolve at neutral pH.)

In Series 2, CS-*g*-K_8F_8 and CS-*g*-$K_{12.5}F_{12.5}$ (#2A-2B, Table 5.2) have much higher MICs, particularly against the bacteria. CS-*g*-$K_{12.5}F_{12.5}$ (#2B) has MICs of 630 – 1250 μg ml^{-1} against the bacterial pathogens. Chitosan with a shorter poly(lysine-*ran*-phenylalanine) graft, CS-*g*-K_8F_8 (#2A), shows even higher MICs, 2500 μg ml^{-1} or greater. These two Series 2 members, *i.e.* CS-*g*-K_8F_8 and CS-*g*-$K_{12.5}F_{12.5}$, show relatively good antifungal activities despite their poor antibacterial activities. We also compared the MICs of CS-*g*-K_nF_n (#2B) with the corresponding values for the polymeric form of the K_nF_n graft (#5C, Table 5.2): the MICs of CS-*g*-$K_{12.5}F_{12.5}$ (#2B) increased more than 5 times for the three bacteria compared with P($K_{12.5}F_{12.5}$) (#5C), which has low MICs for both Gram-negative/positive bacteria (62 μg ml^{-1} for *E. coli*, 31 μg ml^{-1} for *S. aureus*).

Our previous results indicate that the copeptide K_nF_n containing both hydrophobic and cationic amino acid residues (*e.g.* #5C) has better antimicrobial activities than the homopeptide K_{2n} (*e.g.* #5B) due to the requirements of hydrophobicity and cationic charge in antimicrobial biomacromolecules.[55] The current results are unexpected in that the Series 1 molecules have excellent antimicrobial activities in spite of the absence of hydrophobic phenylalanine residues, and CS-*g*-K_{16} and CS-*g*-K_{25} (#1D, #1E) show much better antimicrobial activities than CS-*g*-K_8F_8 and CS-*g*-$K_{12.5}F_{12.5}$ (#2A, #2B).

Among the tested peptidopolysaccharide copolymers, CS-*g*-K_{16} (#1D) has the best antimicrobial activities. Pure polylysine graft in the peptidopolysaccharide copolymer

results in better antimicrobial activity than lysine/phenylalanine copeptide graft. It is also apparent that the chitosan backbone significantly promotes the antimicrobial activity of the graft copolymer. The cationic charge of lysine and the hydrophobicity of chitosan backbone is hypothesized to contribute to the increased efficacy of the graft copolymer. Also, it appears that the antimicrobial activity saturates at high polylysine loading of the copolymer: there is a plateau of very low MICs between the grafting ratio of 9 and 25, with CS-*g*-K_{16} being slightly better than the other two.

Molecular weight is another important factor in tuning the efficacy of synthetic antimicrobial polymers.[114] The 2 series discussed thus far, *i.e.* CS-*g*-K_n and CS-*g*-K_nF_n (#1A-1E, #2A-2B), used chitosan with a relatively low molecular weight of 4.5×10^4 g mol^{-1}. A higher molecular weight chitosan (1.1×10^6 g mol^{-1} in #1B-HMW) was also used to probe the effect of molecular weight on antimicrobial activity. After the multiple reaction steps, the number-average molecular weight (*Mn*) of CS-*g*-K_3 and CS-*g*-K_3-HMW (#1B, #1B-HMW, Table 5.2) determined by GPC were 1.35×10^4 g mol^{-1} and 29.2×10^4 g mol^{-1} respectively (Table 5.1). At the same grafting ratio of lysine, the lower molecular weight CS-*g*-K_3 shows a much lower MIC against all five pathogens. The MICs of CS-*g*-K_3-HMW (#1B-HMW) are 4- or more-fold as large as those of CS-*g*-K_3 (#1B), indicating that the lower molecular weight chitosan results in more effective antimicrobial graft copolymers.

Table 5.2 Antimicrobial and hemolytic activities of peptidopolysaccharides and comparison antimicrobial materials.

No.	Family	Name	MIC [μg ml^{-1}]					HC_{50} [μg ml^{-1}] (a)	Selectivity (b)
			Gram-negative		Gram-positive	Fungi			
			P. aeruginosa	*E. coli*	*S. aureus*	*C. albicans*	*F. solani*		
1A	Peptidopoly-saccharides	CS-*g*-K_1	80	80	160	40	40	>50000	>625
1B		CS-*g*-K_3	20	20	40	20	10	>50000	>2500
1C		CS-*g*-K_9	20	10	20	20	5	>50000	>5000
1D		CS-*g*-K_{16}	20	10	10	20	5	>100000	>10000
1E		CS-*g*-K_{25}	40	10	10	20	5	>50000	>5000
1B-HWM		CS-*g*-K_3-HMW	310	80	160	160	40	>25000	>313
2A		CS-*g*-K_8F_8	>2500	>2500	2500	>2500	160	12500	<5
2B		CS-*g*-$K_{12.5}F_{12.5}$	1250	630	1250	310	80	7500	12
3A	Chitosan derivatives	CS-*g*-PEG	>2500	>2500	1250	1250	630	>25000	10
3B		TMC-Q-*g*-EM[205]	98	200	98	--	24	>25000	>125
3C		DMDC-Q-*g*-EM[205]	98	98	49	--	24	>25000	>250
4A	Natural AMPs	Magainin-2[108]	--	125	--	--	--	>250	>2
4B		Melittin[204]	--	13	--	--	--	2	0.15
5A	Synthetic AMPs	P(K_{16})	>1000	>1000	>1000	>1000	>1000	--	--
5B		P(K_{25})[55]	>1000	>1000	>1000	>1000	>1000	--	--
5C		P($K_{12.5}F_{12.5}$)[55]	250	62	31	250	--	16	0.5
5D		P($K_{10}F_{15}$)[55]	31	31	31	125	--	16	0.5
5E		1-Pro_6[84]	--	5	--	--	--	170	34
5F		$(LLRR)_4$[209]	--	--	--	>50	--	12	<0.5
5G		H1[210]	32	8	32	--	--	128	16
6A	Synthetic Polymers	Polyvinylpridine P(2VP-*co*-PEGMA 300)-HB[122]	--	1.4	--	--	--	1	0.71
6B		Polymethacrylate PB_{27}[204]	--	16	--	--	--	13	0.81
6C		Poly(β-lactam) *p*-(*tert*-Bu)-benzoyl[107]	--	6.25	6.25	--	--	106	17
6D		Polynorbornene $Poly3_{0.8}$-*co*-$PolyP_{0.2}$[115]	--	15	25	--	--	<50	<3.3
6E		Pyridinium methacrylate copolymer B_4[105]	--	15	--	--	--	0.23	0.02

(a) HC_{50}: the concentration which is 50% hemolytic. (b) Selectivity: HC_{50}/MIC(*E. coli*).

5.3.3 Mechanism studies

Field Emission Scanning Electron Microscopy (FESEM) of pathogen cell morphologies is shown in Figure 5.3. Compared with the intact controls (left panel), microbial cells treated with cationic peptidopolysaccharide (CS-*g*-K_{16} at MIC concentration) exhibit distinct changes in their morphology (right panel). Unlike the smooth surfaces of the control cells, wrinkled cell walls can be seen on *E. coli*, *S. aureus* and *C. albicans* cells. Some *P. aeruginosa* cell membranes were damaged to the point that cell contents leaked out (arrows in Figure 5.3b(ii)), while whole cells were collapsed for *S. aureus* and *C. albicans*. *F. solani* cell surfaces were wrinkled and many blebs (white dots in Figure 5.3e(ii)) were observed on the surfaces. All these results indicate that CS-*g*-K_{16} caused severe changes in the microbe cells.

In the bacterial viability study by LIVE/DEAD stain of *E. coli*, the intact bacteria fluoresce green while cationic peptidopolysaccharide (CS-*g*-K_{16} at MIC concentration) treated ones fluoresce red (Figure 5.4). The observed fluorescence behavior indicates that CS-*g*-K_{16} renders *E. coli* cell membrane permeable to propidium iodide.

The permeabilization of bacterial membranes by cationic peptidopolysaccharide was also confirmed by SYTOX Green uptake assay (Figure 5.5). SYTOX is a nucleic acid dye which is only able to penetrate cells with compromised plasma membranes and does not cross the intact membrane of live cells.[211] *E. coli* cells treated with CS-*g*-K_{16} (at MIC concentration) showed bright green fluorescence (Figure 5.5d), while control cells did not show any fluorescence (Figure 5.5b). This result indicates

bacterial membrane disruption and/or permeabilizations induced by CS-*g*-K_{16}.

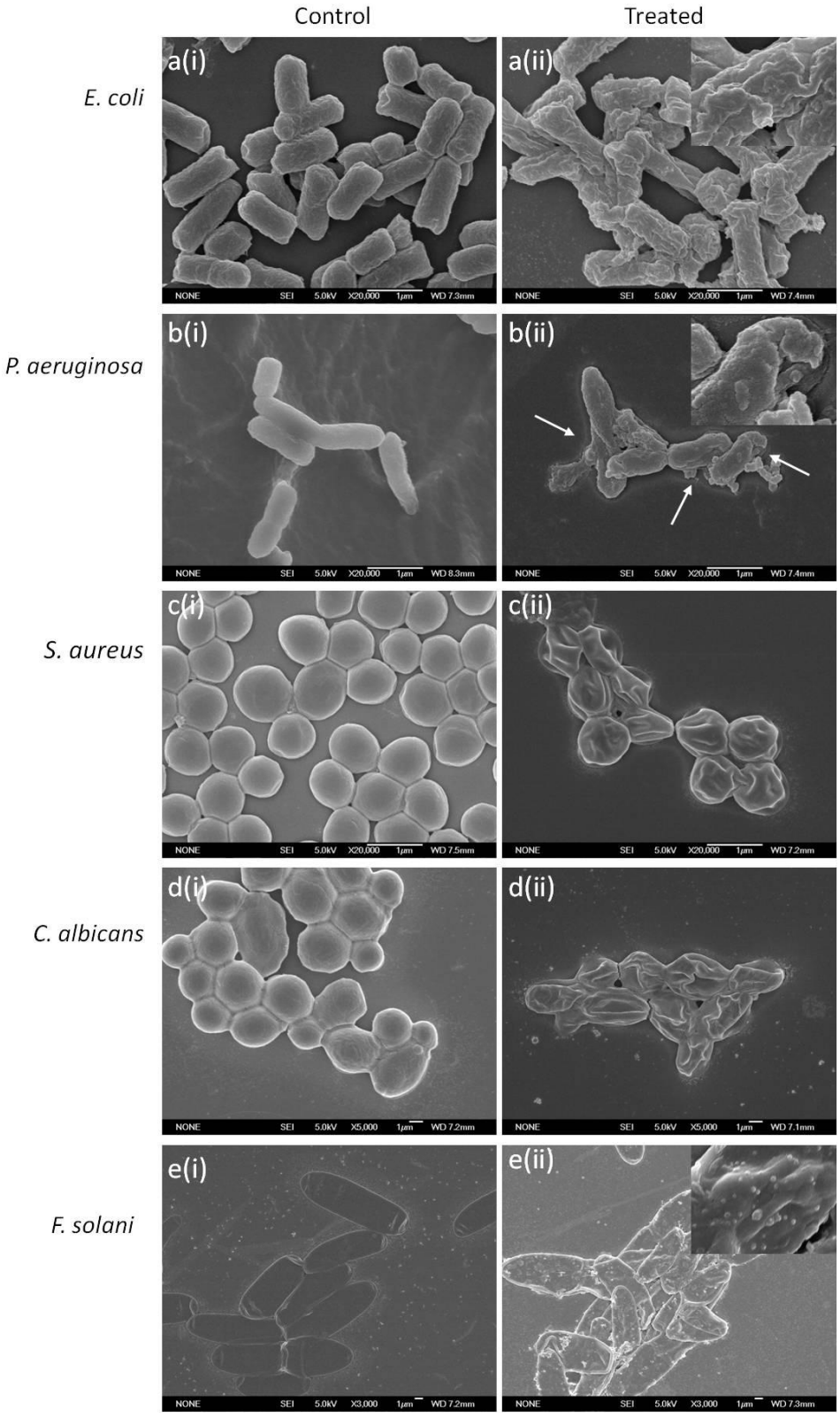

Figure 5.3 Morphology of various pathogens cells: (a) *E. coli*, (b) *P. aeruginosa*, (c) *S. aureus*, (d) *C. albicans* and (d) *F. Solani*, before (i) and after (ii) treatment with CS-*g*-K_{16}.

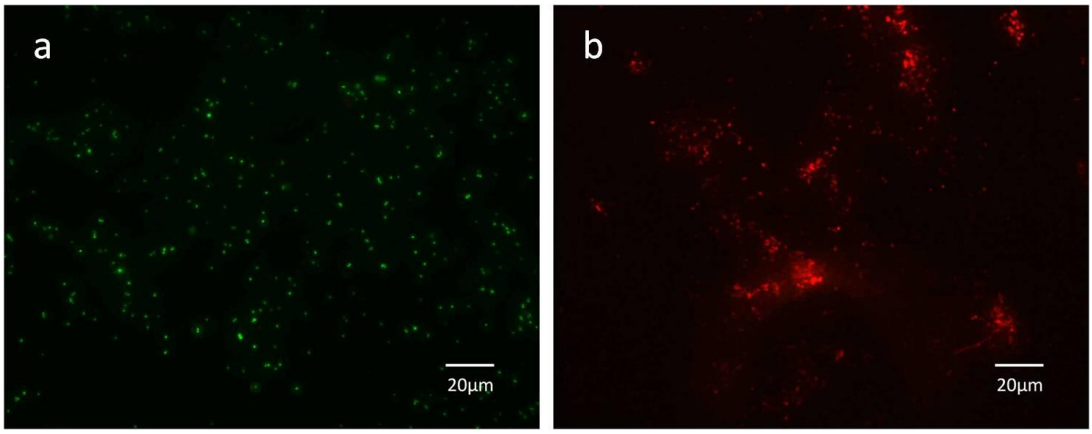

Figure 5.4 LIVE/DEAD bacterial viability assay of *E. coli* (a) control; (b) treated with CS-*g*-K_{16}.

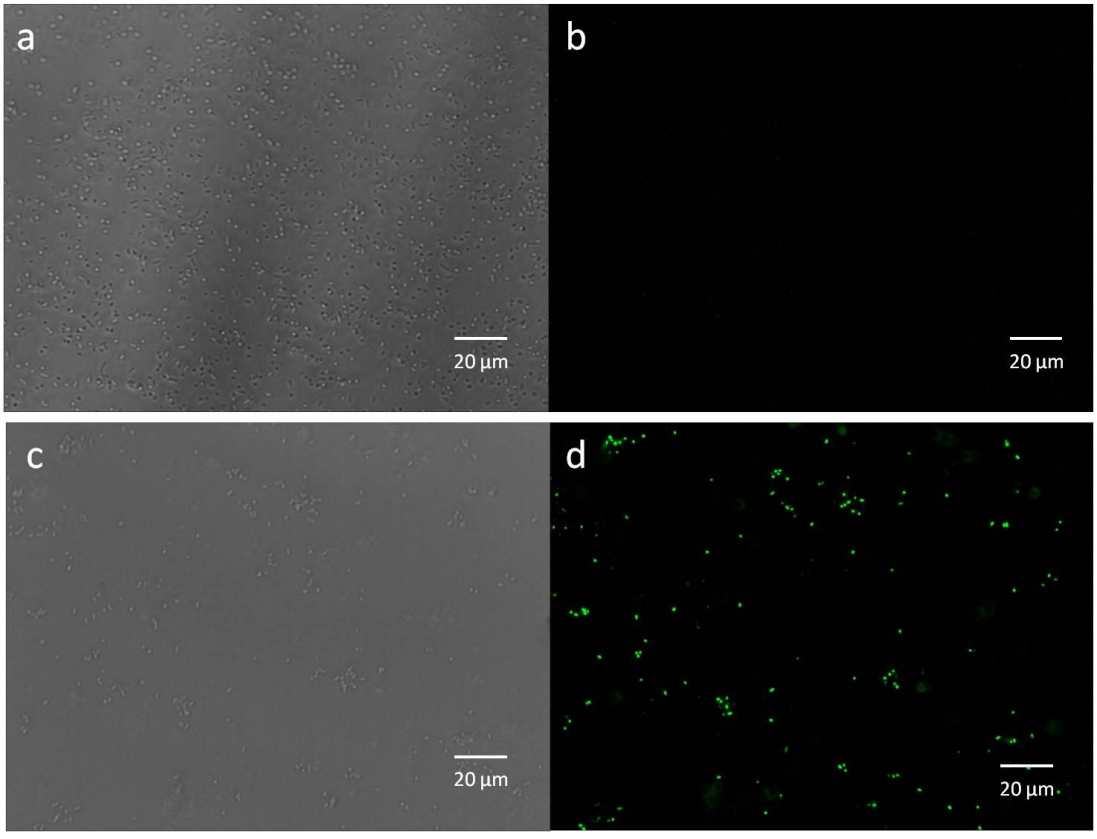

Figure 5.5 Optical (L) and fluorescence (R) images of SYTOX Green assay for (a, b) control, and (c, d) CS-*g*-K_{16} treated bacteria cells (*E. coli*).

Microbe membrane disruption by CS-*g*-K_{16} was also verified by adding the membrane potential sensitive dye $DiSC_3(5)$, which is absorbed into intact membrane bilayers and is released upon subsequent membrane disruption.[212] In Figure 5.6, the first peak indicates the addition of $DiSC_3(5)$ and the gradual incorporation into Gram-negative bacteria *E. coli* membrane. Addition of CS-*g*-K_{16} at the concentration of 100 μg ml^{-1} (at around 650 s), results in an immediate fluorescence increase which indicates release of the dye due to cell membrane disruption. (The fluorescence peak at around 1250s is due to 100% leakage of the dye induced by gramidicin D.)

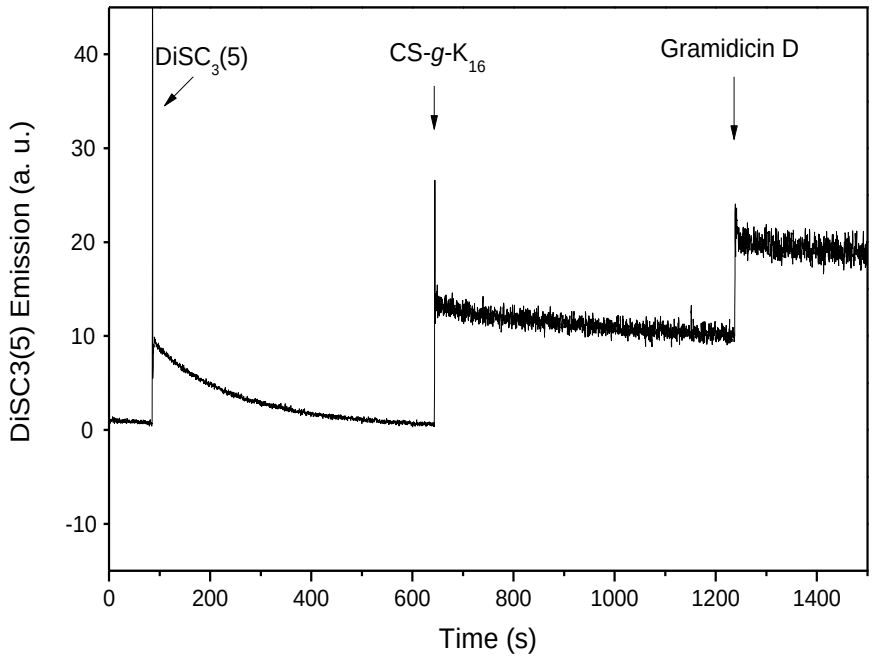

Figure 5.6 Membrane potential sensitive dye $DiSC_3(5)$ leakage from *E. coli* challenged with CS-*g*-K_{16}.

Together with the FESEM morphology study, LIVE/DEAD and SYTOX assays, this result provides strong evidence that CS-*g*-K_{16} acts to disrupt and/or permeabilize the bacterial membrane. In order to determine the size of pores in the disrupted membane induced by the cationic peptidopolysaccharide, the bacteria were treated with fluorescein isothiocyanate (FITC) labeled dextrans with small, medium and high molecular weights (40kDa, 70kDa and 500kDa respectively) (Figure 5.7).[213] In the absence of CS-*g*-K_{16}, FITC-dextrans of different molecular weights are not able to enter into the *E. coli* cells. In the presence of CS-*g*-K_{16} at MIC concentration, FITC-dextran with a molecular weight of 40 kDa (dia. ~ 9 nm) and 70 kDa (dia. ~ 12 nm) were able to penetrate the *E. coli* membrane. The largest FITC-dextran macromolecules (500 kDa, dia. ~ 29 nm) in this test were also able to enter into the *E. coli* cells in the presence of CS-*g*-K_{16}. Thus the diameter of the pores induced by CS-*g*-K_{16} is larger than 29 nm. These results corroborate the FESEM observations that bacterial membrane was damaged by CS-*g*-K_{16} and cell contents leaked out from the pores (Figure 5.3).

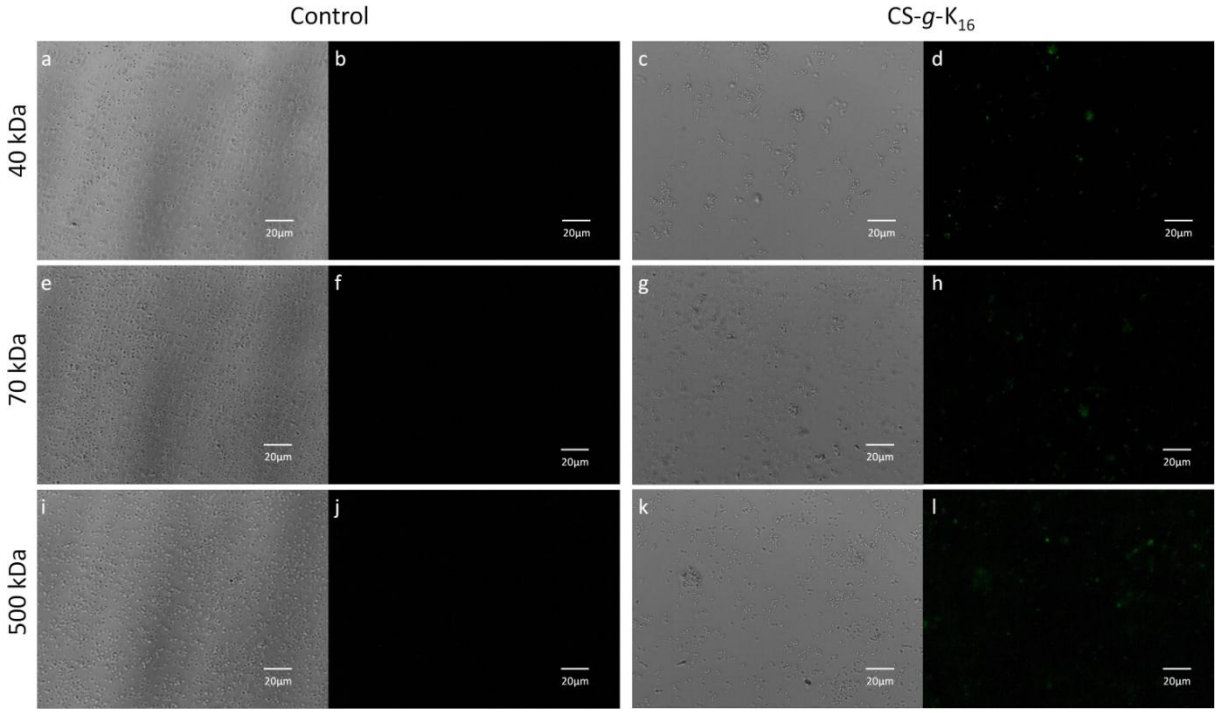

Figure 5.7 Fluorescent staining of bacteria by various FITC-dextrans with different molecular weights. The left side labels denote the molecular weight of FITC-dextran used across the respective row: (a, b, c, d) with 40 kDa, (e, f, g, h) with 70 kDa, and (i, j, k, l) with 500 kDa.

The antimicrobial activity of natural AMPs has generally been attributed to their secondary structures such as α–helix or β–sheet which promote their interaction with the bacterial membrane.[11] Various theories for the action mechanism of α-helical or β-sheet AMPs such as the "barrel-stave", "carpet" and "toroidal" models have been proposed.[13] Circular dichroism (CD) analysis was carried out to assess the degree to which secondary structure might contribute to the antimicrobial activity of CS-*g*-K_{16}. Figure 5.8 shows the CD spectra of CS-*g*-K_{16} in sodium phosphate buffer with 0 μM, 5

μM, 500 μM small unilamellar liposomes (POPC/POPG 4:1). The POPC/POPG lipid vesicle is a mimic of anionic bacterial membranes. Regardless of the presence or absence of the liposomes, CS-*g*-K_{16} gives a typical random coil spectrum. Therefore, unlike most natural AMPs, cationic peptidopolysaccharides exert their antimicrobial activity in the random coil conformation. The possibility that secondary structures may be unnecessary for good antimicrobial activity has also recently been proposed by Tew *et al.*[114]

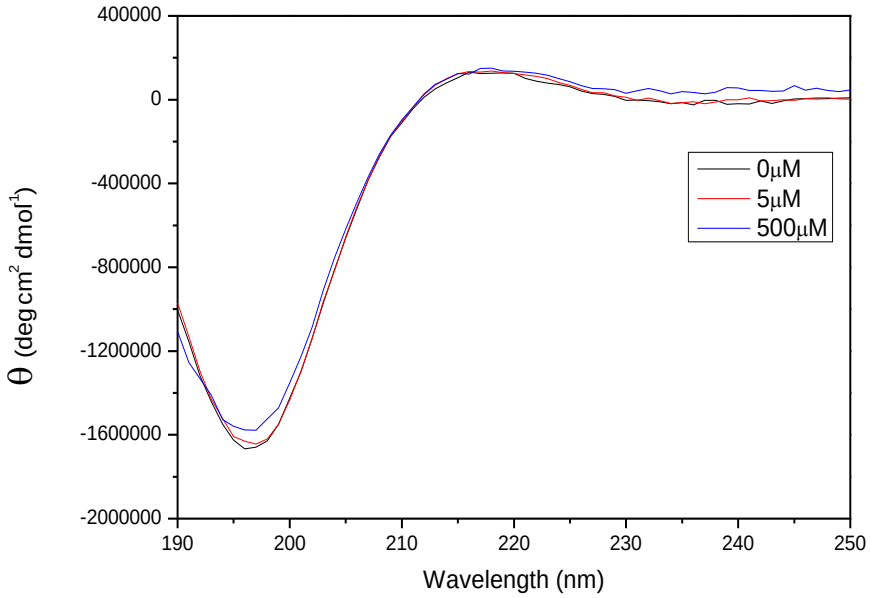

Figure 5.8 CD spectra of CS-*g*-K_{16} in 20 mM sodium phosphate buffer with 0 μM, 5 μM and 500 μM small unilamellar liposomes (POPC/POPG 4:1).

Bacterial cell walls are generally negatively charged, regardless of their specific structure and composition.[37] The Gram-negative bacteria cell wall has two concentric

lipid bilayer membranes: the cytoplasmic (inner) membrane and the outer membrane. The outer leaflet of the outer membrane is mainly composed of highly negatively charged lipopolysaccharides (LPS); the cytoplasmic membrane consists of anionic phospholipids together with zwitterionic phospholipids.[37, 40] The Gram-positive bacteria typically possess a single anionic membrane (the cytoplasmic membrane), and a thick exposed peptidoglycan layer which is rich in anionic teichoic acids (wall teichoic acid (WTA) and lipoteichoic acid (LTA)).[214] So when bacteria, whether Gram-negative or Gram-positive, contact with cationic peptidopolysaccharides, electrostatic interaction between the negatively charged cell wall (due to LPS or teichoic acid) and the positively charged peptidopolysaccharides is inevitable (Figure 5.9).

We propose the following antibacterial mode of action for our cationic peptidopolysaccharides: Firstly, in close proximity to the microbe surface, the cationic peptidopolysaccharide is electrostatically attracted into contact with the anionic microbe cell wall, specifically by the LPS or teichoic acid in Gram-negative and Gram-positive bacteria respectively. The negatively charged bacterial cell wall, which is stabilized by divalent cations, serves as an effective permeability barrier to restrict molecular traffic into and out of the cell.[215] The complexing of cationic peptidopolysaccharides with negative charged cell wall components (such as LPS or teichoic acids) will affect cations such as Mg^{2+} and Ca^{2+} present in the cell wall, alter bacterial surface morphology, increase cell wall permeability and diminish its barrier function.

Secondly, as the cationic peptidopolysaccharide molecules are attracted to and aggregated on/in the cell wall, increasing its permeability, their compatibility with LPS and peptidoglycan, which also contain polysaccharides, enables them to pass through the outer membrane and the peptidoglycan layer and then reach the cytoplasmic membrane.

Thirdly, after passing through the bacterial cell wall barrier, cationic peptidopolysaccharides reach the cytoplasmic membrane and accumulate on/in the cytoplasmic membrane like a "carpet", permeating and then disintegrating the bi-layer when a threshold concentration is reached, leading to the lethal stage.[46] Because of their random coil structure, we postulate that it is more likely that the cationic peptidopolysaccharides exert their antimicrobial activity by a "carpet model" mechanism which does not require specific structure.

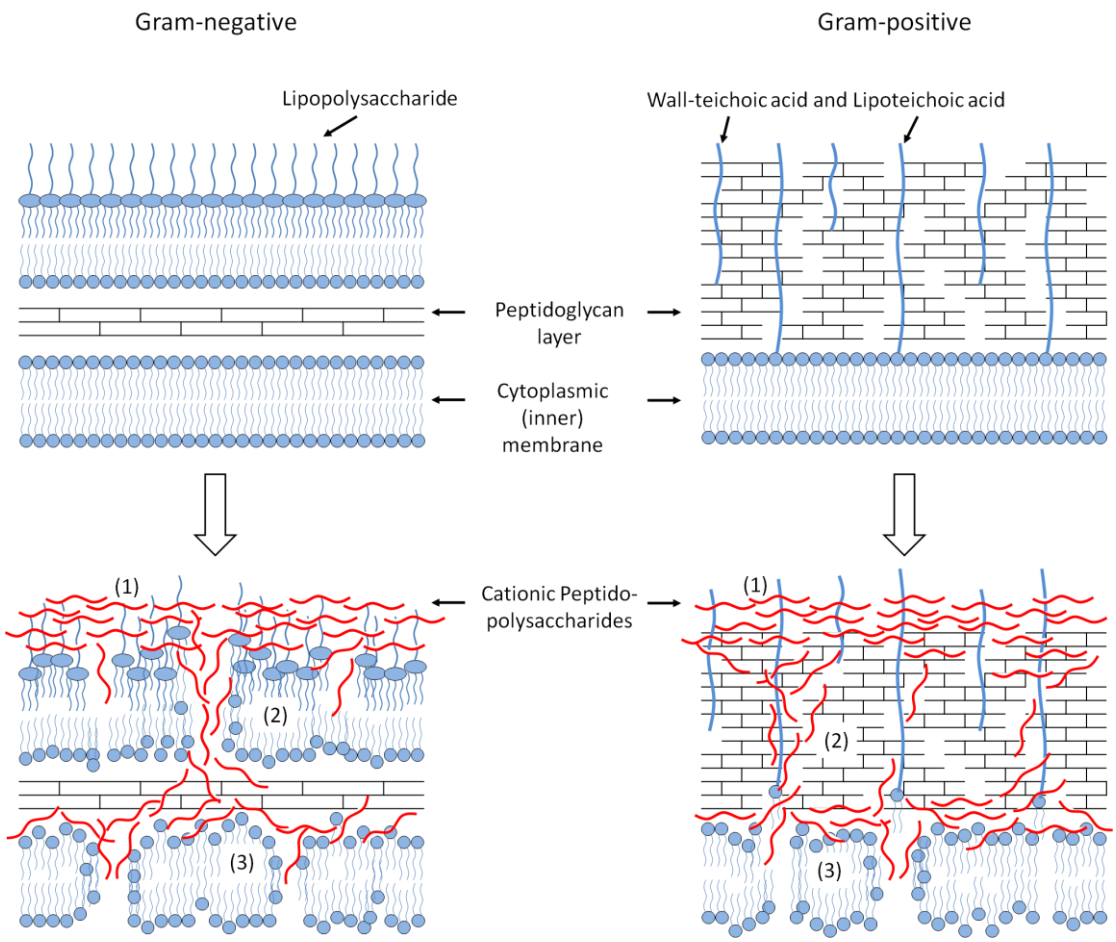

Figure 5.9 The proposed action mode of cationic peptidopolysaccharides on Gram-negative and Gram-positive bacteria: (1) Cationic peptidopolysaccharides aggregate on the cell wall by electrostatic interaction with the anionic bacterial cell wall. (2) The compatibility with LPS and peptidoglycan enables them to pass through the outer membrane and the peptidoglycan layer. (3) Cationic peptidopolysaccharide accumulates on/in the anionic cytoplasmic membrane, permeabilizing and then disintegrating the bi-layer, leading to the lethal stage.

The morphology and membrane depolarization results support our proposed mechanism. The FESEM images exhibit morphology changes of wrinkled or lysed cell walls (Figure 5.3). The $DiSC_3(5)$ dye, which incorporates into the cytoplasmic

membrane, was released after the addition of CS-*g*-K_{16}, which indicates that the cationic peptidopolysaccharides traversed the outer membrane or peptidoglycan matrix successfully and permeabilized the inner membrane (Figure 5.6).

This proposed mechanism can also account for many features of our MIC data. We observed that at low lysine loading (*e.g.* with CS-*g*-K_1 and CS-*g*-K_3), the CS-*g*-K_n series is more effective against Gram-negative bacteria than Gram-positive bacteria. Gram-negative bacterial cell wall is more anionic and hydrophilic than that of Gram-positive bacteria.[216] At low lysine loading, the attraction between the molecule and the cell wall is relatively weak and the higher electrostatic attraction of the more anionic (Gram-negative) cell wall may be significant. At high lysine loading, the attraction is strong for both types of bacteria, so that the differential attraction is less obvious and the antimicrobial activity saturates against both types of bacteria, with similar low MICs. Also, among molecules with similar compositional affinity to cell wall constituents but with different sizes, higher molecular weight molecules should less readily pass through the cell wall, resulting in reduced antimicrobial efficacy. Precisely this effect is observed in the diminished efficacy of the cationic peptidopolysaccharide made with high molecular weight chitosan (#1B-HMW) in comparison with its low MW counterpart with the same length peptide grafts (#1B).

Our cationic peptidopolysaccharides have antifungal activities that are comparable to (in the case of *F. solani*, better than) their antibacterial activities. The fungal cytoplasmic membrane is anionic and is protected by a polysaccharide (mainly chitin, the origin source of chitosan) cell wall.[36] As with bacteria, the cationic

peptidopolysaccharides are able, due their structural affinity to cell wall components, to pass through the polysaccharide fungal cell wall and disrupt the anionic lipid bi-layer, resulting in cell death. The collapse of *C. albicans* cells and the wrinkling of the surface of *F. solani* cells exposed to CS-*g*-K_{16} (Figure 5.3d(ii), e(ii)) suggest severe disruption of the fungal cell wall and membrane.

5.3.4 *In vitro* and *in vivo* biocompatibility studies

We found that Series 1 exhibits extremely low hemolytic activity with human red blood cells: the 50% hemolytic concentration (HC_{50}) for all agents in this series is greater than 50,000 μg ml^{-1} (Table 5.2). For CS-*g*-K_{16}, which has the lowest MICs, even at the highest tested concentration of 100,000 μg ml^{-1}, the hemolytic percentage is below 50% (Table 5.2). The HC_{50} of CS-*g*-K_{16} is thousands of times its MICs for all tested bacteria and fungi, indicating an extremely high degree of selectivity for microbes over human red blood cells. The selectivity of CS-*g*-K_{16} for *E. coli* over human blood red cells is more than 10,000, which is dramatically superior to the selectivity of the related P($K_{10}F_{15}$) polypeptide (Table 5.2) also synthesized by NCA ROP.

The *in vitro* biocompatibility of CS-*g*-K_{16} was also tested by MTT cell viability assay, and the co-culture of human aorta Smooth Muscle Cells (SMCs) and pathogens in the presence and absence of the cationic peptidopolysaccharide. Figure 5.10a shows SMCs viability as determined by the MTT method after exposure to different

concentrations of CS-*g*-K_{16} for 1 h. There is no significant decrease in SMCs survival below 500 μg ml^{-1} of CS-*g*-K_{16}. SMCs proliferation in a culture medium supplemented with 100 μg ml^{-1} CS-*g*-K_{16} is statistically similar to that of the control from 1 to 5 days (Figure 5.10b, $p > 0.05$, no significant difference).

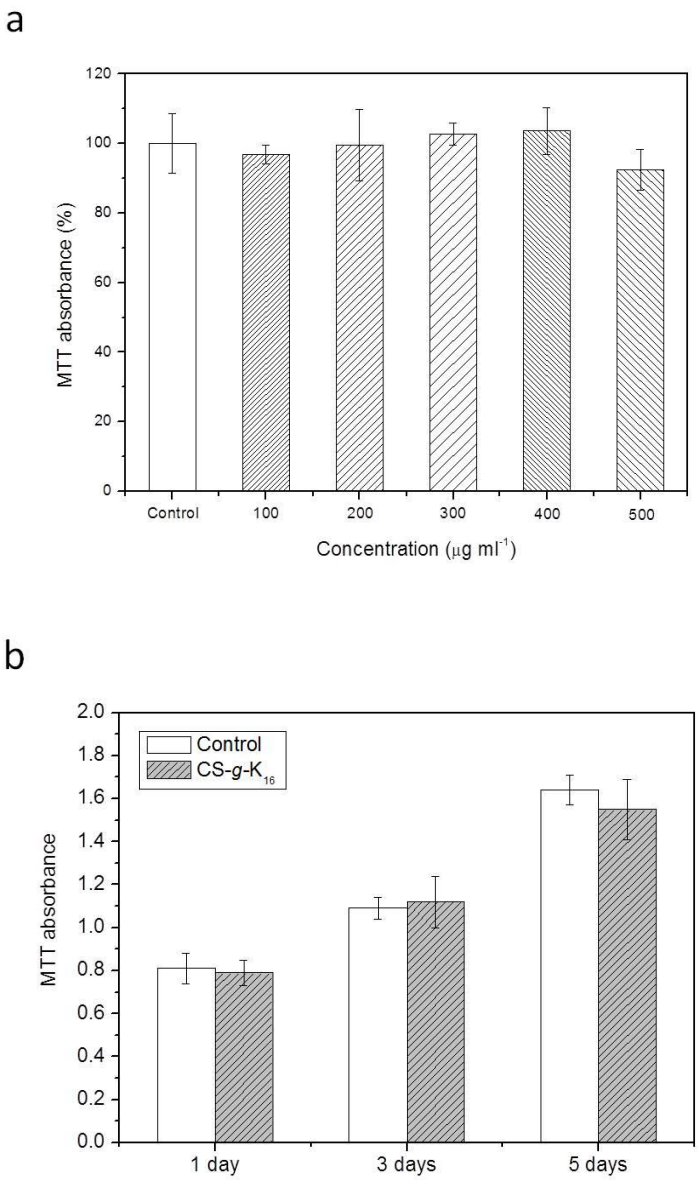

Figure 5.10 MTT of (a) SMCs cultured in a series of concentrations of CS-*g*-K_{16} for 1 h ($p > 0.05$, no significant difference); (b) SMCs cultured with 100 μg ml^{-1} CS-*g*-K_{16} from 1 to 5 days.

In co-culture of SMCs and *E. coli* bacteria, CS-*g*-K_{16} inhibits the bacterial growth but permits SMCs growth. Figures 5.11a and 5.11b shows SMCs cultured 6 h after inoculation of 1×10^5 *E. coli* in culture medium without any antibiotic (Figure 5.11a) and with 100 μg ml^{-1} CS-*g*-K_{16} (Figure 5.11b). The presence of bacteria obviously interfered with SMCs growth: the SMCs detached from the culture plate and have a round shape (Figure 5.11a). In the 100 μg ml^{-1} CS-*g*-K_{16} culture system, the high concentration (10 times MIC) of CS-*g*-K_{16} destroyed all the *E. coli* and the SMCs spread and attached to the culture substrate and showed a normal spindle shape (Figure 5.11b).

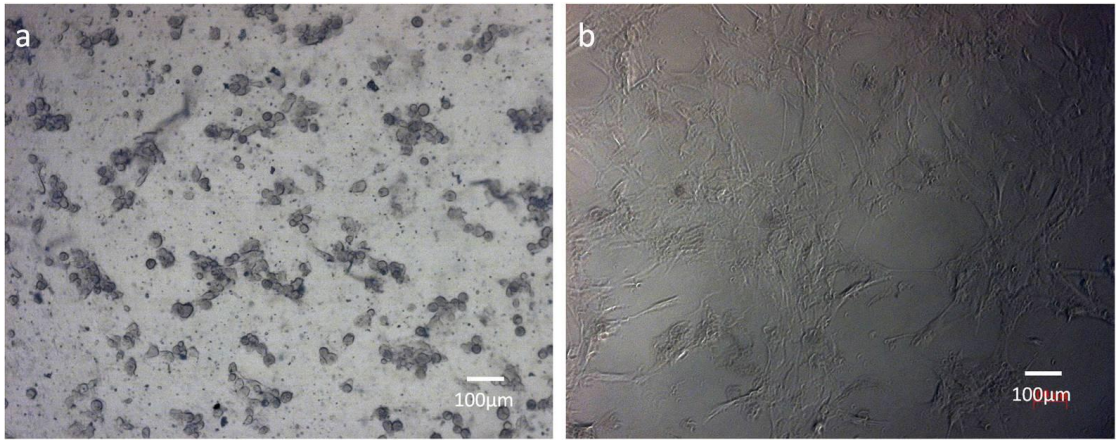

Figure 5.11 Co-culture of SMC with *E. coli* after 6 h incubation: (a) in the culture medium without antibiotic and CS-*g*-K_{16}, bacteria grew well but SMCs detached from the culture dish and changed to round shape; (b) in the culture medium with 100 μg ml^{-1} CS-*g*-K_{16}, bacteria were inhibited and SMCs grew well.

The pro-inflammatory cytokine secretion (specifically TNF-α) of cultured macrophages treated with the peptidopolysaccharide was also characterized. As a first test of the host immune response to the peptidopolysaccharide, we measured the secretion of TNF-α of cultured macrophages when treated with CS-*g*-K_{16}. Figure 5.12 shows the measured secretion of tumor necrosis factor-α (TNF-α) by murine macrophages (raw 264.7) when challenged with CS-g-K_{16}. For all tested concentrations of CS-*g*-K_{16} from 2.5 to 120 μg ml^{-1} (6-24 × MICs for 120 μg ml^{-1}), the TNF-α secretion levels in the 24-hour period are below 100 *p*g ml^{-1}. On the contrary, with LPS at 1μg ml^{-1}, the TNF-α secreted in the 24-hour period is larger than 1000 *p*g ml^{-1}. This preliminary test suggests that the presence of CS-*g*-K_{16} does not trigger the host immune response of macrophages.

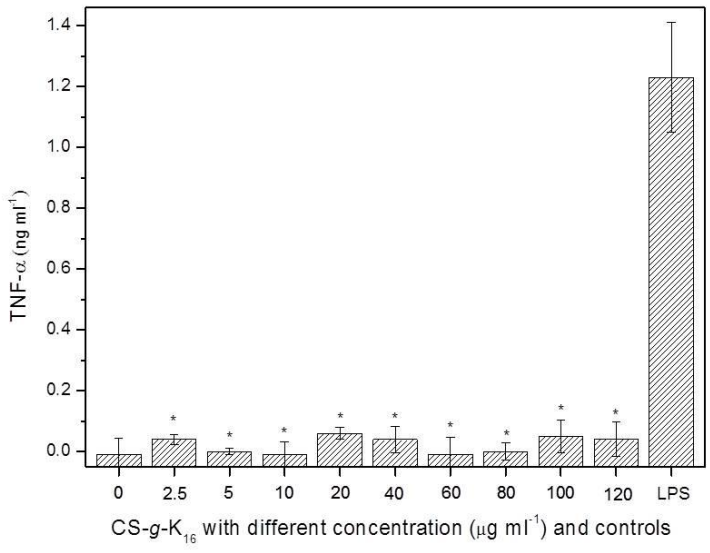

Figure 5.12 Macrophages secretion of TNF-α in the presence of CS-*g*-K_{16} at different concentrations, LPS (1 μg ml^{-1}) was used as positive control. * indiates significantly different from the LPS control ($p < 0.05$, n=4).

Animal toxicity of CS-g-K_{16} was also tested with female BALB/c mice (6-8 weeks, 18-22 g) by tail vein injection at two dosage levels of 5.5 and 17.5 mg kg^{-1} (4-18× and 14-58× MICs, respectively). After 7 days, all the mice (n = 6 in each group) survived and were active; visual inspection of the mice did not suggest any illness. These preliminary *in vitro* and *in vivo* tests suggest non/low-toxicity of CS-g-K_{16} although further tests are needed before this compound can be used in humans. For example, the platelet activation test should also be done in future tests even though the compound is rather non-hemolytic.

Though there is now great interest in AMPs, none of the AMPs have passed approval for clinical use.[32] The reasons include poor *in vivo* antimicrobial activity, salt instability, proteolysis, high cost, high hemolysis and toxicity, *etc*.[32] Various strategies have been investigated to increase the potency of natural AMPs: design of hybrid AMPs through combination of active regions from different natural AMPs[217-218]; mutation of the sequence, amino acid substitution or peptide truncation to screen improved AMPs[219]; cyclization or use of synthetic peptide analogues (such as non-natural β- and γ-amino acids) to improve peptide stability[220]; increase of the concentration of active peptide motif in a molecule with multivalent AMPs, such as dendrimeric, rather than linear peptides[221]; *etc*. Some impressive MICs have been achieved but the selective toxicity of these AMPs and their synthetic analogues are usually not high (*e.g.* Series 4 and 5 in Table 5.2, have selectivities of less than 100). Further, solid phase synthesis is more suitable for small scale synthesis as it involves high cost.

Synthetic antimicrobial polymers which can be produced in large scale and at low cost have received much attention in recent years.[37, 114] Although various synthetic polymers have been designed for antimicrobial applications, only a few of them show potent antimicrobial activity together with non-hemolysis.[77] Most of them mimic the natural AMP structures that typically segregate into distinct cationic and hydrophobic domains or phases.[37, 77] While the antimicrobial activity can be improved significantly by optimizing the cationic/hydrophobic ratio, the hemolysis or cytotoxicity generally is also increased by this optimization. Various optimized synthetic polymers have been shown to have impressive MICs but all are rather hemolytic (#5E - #6E, Table 5.2).[84, 105, 107, 115, 122, 204, 209-210] Among our tested cationic peptidopolysaccharides, CS-*g*-K_{16} exhibits the best performance, with MICs in the range of 5 - 20 μg ml^{-1}, which is comparable to the best reported antimicrobial polymers (#5E - #6E, Table 5.2). However, CS-*g*-K_{16} shows extraordinarily low hemolysis – HC_{50} values that are 3 to 5 orders of magnitude larger than those of the comparison polymers – and excellent biocompatibility compared with other state-of-the-art antimicrobial polymers.

Unlike bacterial and fungal cells, the outer leaflet of mammalian cell membrane consists of zwitterionic phospholipids and cholesterol, which makes the net charge neutral.[47] The absence in mammalian cell membranes of negatively charged targets for cationic antimicrobial molecules makes their hydrophobicity the determinant of their efficacy for membrane disruption and permeabilization.[104, 106, 115, 204] The chitosan backbone is generally thought to be hydrophobic and is a well known non-toxic and low

hemolysis material.[222] So our cationic peptidopolysaccharide has a hydrophobic core flanked by cationic side branches. In the absence of anionic membrane components which would attract the molecule into close contact with the membrane, the hydrophilic branches covering the chitosan hydrophobic core makes the molecule unlikely to penetrate into the hydrophobic interior of an uncharged mammalian lipid bilayer, while the anionic charges in bacterial bilayer make such penetration more likely. Therefore, CS-*g*-K_{16} shows excellent non-hemolysis and biocompatibility as well as potent antimicrobial activity.

5.4 Conclusion

We find that chitosan-*graft*-polylysine, a cationic peptidopolysaccharide, shows outstanding broad spectrum activities against clinically significant bacteria and fungi and high selectivity for the pathogens over mammalian red blood cells. These cationic peptidopolysaccharides were prepared facilely by NCA ring-opening copolymerization of α-amino acids on chitosan. CS-*g*-K_{16} is highly effective against both Gram-negative and Gram-positive bacteria and against fungi with low MICs (5 - 20 μg ml^{-1}) but has high HC_{50} of > 100,000 μg ml^{-1}. CS-*g*-K_{16} destroys bacteria and fungi by penetrating the cell wall and disrupting the microbial membrane. Interestingly, antimicrobial activity is optimized in the CS-*g*-K_n series with grafts containing only cationic residues (lysine), without the presence of hydrophobic residues (phenylalanine). The high antimicrobial efficacy of our CS-*g*-K_n series appears to be due to the resemblance of this molecule's backbone to the pathogen cell wall peptidoglycan and the and selectivity

is due tp the lack of peptidoglycan and charge in mammalian cell membranes. The excellent broad-spectrum antimicrobial activities and high selectivity make cationic peptidopolysaccharides a promising material for in antimicrobial applications.

5.5 Acknowledgements

Part of the work presented in this chapter has been published in *Advanced Materials* (DOI: 10.1002/adma. 201104186). Kai Ye at the School of Chemical and Biomedical Engineering did the animal study in Section 5.3.4.

Chapter 6 Quaternized Chitosan Functionalized Nanomaterials with Enhanced Antimicrobial Activities

6.1 Introduction

In this chapter we want develop an antimicrobial nanomaterial-polysaccharide hybrid materials. The nanomaterial (this material is being patented at this moment, here we use the term 'nanomaterial' or NM instead) is a monolayer of hexagonal sp2-bonded carbon atoms and is known to possess many fascinating properties so as to attract much research interests exploiting its structure and properties.[223] The unique physical, chemical, electrical and mechanical properties of nanomaterial make it useful in widespread applications, such as transparent conductive films, sensors, transistors, solar cells, capacitors, material reinforcement, *etc*.[224-228] NM is rich in oxygenated functional groups, such as carboxyl, carbonyl, phenol hydroxyl and epoxide groups at its edges and basal plane, which makes NM sheets highly amenable to the chemical modifications necessary for various applications. [229]

While most current NM research has focused on electronic applications, the biomedical applications are rapidly evolving in view of the attractive antimicrobial and biocompatible properties of it.[230] They are thought to be potentially useful for biomedical applications such as nano-medicine, photo-thermal therapy, drug delivery, and bacterial inhibition.[142, 231-233] Applications in microbial inhibition are timely considering the threat of antibiotic resistant pathogens, which is vast becoming a global

health crisis. Earlier studies have reported the antimicrobial properties of NM.[140-141] Recent reports have shown that the antimicrobial efficacy of pristine NM is poor,[234-235] and that it lose its efficacy in harsh conditions such as in Luria–Bertani (LB) broth which contains 170 mM NaCl.[236] Several studies have been published on the further modification of NM to improve its antimicrobial activity.[235, 237] Silver nanoparticle (Ag NP) is a well-known biocidal agent, where the incorporation of Ag NPs with NM can be easily done to improve antimicrobial potency by release of silver ions.[134, 234, 238-242] NM based composite materials which release other antimicrobial reagents (*e.g.* quaternary phosphonium salts) were also reported.[235] However, the continued release of antimicrobial reagents is toxic to mammalian cells and poses an environmental hazard in the long term.[243] NM-polymer conjugations have been developed to improve their electrical or biological activities in various applications, such as solar cell, biosensor, drug delivery, *etc*.[244-246] However, covalently functionalized NM-polymer hybrid material with improved antimicrobial activity has not been reported to date.

Previously, we reported a novel and highly effective antimicroibal nanoporous hydrogel coating based on quarternized chitosan derivatives, specifically dimethyldecylammonium chitosan (DMDC) (Figure 6.1a).[247] Hydrogel is a kind of cross-linked polymer network which contains large amounts of water.[248] This kind of soft material has been widely used in biomedical applications.[64] However, the applications of soft hydrogel are limited by their weak mechanical strength and the requirement of a hydrated environment.

In this study, we report a nanomaterial-polymer conjugation based on NM functionalized with one kind of quarternized chitosan (QC), specifically dimethyldecylammonium chitosan (DMDC) to further improve its antimicrobial properties (Figure 6.1). QC molecules were covalently grafted onto NM nanosheets by a coupling reaction between carboxyl and amine groups, with the assistance of 1-ethyl-3-(3-dimethylaminopropyl) carbodiimide (EDC) and *N*-hydroxysuccinimide (NHS) (Figure 6.1b). The obtained nanomaterial-graft-quaternized chitosan (NM-QC) nanosheets have several advantages over pristine NM: Firstly, modification of NM with QC polymers improves the dispersion of the material in the aqueous environment, thus overcoming the aggregation tendencies of NM in solution;[236] Secondly, the use of cationic quaternized chitosan is aimed to increase the charge of NM, for further enhancement of its antimicrobial activity; Thirdly, chitosan derivatives are well-known biocompatible materials, which may prevent the toxicity induced by NM nanosheets.[247, 249] The antimicrobial activity of pristine NM, QC, and NM-QC was investigated for three microbes: Gram-negative bacteria *Escherichia coli* (*E. coli*), Gram-positive bacteria *Staphylococcus aureus* (*S. aureus*), and fungus *Candida. albicans* (*C. albicans*). The antimicrobial efficacy of NM is significantly enhanced after conjugation with QC covalently. A transparent coating of NM-QC nanosheets was fabricated by a Sol-Gel method on glass surface, which inhibit both Gram-negative/positive bacteria and fungi effectively.

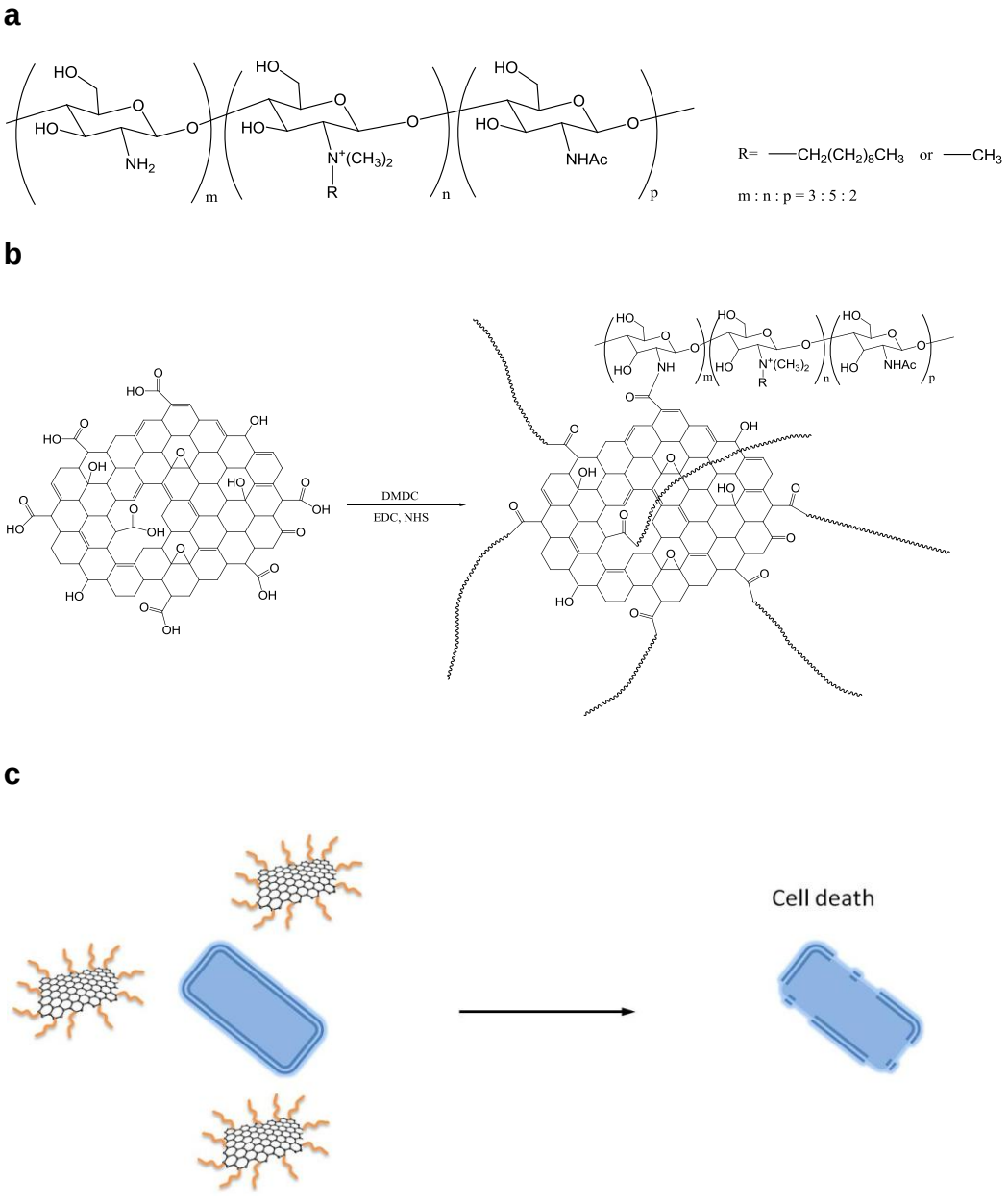

Figure 6.1 (a) Chemical structure of quaternized chitosan: dimethyldecylammonium chitosan (DMDC). (b) Chemical synthesis of NM-QC. (b) Schematic of cationic NM-QC nanosheets' action on the anionic microbial envelope, leading to cell death.

6.2 Experimental Details

Preparation of quaternized chitosan

Chitosan (1 g, 6.2 mmol) was first pre-dissolved in acetic acid (1%, 100 ml), then decanal (0.97 g, 6.2 mmol) was added and stirred for 1 h at room temperature. After this, the pH was increased to 4.5 followed by addition of sodium borohydride (9.3 mmol) and further stirring of the mixture for 1.5 h. The pH was then further increased to 10 by adding NaOH solution (1 M). The white precipitates that formed were filtered and washed with distilled water until neutrality. Soxhlet extraction using ethanol and diethyl ether mixture was performed to remove unreacted reactants. The resulting *N*-decyl chitosan (1 g, 6.2 mmol) was then added to NMP (50 ml) and NaOH solution (1.5M, 15 ml). After 30 min of stirring at 50 ℃, methylation was performed as follows: sodium iodide (1.08 g, 7.2 mmol) and methyl iodide (11.2 g, 78.7 mmol) were added to the chitosan/NMP/NaOH mixture and then reacted for 24 h at 50 ℃. The solution was then suction filtered. After dipping the filtrate into acetone (400ml), the precipitate obtained was filtered and then dried under vacuum to yield the product.

Preparation and characterization of NM-QC nanosheets.

NM nanosheets were chemical exfoliated from natural graphite powder by a modified Hummers method.[250-251] Briefly, NM-QC was prepared by a coupling reaction using 1-ethyl-3-(3-dimethylaminopropyl) carbodiimide hydrochloride (EDC, Sigma) and *N*-hydroxysuccinimide (NHS) described in Figure 6.1.[252] After reaction, the suspension was filtered with polyamide membrane (0.2 μm, Sartorius) and thoroughly washed using deionized water to remove the unreacted regents. The solid residue was dispersed

in water, dialyzed using a cellulose membrane (Sigma, M. W. 10334) for 3 days and then freeze dried. The synthesis of NM-QC was characterized by Fourier transform infrared spectrum (FTIR, Nicolet 5700) and thermogravimetric analysis (TGA, Netzsch STA 409).

Preparation of microbial cells

The following bacteria and fungi strains used were obtained from *American* Type Culture Collection: *Escherichia coli* (ATCC8739), *Staphylococcus aureus* (ATCC6538), *Candida albicans* (ATCC10231). The preparation of bacteria/fungus was described in Chapter 3, section 3.1.

Antimicrobial assay for NM and NM-QC dispersions.

Bacteria or fungi cells were centrifuged and the pellet was re-suspended in water and diluted to the desired concentration. 10^8 CFU cells were inoculated into 1 ml NM/NM-QC dispersions, then incubated at 37 ℃ (28 ℃ for fungi) under shaking conditions at 200 rpm for a desired time. The cell numbers were determined by the plate colony counting method. Briefly, 100 μl of 10-fold dilution of NM/NM-QC treated bacterial suspension were pipetted into a 10 cm culture plate and spread with 45 - 50 ℃ LB agar (YM agar for fungi). The plates were incubated at 37 ℃ (28 ℃ for fungi) overnight for colony formation. The number of colonies was counted and percentage kill determined using Equation below. This experiment was performed in triplicates.

$$\%\text{kill} = \frac{\text{Cell count of control} - \text{Survivor count on sample}}{\text{Cell count of control}} \times 100\%$$

Microbe morphology study

The morphology changes of microorganisms induced by QC, NM and NM-QC were examined with Field Emission Scanning Electron Microscopy (FESEM, JEOL JSM-6701F). Microbe cells were incubated with QC, NM and NM-QC at 100 μg ml^{-1} for 1 h. Other experimental details can be found in Chapter 3, section 3.4.5.

Hemolysis assay

The hemolytic activities of NM and NM-QC were determined following the description in Chapter 3, section 3.3.1.

Oxidative stress assay

Oxidation stress was determined by Ellman's assay which quantifies the loss of thiol groups in glutathione (GSH) after contact with NM or GQ-QC. 225 μl NM or NM-QC dispersions in bicarbonate buffer (50 mM, pH 8.6) was added into equal volumes of GSH bicarbonate buffer solution (0.8 mM) in a cell cultrue plate. The plate was then incubated in dark at room temperature with shaking at 120 rpm for 120 min. After incubation, 785 μl Tris-HCl (50 mM) and 15 μl 5,5-Dithio-bis-2-nitrobenzoic acid (Ellman's reagent, Sigma-Aldrich) were added to each well. After filtration with a 0.45 μm polyethersulfone syringe filter, 200 μl aliquots of filtered solutions from each well were transferred to a new cell culture plate. The absorbance at 412 nm was measured with a microplate spectrophotometer (BIO-RAD, US). Negative control was 0.4 mM GSH solution without NM or NM-QC, positive control was 1 mM H_2O_2 was used as a positive control. The GSH loss can be calculated by equation as follows: GSH loss % = (absorbance of negative control – absorbance of sample)/absorbance of negative

control × 100.

Zeta potential measurement

Zeta potential was determined with an electrokinetic analyzer (Antor Parr), using KCl solution (0.1 mM, pH 5.5) as background electrolyte and PMMA as reference plate.

Preparation of NM-QC coating

NM and NM-QC coating was prepared by Sol-Gel method.[253] Typically, sols were prepared by adding 0.1 ml tetramethyl orthosilicate (TMOS, Sigma-Aldrich) to a 5-mL vial containing a mixture of ethanol (1 ml) and NM/NM-QC suspension in water (1 ml). The vials were capped and the resulting sols were left at room temperature for one day before being used for the coating fabrication. Glass cover slips were cleaned by bath ultrasonication first in NaOH (1M) and then in acetone each for 30 min. After drying under a nitrogen flow, the slips surface were activated with oxygen plasma (March PX-500, Germany) at a radio frequency of 13.56 MHz, gas flow rate of 100 sccm, pressure of 500 mTorr and power of 200 W for 10 minutes. A few drops of NM or NM-QC/TMOS Sols were then deposited on the plasma activated cover slips by spin-coating at 6000 rpm for 2 minutes. The coated thin sol films were gelled at 70 ℃ in an air oven overnight, followed by curing at 130 ℃ for 2 h under a controlled argon gas flow in a tube furnace (2 ℃/min heating and 5 ℃/min cooling rates).

Antimicrobial assay for NM and NM-QC coating

The NM/NM-QC coated glass cover slips were placed in 24-well plates and sterilized under UV light for 1 day. 10 μl bacterial inoculums were pipetted onto the coating surface, then another coated slip was placed over it make the inoculums spread and

contact uniformly between the coatings. Pristine glass slips were used as a control. The inoculated slips were incubated at 37 ℃ (28 ℃ for fungi) and a relative humidity of not less than 90% for 1 h. After incubation, 1 ml of neutralizing broth was added to each well to recover the microbe survivors. A series of 10-fold diluted samples was prepared and plated out in LB agar (YM agar for fungi). The plates were incubated at 37 ℃ (28 ℃ for fungi) overnight and the colony forming units counted. The log reduction of cells was calculated as below equation:

Log reduction = Log (cell count of control) – Log (survivor count on sample)

6.3 Results and Discussion

6.3.1 Characterization of NM-QC nanosheets

NM nanosheets prepared by the exfoliation of oxidized graphite are known to contain abundant oxidized functional groups such as carboxyl, carbonyl, phenol hydroxyl, epoxide groups, etc.[250-251] (Figure 6.1b, left). The carboxyl groups on NM can be activated by carbodiimide and reacted with primary amine groups resulting in amide bond.[252] Quaternized chitosan (specifically dimethyldecylammonium-chitosan) was synthesized as described in Chapter 4, briefly chitosan (82% deacetylated) was *N*-alkylated with decanal and following methylated with methyl iodide.[247] The synthesized QC has a quaternization degree of 56% and molecular weight of 38 kDa. QC was then grafted onto NM nanosheets by 1-ethyl-3-(3-dimethylaminopropyl) carbodiimide (EDC) initiated coupling reaction, in the presence of

N-hydroxysuccinimide to stabilize the active intermediate (Figure 6.1b).[254] Figure 6.2 shows the FITR spectra of pristine NM, QC and NM-QC: The peaks at around 1720 cm^{-1} and 1632 cm^{-1} indicate the C=O stretching of carbonyl and quinone bonds of NM (Figure 6.2a), however, these two peaks were overlapped by the amide I peak (1653 cm^{-1}) of QC in NM-QC (Figure 6.2c).

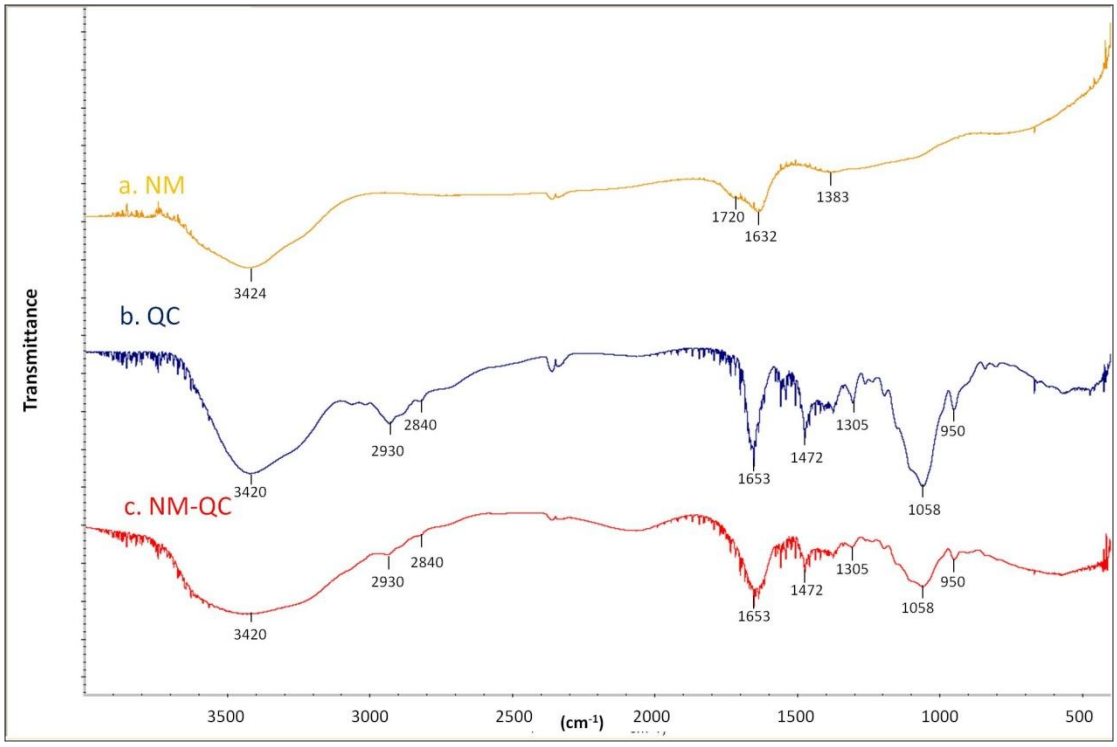

Figure 6.2 FTIR spectra of (a) NM, (b) quaternized chitosan (QC) and (c) NM-QC.

A series of NM-QC derivatives was synthesized by varying the reaction ratio of NM and QC from 1:1 to 1:10 (w/w). TGA analysis was carried out between 50 to 600 °C at a heating rate of 10 °C min^{-1} under protection of nitrogen (Figure 6.3). In Figure 6.3, the curves reveal the thermal stability of NM, NM-QC and QC. The

pristine NM loss 4% of its weight below 100 °C, which is due to the evaporation of absorbed water in its π-stacked strucutre.[255] The major weight loss of pristine NM was observed at 165 – 215 °C, which is likely to be carbon dioxide gas species from the pyrolysis of laible oxygen-cotaining groups.[256] In contrast, QC has less than 2% weight loss below 100 °C. QC loss 35% of its weight between 210 – 250 °C, which is due to the cleavage of substituent groups and decomposition of glucopyranose rings.[257] The weight loss curve of NM-QC has two stages which attribute to the major losses of NM (165 – 195 °C) and QC (210 – 250 °C) respectively. The composition of NM/QC ratio was determined and summarized in Table 6.1. The TGA determined NM/QC ratios were lower than the initial reactant ratio. Between the initial reactant ratio of 1:1 to 1:5, around 50% of QC molecules was successfully grafted onto NM nanosheets. However, only 22% of QC was grafted onto NM nanosheets at the reactant ratio of 1:10, that may attribute to the saturation of carboxyl groups on NM nanosheets. The following antimicrobial activity determination also shows similar results.

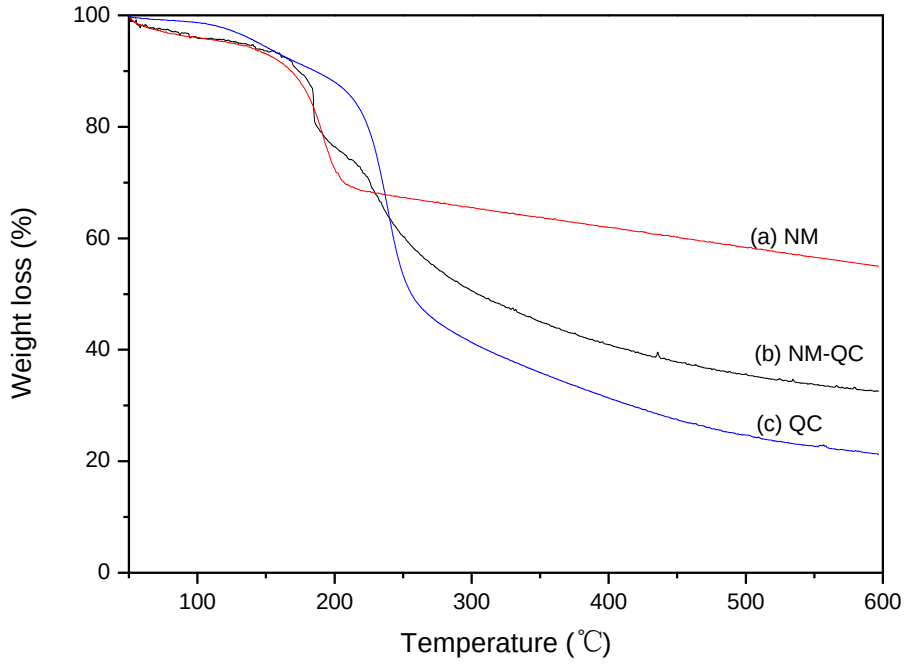

Figure 6.3 TGA curves of (a) NM, (b) NM-QC (1:5) and (c) QC at a heating rate of 10 ˚C per min under nitrogen protection.

Table 6.1 Characteristics and biological activity of NM-QC materials.

Materials	NM/QC ratio determined by TGA	MIC_{90} (μg ml^{-1})			HC_{50} (μg ml^{-1})	Selectivity
		E. coli	*S. aureus*	*C. albicans*		
QC (DMDC)	--	125	63	31	>5000	>160
NM	--	>5000	>5000	>5000	310	<0.1
NM-QC (1:1)	1: 0.54	630	630	160	2500	16
NM-QC (1:2.5)	1: 1.04	160	160	80	5000	63
NM-QC (1:5)	1: 2.07	80	40	40	>5000	>125
NM-QC (1:10)	1: 2.20	80	40	40	>5000	>125

6.3.2 Antimicrobial activity of NM and NM-QC dispersions

There clinically significant microbes, *i.e.* Gram-negative bacteria (*E. coli* ATCC8739), Gram-positive bacteria (*S. aureus* ATCC6538), and fungus (*C. albicans* ATCC10231) were chosen as model pathogens to investigate the antimicrobial activity of NM and NM-QC nanosheets. Firstly, the microbes were inoculated into the NM/NM-QC dispersions (100 μg ml^{-1}) at a concentration of 10^8 CFU ml^{-1}, and the plate colony counting was performed after 1 h incubation. The antimicrobial inhibition of pristine NM for *E. coli*, *S. aureus* and *C. albicans* were 24.8 ± 3.7%, 34.9 ± 4.5% and 18.6 ± 2.2%, respectively (Figure 6.4a). NM nanosheets reportedly disrupt the microbes' cell membrane by their sharp edges, leading to the loss of membrane integrity and leakage of inner components, and eventually cell death.[141] The difference in susceptibility to NM can probably be explained by the difference in cell wall structures between the microbes. Gram-negative bacteria (like *E. coli*) has both an outer membrane and a cytoplasmic membrane while Gram-positive bacteria (like *S. aureus*) only has a cytoplasmic membrane that is protected by a layer of peptidoglycan layer.[215] The cytoplasmic membrane of fungi (like *C. albicans*), on the other hand, is surrounded by a thick carbohydrate cell wall, which is likely to confer more protection to the cell from the physical stress of NM nanosheets, thus explaining its low susceptibility to NM.[258]

Figure 6.4a shows the vast improvement of the antimicrobial activity of NM-QC nanosheets against the three model pathogens compared to pristine NM. NM-QC (1:1) shows significantly higher antimicrobial efficacy than NM, and its %kill for *E. coli*, *S.*

aureus and *C. albicans* are 59.3 ± 3.4%, 63.8 ± 5.8%, 73.9 ± 5.7% respectively. Further, with increasing QC content in the hybrids with NM:QC changing from 1:1 to 1:10 (w/w), the antimicrobial efficacy increases. The %kill of NM-QC (1:5) is 93.6 ± 4.2%, 97.8 ± 1.8% and 99.3 ± 0.4% for three microbes respectively. NM-QC (1:10) inhibited the three microbes at 93.7 ± 1.9%, 98.4 ± 1.5% and 98.2 ± 1.9% respectively, which is similar with NM-QC (1:5). TGA determination also shows NM-QC (1:5) and NM-QC (1:10) has similar NM/QC ratio of 1: 2.07 and 1: 2.20 (Table 6.1). In particular, NM-QC nanosheets showed significantly improved antifungal activity compared to NM. In our previous studies, QC derivatives have shown higher biocidal efficacy towards fungi than bacteria. This may be due to the compatibility of QC derivatives with fungal cell wall which contains significant amount of chitin.[247] As *C. albicans* exhibits low susceptibility to pristine NM, the improved antifungal activity of NM-QC is presumably due to the presence of grafted QC molecules. Since inhibition activities were plateaued at a NM-QC (1:5) and NM-QC (1:10), further antimicrobial characterization studies of NM-QC nanosheets were performed use NM:QC (1:5).

a

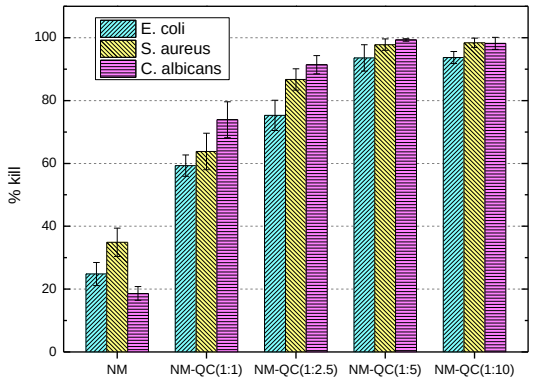

b

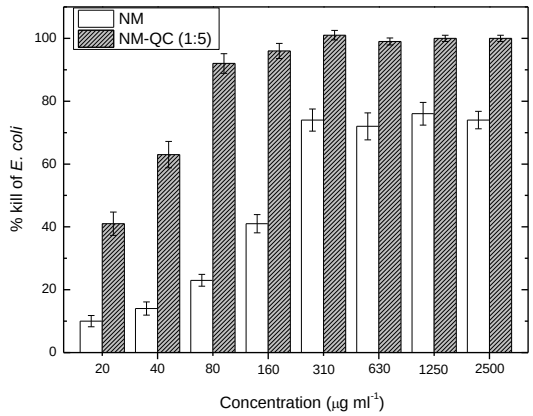

c

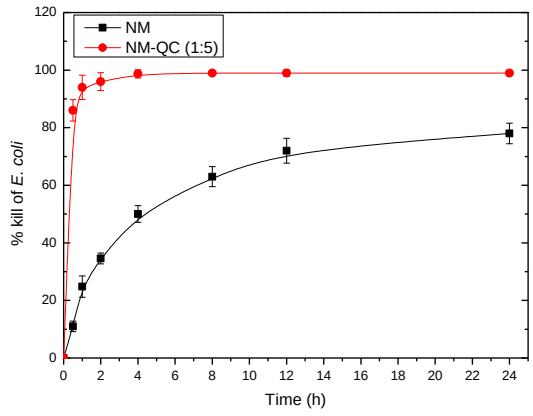

Figure 6.4 (a) Inhibitory rate of microbes after incubation with NM and NM-QC series

(100 μg ml^{-1}) for 1 h at 10^8 CFU ml^{-1}. (b) Antimicrobial efficacy of NM and NM-QC (1:5) at different concentration for *E. coli*. (c) Antimicrobial efficacy of NM and NM-QC (1:5) (100 μg ml^{-1}) at different incubation times ranging from 0.5 h to 24 h.

6.3.3 Concentration and time dependent antimicrobial activity

The concentration- and time-dependent antimicrobial activities were investigated using NM and NM-QC (1:5) with *E. coli*. Both NM and NM-QC showed increased killing efficacy of the microbe after 1 h incubation as the NM and NM-QC concentrations increased from 20 μg ml^{-1} to 2500 μg ml^{-1} (Figure 6.4b). The NM-QC (1:5) generally showed significantly higher antimicrobial activity than pristine NM. At the lower concentration range between 20 to 80 μg ml^{-1}, the percent microbe kill of NM-QC (1:5) were 3-fold higher than NM. NM-QC (1:5) showed 92.4 ± 3.1% inhibitory of *E. coli* at 80 μg ml^{-1}, while NM could only inhibit 23.7 ± 1.9% of *E. coli*. At the higher concentration of 310 μg ml^{-1} and afterwards, NM-QC (1:5) showed nearly 100% *E. coli* inhibition (99.4 ± 0.6%, 99.1 ± 0.8%, 99.3 ± 0.6%, 99.6 ± 0.3% at 310 μg ml^{-1}, 630 μg ml^{-1}, 1250 μg ml^{-1}, 2500 μg ml^{-1} respectively). However, the %kill of NM increased to only 73.6 ± 3.5% at 310 μg ml^{-1} and plateaued at around this value even up to higher concentration of 2500 μg ml^{-1}. Interestingly, the plateaued %kill of NM were at the range of 72.3 ± 4.3% to 76.8 ± 3.6%, which did not reach to 90%.

The time-dependent antimicrobial activity was also investigated by varying the

incubation time from 0.5 h to 24 h of *E. coli* with NM or NM-QC (1:5) dispersions at 100 μg ml^{-1} (Figure 6.4c). The inhibition of *E. coli* by both NM and NM-QC increased in a time-dependent manner at the initial stage of exposure. It is clear that NM-QC (1:5) shows a much faster antimicrobial activity behaviour over pristine NM. The %kill of NM-QC (1:5) reached to >90% (93.6 ± 4.2%) in 1 h, and get into the nearly 100% inhibitory of *E. coli* after 4 h. The %kill of pristine NM took 12 h to increase to 72 ± 4.3%, and the highest efficacy was 78 ± 3.6% at 24 h. Compare with pristine NM, NM-QC acts its antimicrobial activity in a more rapid and sufficient mode than pristine NM.

6.3.4 Antimicrobial activity in the presence of salts

The ability to retain the antimicrobial activity in the presence of salts will be important to broaden the use of NM nanosheets for various antimicrobial applications *e.g.* in ionic physiological environments. Antimicrobial peptides, for example, are strongly disadvantaged by their salt-intolerant behavior, which impedes their development as coating agents.[259] Although the hydrophilic oxygenated groups on the NM nanosheets can help with dispersion stability in water, the Van der Waals interactions that exist among the sheets can still readily induce aggregation.[260] In the presence of counter ions such as Na^+, which are capable of binding to the anionic oxygenated groups and neutralizing it, then aggregation can occur. In a 150 mM NaCl solution, NM nanosheets are observed to aggregate and precipitate in 1 h (Figure 6.5a).

The addition of NaCl from 0 mM to 150 mM resulted in the gradual aggregation of NM, followed by the loss of antimicrobial activity (Figure 6.5b). This aggregation tendency was not observed for NM-QC (1:5) nanosheets which are rich in water-soluble quaternized chitosan side-chains, thereby stabilising the NM nanosheets in solution which is important to retain antimicrobial activity, even in the presence of NaCl up to 150 mM.

a

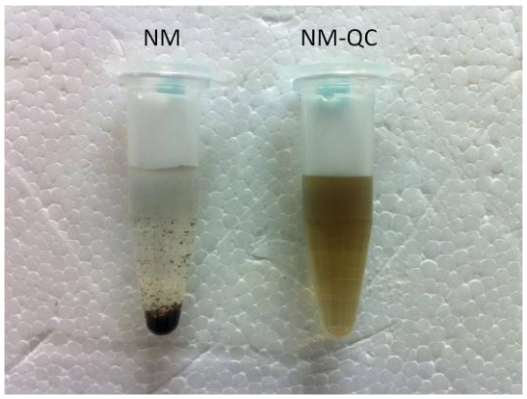

b

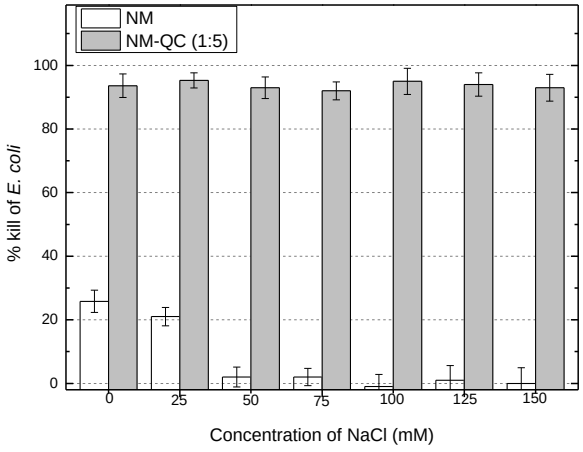

Figure 6.5 (a) Photographs of NM and NM-QC (1:5) (100 μg ml^{-1}) dispersions in presence of NaCl (150 mM) for 1 h. (b) Antimcirobial efficacy of NM and NM-QC (1:5) (100 μg ml^{-1}) in the presence of NaCl for 1 h.

6.3.5 Destruction of microbial membrane

The morphological changes of *E. coli* cells before and after contact with QC, NM and NM-QC (1:5) solution/dispersion (100 μg ml^{-1}) were investigated by field emission scanning electron microscopy (FESEM) (Figure 6.6). QC is a cationic polymer which will achieve antimicrobial activity by disrupting the microbe membrane. QC-treated *E. coli* cells shows wrinkled cell surfaces compared to the smooth surfaces of untreated control cells (Figure 6.6b). NM-treated *E. coli* cells, on the other hand, show a different morphology: physical defects are found especially at the two ends of the cell (arrows in Figure 6.6c), which is likely due to the physical disruption incurred by the sharp nanosheets. NM-QC (1:5) treated cells shows even more drastic morphological changes compared to QC and NM individually. Distinct damages (or holes) on the cells can be clearly seen, where loss of cell integrity is likely to have occurred (arrows in Figure 6.6d).

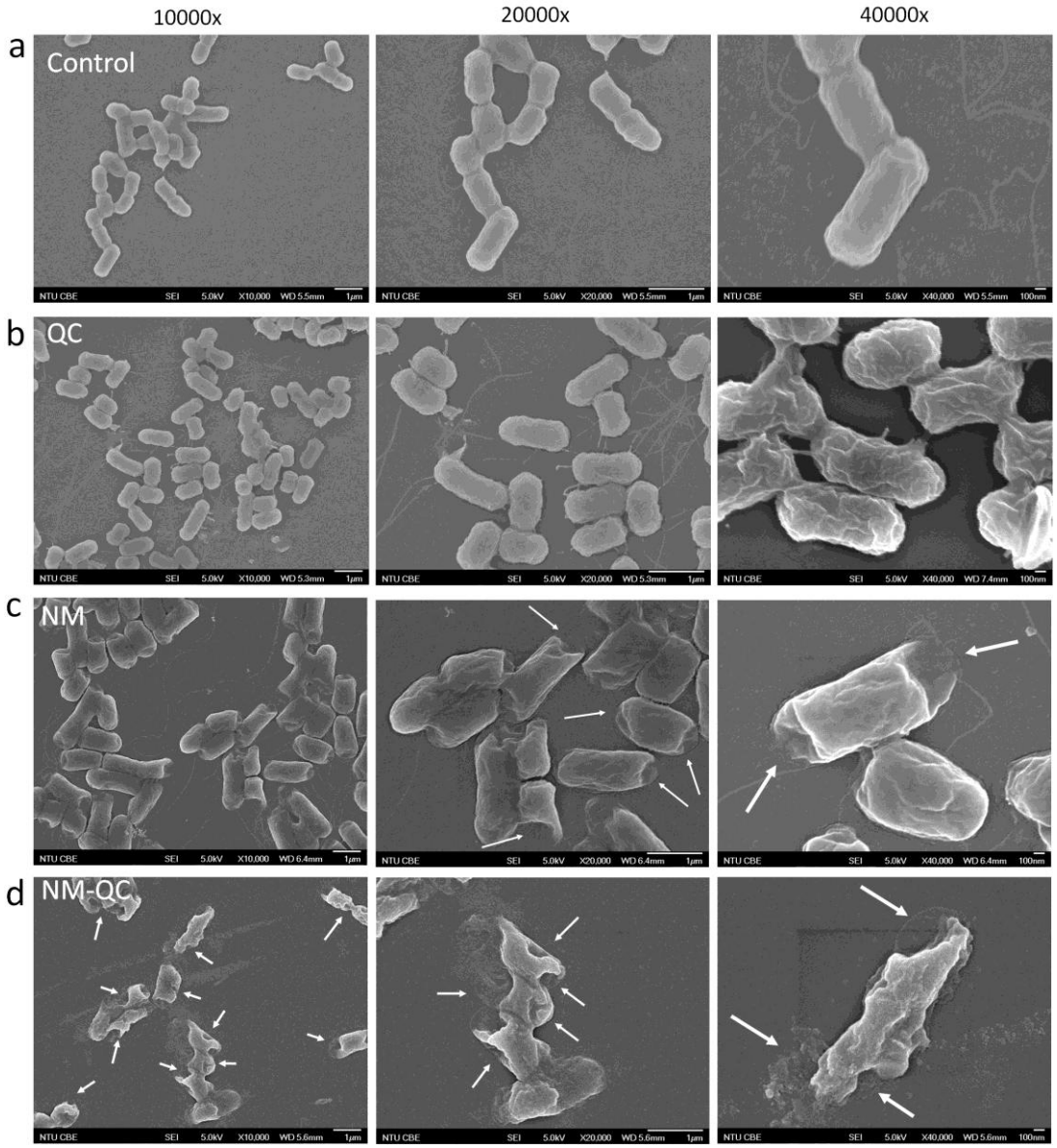

Figure 6.6 Morphology changes of *E. coli* (a) control, treated with (b) quaternized chitosan, (c) NM and (d) NM-QC (1:5) at 100 μg ml^{-1} for 1 h.

6.3.6 Cationic charge and oxidative stress

The charges of NM and NM-QC nanosheets were determined by measuring the zeta potential of them (Figure 6.7a). As expected, the negatively charged groups on the NM nanosheets rendered them a negative potential of -27.9 ±2.9 mV. Grafting of QC on the

NM nanosheets causes the zeta potential to change to positive values. The zeta potential of NM-QC increased from 3.5 ±1.9 mV to 12.6 ±2.3 mV with increasing NM/QC ratio. This also corroborates that the NM-QC nanosheets comprise the cationic polymer which is covalently grafted onto the NM.

In previous studies, oxidative stress was considered as one of the factors which led the antimicrobial activity of NM-based materials.[140] Oxidative stress has also been determined by Ellman's assay which quantify the loss of thiol groups on GSH after contact with NM and NM-QC (1:5) nanosheets.[261] Although the oxidation activity of NM and NM-QC (1:5) both increased following their concentration increases (Figure 6.7b), NM demonstrated higher oxidization ability than NM-QC (1:5) at the same concentration.

As the oxidization ability of NM-QC (1:5) is lower than pristine NM, the improved antimicrobial activity of NM-QC (1:5) should not be attributed to the oxidization stress. The increased charge state of NM-QC (1:5) may play a more important role in the enhanced antimicrobial activity. The microbial membranes are composed of anionic molecules such as lipopolisaccharides, lipoteichoic acids, anionic phospholipids, *etc*. The sharp NM nanosheets are harmful to microbes, only when they collide together occasionally in suspension. Moreover, their anionic microbe surface charge results in electrostatic repulsion of NM nanosheets. Unlike pristine NM, the grafting of cationic QC endows NM-QC nanosheets with positive charge, which should attract suspended NM-QC nanosheets into physical contact with anionic microbe surfaces. This is a plausible account of the observed superior antimicrobial activity of NM-QC with

respect to GO (Figure 6.4c).

a

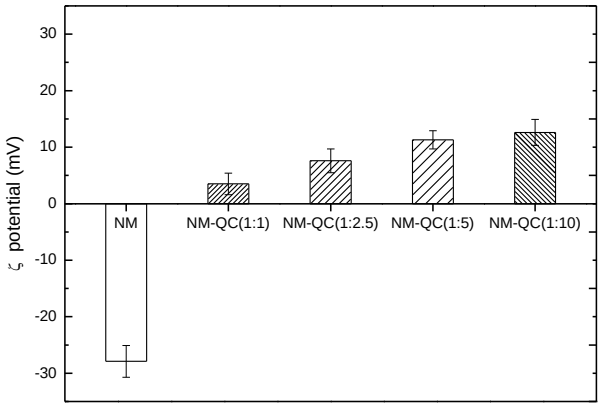

b

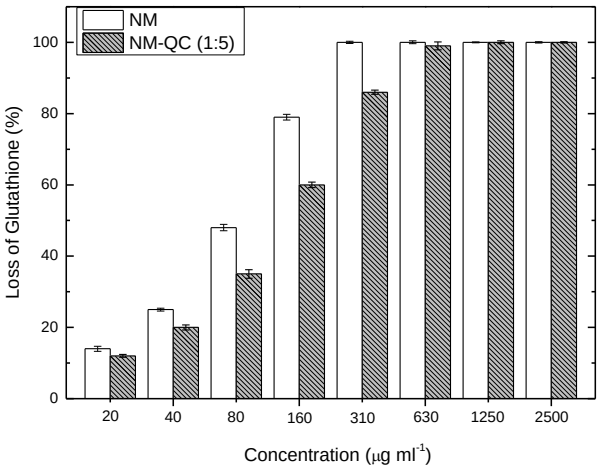

Figure 6.7 (a) Zeta potential of NM and NM-QC series. (b) Oxidation of glutathione by NM and NM-QC.

6.3.7 Hemolytic activity of human red blood cells

Hemolytic activity of human red blood cells (RBCs) is an important criteria in the biocompatibility determination of antimicrobial materials.[204] The significant hemolytic activity of NM has been reported, which limits its applications in the biomedical area.[262] The concentration of NM and NM-QC required to incur 50% hemolysis of RBCs (HC_{50}) was measured (Table 6.1). The HC_{50} of pristine NM is 310 μg ml^{-1}, while the NM-QC series generally showed a much higher HC_{50}. NM-QC (1:1) and (1:2.5) has their HC_{50} at 2,500 and 5,000 μg ml^{-1} respectively, the higher QC ratio of (1:5) and (1:10) show larger HC_{50} >5,000 μg ml^{-1}. Compared with their minimum inhibitory concentration which inhibit more than 90% microbe growth (MIC_{90}), the selectivity of the desired NM-QC (1:5) nanoflakes is calculated to be >125. The sharp edges of pristine NM are expected to be harmful to mammalian cells, leading to the lysis of 50% of RBCs at the concentration of 310 μg ml^{-1}. Our previous results demonstrate that quaternized chitosan derivatives are biocompatible materials having low hemolytic activity; they disrupt the microbial membrane but are non-toxic to mammalian cells.[247] The presence of QC molecules surrounding NM-QC nanosheets may function as a biocompatible protection layer which lowers the toxicity to mammalian cells. Thus NM-QC shows a much improved HC_{50} compared with pristine NM.

6.3.8 Preparation and antimicrobial activity of NM-QC coating

NM-QC nanosheets were fabricated as a transparent nanoporous antimicrobial surface coating by a Sol-Gel method (Figure 6.8).[253] NM-QC Sol was spin-coated on an oxygen plasma treated glass surface, where the coating was formed by subsequent gelation. Antimicrobial assay on this coating was performed on NM and NM-QC coating, and the plasma-treated glass slip was used as a control. The log reduction of three microbes was recorded by colony plate counting. NM only shows a log reduction of 0.18 ± 0.01 to 0.30 ± 0.04, while NM-QC shows a much higher reduction; the log reductions of NM-QC (1:5) and NM-QC (1:10) above 2 indicates inhibitory values which are larger than 99% (Figure 6.8e).

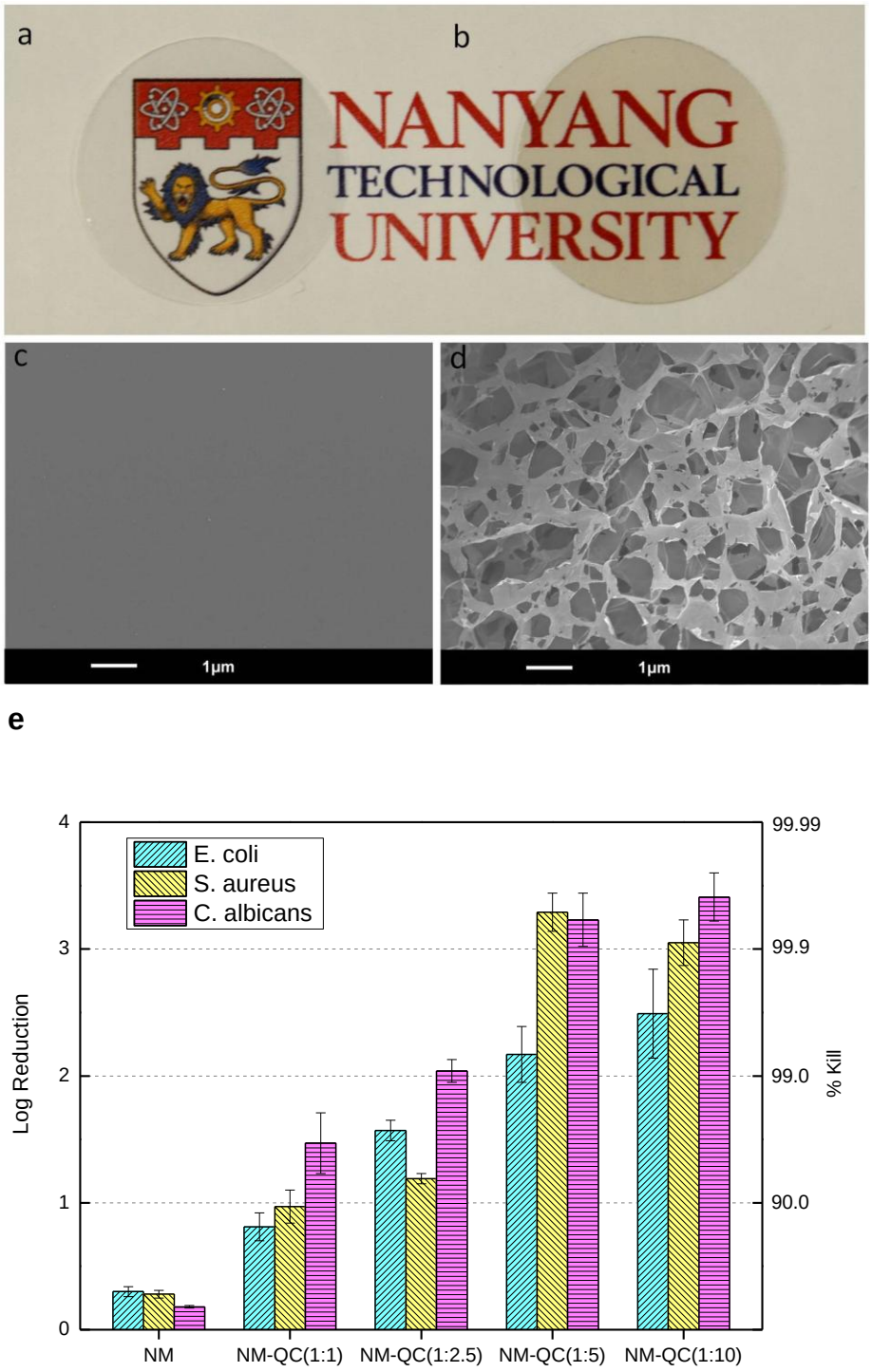

Figure 6.8 Photographs of (a) pristine and (b) transparent NM-QC (1:5) coating glass slip; SEM images of (c) pristine and (d) NM-QC coated glass slip; (c) Log reduction of 3 bacteria and fungi after contacted with the NM and NM-QC coatings.

6.4 Conclusions

The carboxyl groups on NM nanosheets render it anionic, which is the same charge state as microbial membranes. The occurrence of electrostatic repulsive forces between NM and microbial cells can therefore impede the rate at which they make contact, which explains the more gradual manner NM damages membranes. Quaternized chitosan which are cationic polysaccharides, changes the charge state of NM from anionic to cationic, when functionalized to the NM nanosheets. In cationic NM-QC dispersions, the cationic nanosheets are electrostatically drawn to the anionic microbial cells, where both the cationic charge and sharp edges of the NM-QC nanosheets synergistically disrupt the anionic microbial membranes rapidly and efficiently. NM-QC therefore shows enhanced antimicrobial activity over pristine NM. The increase in charge state of NM-QC did not compromise biocompatibility properties of the nanosheets, as indicated by an improved HC_{50} for the NM-QC series compared to NM alone. A coating of NM-QC is efficiently antimicrobial and transparent, which opens the way for the use of NM-QC nanosheets for antimicrobial applications in biomedical and other fields.

6.5 Acknowledgements

Wang Jing at the School of Chemical and Biomedical Engineering helped in the preparation of NM nanosheets.

Chapter 7 Conclusion and Directions for Future Research

7.1 Conclusion

We have developed a nanoporous antimicrobial hydrogel based on polysaccharide derivatives, specifically quaternized ammonium-chitosan-*graft*-poly(*e*thylene glycol) *m*ethacrylate (qC-*g*-EM), and poly(ethylene glycol) diacrylate. The optimized formulation (DMDC-Q-*g*-EM) shows excellent broad-spectrum antimicrobial efficacy of more than 99% kill against both Gram-negative and Gram-positive bacteria, and fungus. Further, a new killing mechanism which is active in this new class of highly hydrated cationic antimicrobial hydrogels has been proposed and tested experimentally. This polycationic hydrogel attract parts of the anionic microbial membrane into its internal nanopores, like an “anion sponge”, leading to microbial membrane disruption. We have also demonstrated a thin uniform adherent coating of the hydrogel by simple UV immobilization. Animal study shows that DMDC-Q-*g*-EM hydrogel coating is biocompatible with rabbit conjunctiva and has no toxicity to the epithelial cells or the underlying stroma. Such antimicrobial and biocompatible coating has a promising potential in reducing the risk of infections related with biomedical devices and implants.

Peptidopolysaccharides, a novel class of antimicrobial polymers, which possess mimicry of the bacterial membrane component peptidoglycan, were designed, synthesized and tested and were shown to have excellent broad-spectrum antimicrobial

activity and high selectivity. The optimum tested peptidopolysaccharide, specifically a copolymer of chitosan and polylysine (CS-*g*-K_{16}), is effective against clinically significant Gram-negative and Gram-positive bacteria and fungi with low minimum inhibitory concentrations (5 - 20 μg ml^{-1}), high selectivity (> 5,000 - 10,000) and low toxicity to mammalian cells. Our preliminary immune response study shows low/non secretion of tumor necrosis factor-α by cultured macrophages when challenged with CS-*g*-K_{16}, suggesting that the compound stimulates little or no inflammatory response. The cationic charge of our peptidopolysaccharides causes them to target the anionic microbial cell envelope, and their structural affinity with microbial cell wall constituents promotes their penetration of the microbe cell wall to reach the cytoplasmic membrane, where the peptidopolysaccharide acts as an effective membrane disruptor. The combination of these features (*i.e.* cationic charge and petidoglycan mimicry) results in excellent antimicrobial activity and selectivity. This class of antimicrobial peptidopolysaccharides reveals a new direction for the design of antimicrobial molecules.

Nanomaterial (NM) was grafted with quaternized chitosan (QC) by a facile single-step carbodiimide coupling reaction. The NM-QC hybrid shows broad-spectrum antimicrobial activity for Gram-negative and Gram-positive bacteria, and fungi. The antimicrobial efficacy of NM was improved significantly by conjugation of QC. FESEM analysis shows that NM-QC induces more significant microbial cell wall/membrane damage than the individual constitutent, where obvious holes can be observed with NM-QC treated cells. QC appeared to have only a membrane-wrinkling

effect while NM incurred only relatively minor morphology changes. The synergistic combination of NM and QC confers the NM-QC unique properties: it comprises a condensed carrier of quaternized chitosan, where the cationic charge of the QC groups is responsible for electrostatic-driven contact with the anionic microbial cell envelope and the sharp edges of the NM would further enhance membrane disruption. Importantly, the chitosan groups confer the nanomaterials good biocompatibility properties, as demonstrated by the reduced hemolytic activity. Furthermore, NM-QC was deposited on the surface of glass slips forming a transparent nanoporous coating with antimicrobial activity. Such transparent antimicrobial coating should have good prospects in applications for preventing microorganisms colonization on healthcare and household devices.

7.2 Directions for Future Research

7.2.1 Polysaccharides based antimicrobial materials

The bacterial cell wall and membrane are rich in polysaccharides components, such as LPS and peptidoglycan. The microbial cytoplasmic membrane is surrounded by cell wall, a barrier which must be penetrated by all effective antimicrobial molecules. However, the structural affinity of antimicrobial molecules with the microbial cell wall has generally not been considered in previous designs of cationic antimicrobial polymers. Peptidoglycan is a common component of the bacteria cell wall, a feature absent from animal cells, so that peptidoglycan-mimicry may be exploited to achieve

high antimicrobial activity with low hemolytic activity. Our quaternized ammonium chitosan derivatives and peptidopolysaccharides both show excellent broad-spectrum and biocompatibility, which indicate polysaccharides such as chitosan is a good backbone for antimicrobial applications. Further modifications of chitosan by grafting with other amino acids such as arginine or other positive charged analogues, should have a probability of success on antimicrobial materials. On the other side, there are other kinds of polysaccharides (*e.g.*, dextran, starches, cellulose, pectins) which may be adopted for antimicrobial applications.

7.2.2 Nanoporous antimicrobial coatings

Unlike the conventional antimicrobial coating formed by immobilization of antimicrobial molecules, nanoporous hydrogel coating reveals a new strategy for the design of contact-active antimicrobial surfaces. The conventional theories believe antimicrobial molecules act their efficacy by extending from the immobilized site and then “inserting” into the bacterial envelope, therefore long spacer are needed based on this understanding. However, our cationic nanoporous hydrogel coating suggested a different mechanism: the immobilized and cross-linked cationic hydrogel disrupt the anionic bacterial membrane components by “suctioning mode” like a sponge. Therefore, other coating can be proposed by this theory using membrane disrupting molecules and porous structures.

7.2.3 Hybrid antimicrobial materials

More multi-functional hybrid antimicrobial materials have been developed recently. Our polysaccharide-nanomaterial hybrid shows an enhanced antimicrobial activity. The unique properties of nanomaterials (*e.g.*, super specific area, strong mechanical modulus, electronic properties) may promote the activity or broaden the application areas of antimicrobial molecules. Therefore polymer/peptide-nanomaterial hybrid antimicrobial materials have vast prospects for further investigation. Besides their antimicrobial activity, it is critical to evaluate the biocompatibility of these nanomaterial based hybrid materials. Their cytotoxicity to mammalian cells must be investigated before their application in biomedical devices.

References

1. Young, D.; Hussell, T.; Dougan, G., Chronic bacterial infections: living with unwanted guests. *Nature Immunology* **2002,** *3* (11), 1026-1032.

2. von Nussbaum, F.; Brands, M.; Hinzen, B.; Weigand, S.; Habich, D., Antibacterial natural products in medicinal chemistry - Exodus or revival? *Angewandte Chemie-International Edition* **2006,** *45* (31), 5072-5129.

3. Payne, D. J.; Gwynn, M. N.; Holmes, D. J.; Pompliano, D. L., Drugs for bad bugs: confronting the challenges of antibacterial discovery. *Nature Reviews Drug Discovery* **2007,** *6* (1), 29-40.

4. Neu, H. C., The crisis in antibiotic-resistance. *Science* **1992,** *257* (5073), 1064-1073.

5. Klevens, R. M.; Edwards, J. R.; Richards, C. L.; Horan, T. C.; Gaynes, R. P.; Pollock, D. A.; Cardo, D. M., Estimating health care-associated infections and deaths in US hospitals, 2002. *Public Health Rep.* **2007,** *122* (2), 160-166.

6. Klevens, R. M.; Morrison, M. A.; Nadle, J.; Petit, S.; Gershman, K.; Ray, S.; Harrison, L. H.; Lynfield, R.; Dumyati, G.; Townes, J. M.; Craig, A. S.; Zell, E. R.; Fosheim, G. E.; McDougal, L. K.; Carey, R. B.; Fridkin, S. K.; Investigators, A. B. M., Invasive methicillin-resistant Staphylococcus aureus infections in the United States. *Jama-Journal of the American Medical Association* **2007,** *298* (15), 1763-1771.

7. Levy, S. B.; Marshall, B., Antibacterial resistance worldwide: causes, challenges and responses. *Nature Medicine* **2004,** *10* (12), S122-S129.

8. Gordon, Y. J.; Romanowski, E. G.; McDermott, A. M., A review of antimicrobial peptides and their therapeutic potential as anti-infective drugs. *Current Eye Research* **2005,** *30* (7), 505-515.

9. Boman, H. G., Antibacterial peptides - key components needed in immunity. *Cell* **1991,** *65* (2), 205-207.

10. Marr, A. K.; Gooderham, W. J.; Hancock, R. E. W., Antibacterial peptides for therapeutic use: obstacles and realistic outlook. *Current Opinion in Pharmacology* **2006,** *6* (5), 468-472.

11. Zasloff, M., Antimicrobial peptides of multicellular organisms. *Nature* **2002,** *415* (6870), 389-395.

12. Breithaupt, H., The new antibiotics. *Nature Biotechnology* **1999,** *17* (12), 1165-1169.

13. Brogden, K. A., Antimicrobial peptides: Pore formers or metabolic inhibitors in bacteria? *Nature Reviews Microbiology* **2005,** *3* (3), 238-250.

14. Li, P.; Li, X.; Saravanan, R.; Li, C. M.; Leong, S. S. J., Antimicrobial macromolecules: synthesis methods and future applications. *RSC Advances* **2012**.

15. Gristina, A. G., Biomaterial-centered infection: microbial adhesion versus tissue integration. *Science* **1987,** *237* (4822), 1588-1595.

16. Darouiche, R. O., Device-associated infections: A macroproblem that starts with microadherence. *Clinical Infectious Diseases* **2001,** *33* (9), 1567-1572.

17. von Eiff, C.; Jansen, B.; Kohnen, W.; Becker, K., Infections associated with medical devices - Pathogenesis, management and prophylaxis. *Drugs* **2005,** *65* (2), 179-214.

18. Hetrick, E. M.; Schoenfisch, M. H., Reducing implant-related infections: active release strategies. *Chemical Society Reviews* **2006,** *35* (9), 780-789.

19. Huang, J. Y.; Murata, H.; Koepsel, R. R.; Russell, A. J.; Matyjaszewski, K., Antibacterial polypropylene via surface-initiated atom transfer radical polymerization. *Biomacromolecules* **2007,** *8* (5), 1396-1399.

20. Barr, J. T., Contact Lens Spectrum's Annual Report 2004. *Contact Lens Spectrum* **2005** *January 2005* (January 2005).

21. Fleiszig, S. M. J.; Evans, D. J., Pathogenesis of Contact Lens-Associated Microbial Keratitis. *Optometry and Vision Science* **2010,** *87* (4), 225-232.

22. Erie, J. C.; Nevitt, M. P.; Hodge, D. O.; Ballard, D., Incidence of ulcerative keratitis in a defined population from 1950 through 1988. *Arch. Ophthalmol.* **1993,** *111* (12), 1665-1671.

23. Cheng, K. H.; Leung, S. L.; Hoekman, H. W.; Beekhuis, W. H.; Mulder, P. G. H.; Geerards, A. J. M.; Kijlstra, A., Incidence of contact-lens-associated microbial keratitis and its related morbidity. *Lancet* **1999,** *354* (9174), 181-185.

24. Neumaier-Ammerer, B.; Stolba, U.; Feichtinger, H.; Binder, S., Contact lens related corneal infiltrates and ulcers - a retrospective study of 134 eyes. *Spektrum Der Augenheilkunde* **2008,** *22* (5), 297-300.

25. Trautner, B. W.; Darouiche, R. O., Catheter-associated infections - Pathogenesis affects prevention. *Archives of Internal Medicine* **2004,** *164* (8), 842-850.

26. Noimark, S.; Dunnill, C. W.; Wilson, M.; Parkin, I. P., The role of surfaces in catheter-associated infections. *Chemical Society Reviews* **2009,** *38* (12), 3435-3448.

27. Darouiche, R. O., Current concepts - Treatment of infections associated with surgical implants. *N. Engl. J. Med.* **2004,** *350* (14), 1422-1429.

28. O'Grady, N. P.; Alexander, M.; Dellinger, E. P.; Gerberding, J. L.; Heard, S. O.; Maki, D. G.; Masur, H.; McCormick, R. D.; Mermel, L. A.; Pearson, M. L.; Raad, II; Randolph, A.; Weinstein, R. A., Guidelines for the prevention of intravascular catheter-related infections. *Infection Control and Hospital Epidemiology* **2002,** *23* (12), 759-769.

29. Maki, D. G.; Kluger, D. M.; Crnich, C. J., The risk of bloodstream infection in adults with different intravascular devices: A systematic review of 200 published prospective studies. *Mayo Clinic Proceedings* **2006,** *81* (9), 1159-1171.

30. Muto, C.; Herbert, C.; Harrison, E.; Edwards, J. R.; Horan, T.; Andrus, M.; Jernigan, J. A.; Kutty, P. K.; Cdc, Reduction in central line-associated bloodstream infections among patients in intensive care units - Pennsylvania, April 2001-March 2005 (Reprinted from MMWR, vol 54, pg 1013-1016, 2005). *Jama-Journal of the American Medical Association* **2006,** *295* (3), 269-270.

31. Epand, R. M.; Vogel, H. J., Diversity of antimicrobial peptides and their mechanisms of action. *Biochimica Et Biophysica Acta-Biomembranes* **1999,** *1462* (1-2), 11-28.

32. Hancock, R. E. W.; Sahl, H. G., Antimicrobial and host-defense peptides as new anti-infective therapeutic strategies. *Nature Biotechnology* **2006,** *24* (12), 1551-1557.

33. Gabriel, G. J.; Tew, G. N., Conformationally rigid proteomimetics: a case study in designing antimicrobial aryl oligomers. *Organic & Biomolecular Chemistry* **2008,** *6* (3), 417-423.

34. Lienkamp, K.; Madkour, A.; Tew, G., Antibacterial Peptidomimetics: Polymeric Synthetic Mimics of Antimicrobial Peptides. Springer Berlin Heidelberg: 2010; pp 1-32.

35. Dowhan, W., Molecular basis for membrane phospholipid diversity: Why are there so many lipids? *Annual Review of Biochemistry* **1997,** *66*, 199-232.

36. Theis, T.; Stahl, U., Antifungal proteins: targets, mechanisms and prospective applications. *Cellular and Molecular Life Sciences* **2004,** *61* (4), 437-455.

37. Gabriel, G. J.; Som, A.; Madkour, A. E.; Eren, T.; Tew, G. N., Infectious disease: Connecting innate immunity to biocidal polymers. *Materials Science & Engineering R-Reports* **2007,** *57* (1-6), 28-64.

38. Lohner, K.; Prenner, E. J., Differential scanning calorimetry and X-ray diffraction studies of the specificity of the interaction of antimicrobial peptides with membrane-mimetic systems. *Biochimica Et Biophysica Acta-Biomembranes* **1999,** *1462* (1-2), 141-156.

39. Albelo, S. T.; Domenech, C. E., Carbons from choline present in the phospholipids of Pseudomonas aeruginosa. *Fems Microbiology Letters* **1997,** *156* (2), 271-274.

40. Beveridge, T. J., Structures of gram-negative cell walls and their derived membrane vesicles. *Journal of Bacteriology* **1999,** *181* (16), 4725-4733.

41. Nikaido, H., Molecular basis of bacterial outer membrane permeability revisited. *Microbiology and Molecular Biology Reviews* **2003,** *67* (4), 593-656.

42. Fischer, W., Lipoteichoic acid and lipids in the membrane of Staphylococcus aureus. *Medical Microbiology and Immunology* **1994,** *183* (2), 61-76.

43. Xia, G. Q.; Kohler, T.; Peschel, A., The wall teichoic acid and lipoteichoic acid polymers of Staphylococcus aureus. *International Journal of Medical Microbiology* **2010,** *300* (2-3), 148-154.

44. Hone, D. M., Crowley, Richard, Shata, Mohamed Tarek. Adjuvant comprising a lipopolysaccharide antagonist. 2004.

45. Bhavsar, A. P.; Erdman, L. K.; Schertzer, J. W.; Brown, E. D., Teichoic acid is an essential polymer in Bacillus subtilis that is functionally distinct from teichuronic acid. *Journal of Bacteriology* **2004,** *186* (23), 7865-7873.

46. Shai, Y., Mode of action of membrane active antimicrobial peptides. *Biopolymers* **2002,** *66* (4), 236-248.

47. Yeaman, M. R.; Yount, N. Y., Mechanisms of antimicrobial peptide action and resistance. *Pharmacological Reviews* **2003,** *55* (1), 27-55.

48. Shai, Y., Mechanism of the binding, insertion and destabilization of phospholipid bilayer membranes by alpha-helical antimicrobial and cell non-selective

membrane-lytic peptides. *Biochimica Et Biophysica Acta-Biomembranes* **1999,** *1462* (1-2), 55-70.

49. Matsuzaki, K., Magainins as paradigm for the mode of action of pore forming polypeptides. *Biochimica Et Biophysica Acta-Reviews on Biomembranes* **1998,** *1376* (3), 391-400.

50. Oren, Z.; Shai, Y., Mode of action of linear amphipathic alpha-helical antimicrobial peptides. *Biopolymers* **1998,** *47* (6), 451-463.

51. Yang, L.; Harroun, T. A.; Weiss, T. M.; Ding, L.; Huang, H. W., Barrel-stave model or toroidal model? A case study on melittin pores. *Biophysical Journal* **2001,** *81* (3), 1475-1485.

52. Liu, D. H.; DeGrado, W. F., De novo design, synthesis, and characterization of antimicrobial beta-peptides. *Journal of the American Chemical Society* **2001,** *123* (31), 7553-7559.

53. Yan, L. Z.; Dawson, P. E., Synthesis of peptides and proteins without cysteine residues by native chemical ligation combined with desulfurization. *Journal of the American Chemical Society* **2001,** *123* (4), 526-533.

54. Engler, A. C.; Shukla, A.; Puranam, S.; Buss, H. G.; Jreige, N.; Hammond, P. T., Effects of Side Group Functionality and Molecular Weight on the Activity of Synthetic Antimicrobial Polypeptides. *Biomacromolecules* **2011,** *12* (5), 1666-1674.

55. Zhou, C. C.; Qi, X. B.; Li, P.; Chen, W. N.; Mouad, L.; Chang, M. W.; Leong, S. S. J.; Chan-Park, M. B., High Potency and Broad-Spectrum Antimicrobial Peptides Synthesized via Ring-Opening Polymerization of alpha-Aminoacid-N-carboxyanhydrides. *Biomacromolecules* **2010,** *11* (1), 60-67.

56. Doty, P.; Bradbury, J. H.; Holtzer, A. M., Polypeptides. 4. The molecular weight, configuration and association of poly-gamma-benzyl-L-glutamate in various solvents. *Journal of the American Chemical Society* **1956,** *78* (5), 947-954.

57. Lundberg, R. D.; Doty, P., Polypeptides. 17. A study of the kenetics of the primary amine-initiated polymerization of N-carboxy-anhydrides with special reference to configurational and stereochemical effects. *Journal of the American Chemical Society* **1957,** *79* (15), 3961-3972.

58. Deming, T. J., Living Polymerization of a-Amino Acid-N-Carboxyanhydrides. *J. Polym. Sci. Part A: Polym. Chem.* **2000,** *38*, 3011.

59. Deming, T. J., Synthetic polypeptides for biomedical applications. *Prog.*

Polym. Sci. **2007,** *32* (8-9), 858-875.

60. Wyrsta, M. D.; Cogen, A. L.; Deming, T. J., A parallel synthetic approach for the analysis of membrane interactive copolypeptides. *J Am Chem Soc* **2001,** *123* (51), 12919-20.

61. Deming, T. J., Facile synthesis of block copolypeptides of defined architecture. *Nature* **1997,** *390* (6658), 386-9.

62. Costa, F.; Carvalho, I. F.; Montelaro, R. C.; Gomes, P.; Martins, M. C. L., Covalent immobilization of antimicrobial peptides (AMPs) onto biomaterial surfaces. *Acta Biomaterialia* **2011,** *7* (4), 1431-1440.

63. Onaizi, S. A.; Leong, S. S. J., Tethering antimicrobial peptides: Current status and potential challenges. *Biotechnology Advances* **2011,** *29* (1), 67-74.

64. Peppas, N. A.; Hilt, J. Z.; Khademhosseini, A.; Langer, R., Hydrogels in biology and medicine: From molecular principles to bionanotechnology. *Advanced Materials* **2006,** *18* (11), 1345-1360.

65. Schierholz, J. M.; Beuth, J., Implant infections: a haven for opportunistic bacteria. *J. Hosp. Infect.* **2001,** *49* (2), 87-93.

66. Maziad, N. A.; Ei-Aal, S. E. A.; El-Kelesh, N. A., Equilibrium Adsorption Isotherm and Controlled Release of Antibiotic Drug Chloroamphenicol from Poly(2-vinyl pyridine/acrylic acid) Hydrogels Prepared by Gamma Radiation. *Journal of Applied Polymer Science* **2009,** *111* (3), 1369-1380.

67. Ayhan, F.; Ozkan, S., Gentamicin release from photopolymerized PEG diacrylate and pHEMA hydrogel discs and their in vitro antimicrobial activities. *Drug Delivery* **2007,** *14* (7), 433-439.

68. Nurkeeva, Z. S.; Khutoryanskiy, V. V.; Mun, G. A.; Sherbakova, M. V.; Ivaschenko, A. T.; Aitkhozhina, N. A., Polycomplexes of poly(acrylic acid) with streptomycin sulfate and their antibacterial activity. *European Journal of Pharmaceutics and Biopharmaceutics* **2004,** *57* (2), 245-249.

69. Zumbuehl, A.; Ferreira, L.; Kuhn, D.; Astashkina, A.; Long, L.; Yeo, Y.; Iaconis, T.; Ghannoum, M.; Fink, G. R.; Langer, R.; Kohane, D. S., Antifungal hydrogels. *Proceedings of the National Academy of Sciences of the United States of America* **2007,** *104* (32), 12994-12998.

70. Ying, L.; Sun, J. A.; Jiang, G. Q.; Jia, Z.; Ding, F. X., In vitro evaluation of lysozyme-loaded microspheres in thermosensitive methyleellulose-based hydrogel.

Chinese Journal of Chemical Engineering **2007,** *15* (4), 566-572.

71. Yu, H. J.; Xu, X. Y.; Chen, X. S.; Lu, T. C.; Zhang, P. B.; Jing, X. B., Preparation and antibacterial effects of PVA-PVP hydrogels containing silver nanoparticles. *Journal of Applied Polymer Science* **2007,** *103* (1), 125-133.

72. Punyani, S.; Narayanan, P.; Vasudevan, P.; Singh, H., Sustained release of iodine from a polymeric hydrogel device for water disinfection. *Journal of Applied Polymer Science* **2007,** *103* (5), 3334-3340.

73. Salick, D. A.; Kretsinger, J. K.; Pochan, D. J.; Schneider, J. P., Inherent antibacterial activity of a peptide-based beta-hairpin hydrogel. *J. Am. Chem. Soc.* **2007,** *129* (47), 14793-14799.

74. Gabriel, M.; Nazmi, K.; Veerman, E. C.; Amerongen, A. V. N.; Zentner, A., Preparation of LL-37-grafted titanium surfaces with bactericidal activity. *Bioconjugate Chemistry* **2006,** *17* (2), 548-550.

75. Poelstra, K. A.; Barekzi, N. A.; Rediske, A. M.; Felts, A. G.; Slunt, J. B.; Grainger, D. W., Prophylactic treatment of gram-positive and gram-negative abdominal implant infections using locally delivered polyclonal antibodies. *J. Biomed. Mater. Res.* **2002,** *60* (1), 206-215.

76. Som, A.; Vemparala, S.; Ivanov, I.; Tew, G. N., Synthetic mimics of antimicrobial peptides. *Biopolymers* **2008,** *90* (2), 83-93.

77. Tew, G. N.; Scott, R. W.; Klein, M. L.; Degrado, W. F., De Novo Design of Antimicrobial Polymers, Foldamers, and Small Molecules: From Discovery to Practical Applications. *Accounts of Chemical Research* **2010,** *43* (1), 30-39.

78. Goodman, C. M.; Choi, S.; Shandler, S.; DeGrado, W. F., Foldamers as versatile frameworks for the design and evolution of function. *Nature Chemical Biology* **2007,** *3* (5), 252-262.

79. Arnt, L.; Tew, G. N., New poly(phenyleneethynylene)s with cationic, facially amphiphilic structures. *Journal of the American Chemical Society* **2002,** *124* (26), 7664-7665.

80. Claudon, P.; Violette, A.; Lamour, K.; Decossas, M.; Fournel, S.; Heurtault, B.; Godet, J.; Mely, Y.; Jamart-Gregoire, B.; Averlant-Petit, M. C.; Briand, J. P.; Duportail, G.; Monteil, H.; Guichard, G., Consequences of Isostructural Main-Chain Modifications for the Design of Antimicrobial Foldamers: Helical Mimics of Host-Defense Peptides Based on a Heterogeneous Amide/Urea Backbone. *Angewandte Chemie-International Edition* **2010,** *49* (2), 333-336.

81. Horne, W. S.; Gellman, S. H., Foldamers with Heterogeneous Backbones. *Accounts of Chemical Research* **2008,** *41* (10), 1399-1408.

82. Schmitt, M. A.; Weisblum, B.; Gellman, S. H., Unexpected relationships between structure and function in alpha,beta-peptides: Antimicrobial foldamers with heterogeneous backbones. *Journal of the American Chemical Society* **2004,** *126* (22), 6848-6849.

83. Violette, A.; Fournel, S.; Lamour, K.; Chaloin, O.; Frisch, B.; Briand, J. P.; Monteil, H.; Guichard, G., Mimicking helical antibacterial peptides with nonpeptidic folding oligomers. *Chemistry & Biology* **2006,** *13* (5), 531-538.

84. Chongsiriwatana, N. P.; Patch, J. A.; Czyzewski, A. M.; Dohm, M. T.; Ivankin, A.; Gidalevitz, D.; Zuckermann, R. N.; Barron, A. E., Peptoids that mimic the structure, function, and mechanism of helical antimicrobial peptides. *Proceedings of the National Academy of Sciences of the United States of America* **2008,** *105* (8), 2794-2799.

85. Patch, J. A.; Barron, A. E., Helical peptoid mimics of magainin-2 amide. *Journal of the American Chemical Society* **2003,** *125* (40), 12092-12093.

86. Choi, S.; Isaacs, A.; Clements, D.; Liu, D. H.; Kim, H.; Scott, R. W.; Winkler, J. D.; DeGrado, W. F., De novo design and in vivo activity of conformationally restrained antimicrobial arylamide foldamers. *Proceedings of the National Academy of Sciences of the United States of America* **2009,** *106* (17), 6968-6973.

87. Liu, D. H.; Choi, S.; Chen, B.; Doerksen, R. J.; Clements, D. J.; Winkler, J. D.; Klein, M. L.; DeGrado, W. F., Nontoxic membrane-active antimicrobial arylamide oligomers. *Angewandte Chemie-International Edition* **2004,** *43* (9), 1158-1162.

88. Mensa, B.; Kim, Y. H.; Choi, S.; Scott, R.; Caputo, G. A.; DeGrado, W. F., Antibacterial Mechanism of Action of Arylamide Foldamers. *Antimicrobial Agents and Chemotherapy* **2011,** *55* (11), 5043-5053.

89. Tang, H.; Doerksen, R. J.; Jones, T. V.; Klein, M. L.; Tew, G. N., Biomimetic facially amphiphilic antibacterial oligomers with conformationally stiff backbones. *Chemistry & Biology* **2006,** *13* (4), 427-435.

90. Tew, G. N.; Clements, D.; Tang, H. Z.; Arnt, L.; Scott, R. W., Antimicrobial activity of an abiotic host defense peptide mimic. *Biochimica Et Biophysica Acta-Biomembranes* **2006,** *1758* (9), 1387-1392.

91. Tang, H. Z.; Doerksen, R. J.; Tew, G. N., Synthesis of urea oligomers and their antibacterial activity. *Chemical Communications* **2005,** (12), 1537-1539.

92. Ishitsuka, Y.; Arnt, L.; Majewski, J.; Frey, S.; Ratajczek, M.; Kjaer, K.; Tew, G. N.; Lee, K. Y. C., Amphiphilic poly(phenyleneethynylene)s can mimic antimicrobial peptide membrane disordering effect by membrane insertion. *Journal of the American Chemical Society* **2006,** *128* (40), 13123-13129.

93. Yang, L. H.; Gordon, V. D.; Mishra, A.; Sorn, A.; Purdy, K. R.; Davis, M. A.; Tew, G. N.; Wong, G. C. L., Synthetic antimicrobial, oligomers induce a composition-dependent topological transition in membranes. *Journal of the American Chemical Society* **2007,** *129* (40), 12141-12147.

94. Slutsky, M. M.; Phillip, J. S.; Tew, G. N., Synthesis and characterization of amphiphilic o-phenylene ethynylene oligomers. *New Journal of Chemistry* **2008,** *32* (4), 670-675.

95. Som, A.; Tew, G. N., Influence of lipid composition on membrane activity of antimicrobial phenylene ethynylene oligomers. *Journal of Physical Chemistry B* **2008,** *112* (11), 3495-3502.

96. Scott, R. W.; DeGrado, W. F.; Tew, G. N., De novo designed synthetic mimics of antimicrobial peptides. *Current Opinion in Biotechnology* **2008,** *19* (6), 620-627.

97. Lienkamp, K.; Madkour, A.; Tew, G., Antibacterial Peptidomimetics: Polymeric Synthetic Mimics of Antimicrobial Peptides. In *Polymer Composites – Polyolefin Fractionation – Polymeric Peptidomimetics – Collagens*, Abe, A.; Kausch, H.-H.; Möller, M.; Pasch, H., Eds. Springer Berlin Heidelberg: 2013; Vol. 251, pp 141-172.

98. Lienkamp, K.; Madkour, A. E.; Musante, A.; Nelson, C. F.; Nusslein, K.; Tew, G. N., Antimicrobial polymers prepared by ROMP with unprecedented selectivity: A molecular construction kit approach. *Journal of the American Chemical Society* **2008,** *130* (30), 9836-9843.

99. Kuroda, K.; DeGrado, W. F., Amphiphilic polymethacrylate derivatives as antimicrobial agents. *Journal of the American Chemical Society* **2005,** *127* (12), 4128-4129.

100. Allison, B. C.; Applegate, B. M.; Youngblood, J. P., Hemocompatibility of hydrophilic antimicrobial copolymers of alkylated 4-vinylpyridine. *Biomacromolecules* **2007,** *8* (10), 2995-2999.

101. Oda, Y.; Kanaoka, S.; Sato, T.; Aoshima, S.; Kuroda, K., Block versus Random Amphiphilic Copolymers as Antibacterial Agents. *Biomacromolecules* **2011,** *12* (10), 3581-3591.

102. Ilker, M. F.; Nusslein, K.; Tew, G. N.; Coughlin, E. B., Tuning the hemolytic and antibacterial activities of amphiphilic polynorbornene derivatives. *Journal of the American Chemical Society* **2004,** *126* (48), 15870-15875.

103. Al-Badri, Z. M.; Som, A.; Lyon, S.; Nelson, C. F.; Nusslein, K.; Tew, G. N., Investigating the Effect of Increasing Charge Density on the Hemolytic Activity of Synthetic Antimicrobial Polymers. *Biomacromolecules* **2008,** *9* (10), 2805-2810.

104. Glukhov, E.; Burrows, L. L.; Deber, C. M., Membrane interactions of designed cationic antimicrobial peptides: The two thresholds. *Biopolymers* **2008,** *89* (5), 360-371.

105. Sambhy, V.; Peterson, B. R.; Sen, A., Antibacterial and hemolytic activities of pyridinium polymers as a function of the spatial relationship between the positive charge and the pendant alkyl tail. *Angewandte Chemie-International Edition* **2008,** *47* (7), 1250-1254.

106. Kuroda, K.; Caputo, G. A.; DeGrado, W. F., The Role of Hydrophobicity in the Antimicrobial and Hemolytic Activities of Polymethacrylate Derivatives. *Chemistry-a European Journal* **2009,** *15* (5), 1123-1133.

107. Mowery, B. P.; Lindner, A. H.; Weisblum, B.; Stahl, S. S.; Gellman, S. H., Structure-activity Relationships among Random Nylon-3 Copolymers That Mimic Antibacterial Host-Defense Peptides. *Journal of the American Chemical Society* **2009,** *131* (28), 9735-9745.

108. Palermo, E. F.; Sovadinova, I.; Kuroda, K., Structural Determinants of Antimicrobial Activity and Biocompatibility in Membrane-Disrupting Methacrylamide Random Copolymers. *Biomacromolecules* **2009,** *10* (11), 3098-3107.

109. Dizman, B.; Elasri, M. O.; Mathias, L. J., Synthesis and antibacterial activities of water-soluble methacrylate polymers containing quaternary ammonium compounds. *Journal of Polymer Science Part a-Polymer Chemistry* **2006,** *44* (20), 5965-5973.

110. Gabriel, G. J.; Maegerlein, J. A.; Nelson, C. E.; Dabkowski, J. M.; Eren, T.; Nusslein, K.; Tew, G. N., Comparison of Facially Amphiphilic versus Segregated Monomers in the Design of Antibacterial Copolymers. *Chemistry-a European Journal* **2009,** *15* (2), 433-439.

111. Chakrabarty, S.; King, A.; Kurt, P.; Zhang, W.; Ohman, D. E.; Wood, L. F.; Lovelace, C.; Rao, R.; Wynne, K. J., Highly Effective, Water-Soluble, Hemocompatible 1,3-Propylene Oxide-Based Antimicrobials: Poly (3,3-quaternary/PEG)-copolyoxetanes. *Biomacromolecules* **2011,** *12* (3), 757-769.

112. Krishnan, S.; Ward, R. J.; Hexemer, A.; Sohn, K. E.; Lee, K. L.; Angert, E. R.; Fischer, D. A.; Kramer, E. J.; Ober, C. K., Surfaces of fluorinated pyridinium block copolymers with enhanced antibacterial activity. *Langmuir* **2006,** *22* (26), 11255-11266.

113. Fu, G. D.; Yao, F.; Li, Z. G.; Li, X. S., Solvent-resistant antibacterial microfibers of self-quaternized block copolymers from atom transfer radical polymerization and electrospinning. *Journal of Materials Chemistry* **2008,** *18* (8), 859-867.

114. Lienkamp, K.; Tew, G. N., Synthetic Mimics of Antimicrobial Peptides-A Versatile Ring-Opening Metathesis Polymerization Based Platform for the Synthesis of Selective Antibacterial and Cell-Penetrating Polymers. *Chemistry-a European Journal* **2009,** *15* (44), 11784-11800.

115. Colak, S.; Nelson, C. F.; Nusslein, K.; Tew, G. N., Hydrophilic Modifications of an Amphiphilic Polynorbornene and the Effects on its Hemolytic and Antibacterial Activity. *Biomacromolecules* **2009,** *10* (2), 353-359.

116. Lienkamp, K.; Kumar, K. N.; Som, A.; Nusslein, K.; Tew, G. N., "Doubly Selective" Antimicrobial Polymers: How Do They Differentiate between Bacteria? *Chemistry-a European Journal* **2009,** *15* (43), 11710-11714.

117. Lienkamp, K.; Madkour, A. E.; Kumar, K. N.; Nusslein, K.; Tew, G. N., Antimicrobial Polymers Prepared by Ring-Opening Metathesis Polymerization: Manipulating Antimicrobial Properties by Organic Counterion and Charge Density Variation. *Chemistry-a European Journal* **2009,** *15* (43), 11715-11722.

118. Venkataraman, S.; Zhang, Y.; Liu, L. H.; Yang, Y. Y., Design, syntheses and evaluation of hemocompatible pegylated-antimicrobial polymers with well-controlled molecular structures. *Biomaterials* **2010,** *31* (7), 1751-1756.

119. Palermo, E. F.; Kuroda, K., Chemical Structure of Cationic Groups in Amphiphilic Polymethacrylates Modulates the Antimicrobial and Hemolytic Activities. *Biomacromolecules* **2009,** *10* (6), 1416-1428.

120. Stratton, T. R.; Rickus, J. L.; Youngblood, J. P., In Vitro Biocompatibility Studies of Antibacterial Quaternary Polymers. *Biomacromolecules* **2009,** *10* (9), 2550-2555.

121. Stratton, T. R.; Howarter, J. A.; Allison, B. C.; Applegate, B. M.; Youngblood, J. P., Structure-Activity Relationships of Antibacterial and Biocompatible Copolymers. *Biomacromolecules* **2010,** *11* (5), 1286-1290.

122. Stratton, T. R.; Applegate, B. M.; Youngblood, J. P., Effect of Steric Hindrance on the Properties of Antibacterial and Biocompatible Copolymers. *Biomacromolecules* **2011,** *12* (1), 50-56.

123. Mowery, B. P.; Lee, S. E.; Kissounko, D. A.; Epand, R. F.; Epand, R. M.; Weisblum, B.; Stahl, S. S.; Gellman, S. H., Mimicry of antimicrobial host-defense peptides by random copolymers. *Journal of the American Chemical Society* **2007,** *129* (50), 15474-+.

124. Epand, R. F.; Mowery, B. P.; Lee, S. E.; Stahl, S. S.; Lehrer, R. I.; Gellman, S. H.; Epand, R. M., Dual mechanism of bacterial lethality for a cationic sequence-random copolymer that mimics host-defense antimicrobial peptides. *Journal of Molecular Biology* **2008,** *379* (1), 38-50.

125. Park, D.; Finlay, J. A.; Ward, R. J.; Weinman, C. J.; Krishnan, S.; Paik, M.; Sohn, K. E.; Callow, M. E.; Callow, J. A.; Handlin, D. L.; Willis, C. L.; Fischer, D. A.; Angert, E. R.; Kramer, E. J.; Ober, C. K., Antimicrobial Behavior of Semifluorinated-Quaternized Triblock Copolymers against Airborne and Marine Microorganisms. *Acs Applied Materials & Interfaces* **2010,** *2* (3), 703-711.

126. Sellenet, P. H.; Allison, B.; Applegate, B. M.; Youngblood, J. P., Synergistic activity of hydrophilic modification in antibiotic polymers. *Biomacromolecules* **2007,** *8* (1), 19-23.

127. Palermo, E. F.; Lee, D. K.; Ramamoorthy, A.; Kuroda, K., Role of Cationic Group Structure in Membrane Binding and Disruption by Amphiphilic Copolymers. *Journal of Physical Chemistry B* **2011,** *115* (2), 366-375.

128. Park, E. S.; Kim, H. S.; Kim, M. N.; Yoon, J. S., Antibacterial activities of polystyrene-block-poly(4-vinyl pyridine) and poly(styrene-random-4-vinyl pyn'dine). *European Polymer Journal* **2004,** *40* (12), 2819-2822.

129. Palermo, E. F.; Kuroda, K., Structural determinants of antimicrobial activity in polymers which mimic host defense peptides. *Applied Microbiology and Biotechnology* **2010,** *87* (5), 1605-1615.

130. Gademann, K., Natural product hybrids. *Chimia* **2006,** *60* (12), 841-845.

131. Hudson, S. P.; Langer, R.; Fink, G. R.; Kohane, D. S., Injectable in situ cross-linking hydrogels for local antifungal therapy. *Biomaterials* **2010,** *31* (6), 1444-1452.

132. Wach, J. Y.; Bonazzi, S.; Gademann, K., Antimicrobial surfaces through natural product hybrids. *Angewandte Chemie-International Edition* **2008,** *47* (37),

7123-7126.

133. Liu, L. H.; Xu, K. J.; Wang, H. Y.; Tan, P. K. J.; Fan, W. M.; Venkatraman, S. S.; Li, L. J.; Yang, Y. Y., Self-assembled cationic peptide nanoparticles as an efficient antimicrobial agent. *Nature Nanotechnology* **2009,** *4* (7), 457-463.

134. Nederberg, F.; Zhang, Y.; Tan, J. P. K.; Xu, K. J.; Wang, H. Y.; Yang, C.; Gao, S. J.; Guo, X. D.; Fukushima, K.; Li, L. J.; Hedrick, J. L.; Yang, Y. Y., Biodegradable nanostructures with selective lysis of microbial membranes. *Nature Chemistry* **2011,** *3* (5), 409-414.

135. Qi, X. B.; Poernomo, G.; Wang, K. A.; Chen, Y. A.; Chan-Park, M. B.; Xu, R.; Chang, M. W., Covalent immobilization of nisin on multi-walled carbon nanotubes: superior antimicrobial and anti-biofilm properties. *Nanoscale* **2011,** *3* (4), 1874-1880.

136. Liu, Y. X.; Chan-Park, M. B., Hydrogel based on interpenetrating polymer networks of dextran and gelatin for vascular tissue engineering. *Biomaterials* **2009,** *30* (2), 196-207.

137. Wang, H. Y.; Xu, K. J.; Liu, L. H.; Tan, J. P. K.; Chen, Y. B.; Li, Y. T.; Fan, W. M.; Wei, Z. Q.; Sheng, J. F.; Yang, Y. Y.; Li, L. J., The efficacy of self-assembled cationic antimicrobial peptide nanoparticles against Cryptococcus neoformans for the treatment of meningitis. *Biomaterials* **2010,** *31* (10), 2874-2881.

138. Darling, S. B., Directing the self-assembly of block copolymers. *Progress in Polymer Science* **2007,** *32* (10), 1152-1204.

139. Liu, S. B.; Wei, L.; Hao, L.; Fang, N.; Chang, M. W.; Xu, R.; Yang, Y. H.; Chen, Y., Sharper and Faster "Nano Darts" Kill More Bacteria: A Study of Antibacterial Activity of Individually Dispersed Pristine Single-Walled Carbon Nanotube. *Acs Nano* **2009,** *3* (12), 3891-3902.

140. Liu, S. B.; Zeng, T. H.; Hofmann, M.; Burcombe, E.; Wei, J.; Jiang, R. R.; Kong, J.; Chen, Y., Antibacterial Activity of Graphite, Graphite Oxide, Graphene Oxide, and Reduced Graphene Oxide: Membrane and Oxidative Stress. *Acs Nano* **2011,** *5* (9), 6971-6980.

141. Akhavan, O.; Ghaderi, E., Toxicity of Graphene and Graphene Oxide Nanowalls Against Bacteria. *Acs Nano* **2010,** *4* (10), 5731-5736.

142. Hu, W. B.; Peng, C.; Luo, W. J.; Lv, M.; Li, X. M.; Li, D.; Huang, Q.; Fan, C. H., Graphene-Based Antibacterial Paper. *Acs Nano* **2010,** *4* (7), 4317-4323.

143. Vasilev, K.; Cook, J.; Griesser, H. J., Antibacterial surfaces for biomedical

devices. *Expert Review of Medical Devices* **2009,** *6* (5), 553-567.

144. Tiller, J. C.; Liao, C. J.; Lewis, K.; Klibanov, A. M., Designing surfaces that kill bacteria on contact. *Proceedings of the National Academy of Sciences of the United States of America* **2001,** *98* (11), 5981-5985.

145. Tiller, J. C., Antimicrobial Surfaces. In *Bioactive Surfaces*, Borner, H. G.; Lutz, J. F., Eds. 2011; Vol. 240, pp 193-217.

146. Johnson, J. R.; Kuskowski, M. A.; Wilt, T. J., Systematic review: Antimicrobial urinary catheters to prevent catheter-associated urinary tract infection in hospitalized patients. *Annals of Internal Medicine* **2006,** *144* (2), 116-126.

147. Tiller, J. C.; Sprich, C.; Hartmann, L., Amphiphilic conetworks as regenerative controlled releasing antimicrobial coatings. *Journal of Controlled Release* **2005,** *103* (2), 355-367.

148. Kumar, A.; Vemula, P. K.; Ajayan, P. M.; John, G., Silver-nanoparticle-embedded antimicrobial paints based on vegetable oil. *Nature Materials* **2008,** *7* (3), 236-241.

149. Ho, C. H.; Tobis, J.; Sprich, C.; Thomann, R.; Tiller, J. C., Nanoseparated polymeric networks with multiple antimicrobial properties. *Advanced Materials* **2004,** *16* (12), 957-+.

150. Kristinsson, K. G.; Jansen, B.; Treitz, U.; Schumacher-Perdreau, F.; Peters, G.; Pulverer, G., Antimicrobial Activity of Polymers Coated with Iodine-Complexed Polyvinylpyrrolidone *J Biomater Appl* **1991,** *5*, 173-184.

151. Cohen, M. L., Changing patterns of infectious disease. *Nature* **2000,** *406* (6797), 762-767.

152. Bullen, J. J.; Rogers, H. J.; Spalding, P. B.; Ward, C. G., Iron and infection: the heart of the matter. *FEMS Immunol. Med. Microbiol.* **2005,** *43* (3), 325-330.

153. Raulio, M.; Jarn, M.; Ahola, J.; Peltonen, J.; Rosenholm, J. B.; Tervakangas, S.; Kolehmainen, J.; Ruokolainen, T.; Narko, P.; Salkinoja-Salonen, M., Microbe repelling coated stainless steel analysed by field emission scanning electron microscopy and physicochemical methods. *J. Ind. Microbiol. Biotechnol.* **2008,** *35* (7), 751-760.

154. Liu, C.; Zhao, Q.; Liu, Y.; Wang, S.; Abel, E. W., Reduction of bacterial adhesion on modified DLC coatings. *Colloids and Surfaces B-Biointerfaces* **2008,** *61* (2), 182-187.

155. Park, K. D.; Kim, Y. S.; Han, D. K.; Kim, Y. H.; Lee, E. H. B.; Suh, H.; Choi, K. S., Bacterial adhesion on PEG modified polyurethane surfaces. *Biomaterials* **1998,** *19* (7-9), 851-859.

156. Cunliffe, D.; Smart, C. A.; Alexander, C.; Vulfson, E. N., Bacterial adhesion at synthetic surfaces. *Appl. Environ. Microbiol.* **1999,** *65* (11), 4995-5002.

157. Benesch, J.; Svedhem, S.; Svensson, S. C. T.; Valiokas, R.; Liedberg, B.; Tengvall, P., Protein adsorption to oligo(ethylene glycol) self-assembled monolayers: Experiments with fibrinogen, heparinized plasma, and serum. *J. Biomater. Sci.-Polym. Ed.* **2001,** *12* (6), 581-597.

158. Kingshott, P.; Wei, J.; Bagge-Ravn, D.; Gadegaard, N.; Gram, L., Covalent attachment of poly(ethylene glycol) to surfaces, critical for reducing bacterial adhesion. *Langmuir* **2003,** *19* (17), 6912-6921.

159. Desai, N. P.; Hossainy, S. F. A.; Hubbell, J. A., Surface-immobilized polyethylene oxide for bacterial repellence. *Biomaterials* **1992,** *13* (7), 417-420.

160. Chen, H.; Yuan, L.; Song, W.; Wu, Z. K.; Li, D., Biocompatible polymer materials: Role of protein-surface interactions. *Progress in Polymer Science* **2008,** *33* (11), 1059-1087.

161. Fuchs, A. D.; Tiller, J. C., Contact-active antimicrobial coatings derived from aqueous suspensions. *Angewandte Chemie-International Edition* **2006,** *45* (40), 6759-6762.

162. Waschinski, C. J.; Zimmermann, J.; Salz, U.; Hutzler, R.; Sadowski, G.; Tiller, J. C., Design of contact-active antimicrobial acrylate-based materials using biocidal macromers. *Advanced Materials* **2008,** *20* (1), 104-+.

163. Ferreira, L.; Zumbuehl, A., Non-leaching surfaces capable of killing microorganisms on contact. *Journal of Materials Chemistry* **2009,** *19* (42), 7796-7806.

164. Girshevitz, O.; Nitzan, Y.; Sukenik, C. N., Solution-deposited amorphous titanium dioxide on silicone rubber: A conformal, crack-free antibacterial coating. *Chem. Mat.* **2008,** *20* (4), 1390-1396.

165. Etienne, O.; Gasnier, C.; Taddei, C.; Voegel, J. C.; Aunis, D.; Schaaf, P.; Metz-Boutigue, M. H.; Bolcato-Bellemin, A. L.; Egles, C., Antifungal coating by biofunctionalized polyelectrolyte multilayered films. *Biomaterials* **2005,** *26* (33), 6704-6712.

166. Lee, S. B.; Koepsel, R. R.; Morley, S. W.; Matyjaszewski, K.; Sun, Y. J.; Russell, A. J., Permanent, nonleaching antibacterial surfaces. 1. Synthesis by atom transfer radical polymerization. *Biomacromolecules* **2004,** *5* (3), 877-882.

167. Murata, H.; Koepsel, R. R.; Matyjaszewski, K.; Russell, A. J., Permanent, non-leaching antibacterial surfaces - 2: How high density cationic surfaces kill bacterial cells. *Biomaterials* **2007,** *28* (32), 4870-4879.

168. Huang, J. Y.; Koepsel, R. R.; Murata, H.; Wu, W.; Lee, S. B.; Kowalewski, T.; Russell, A. J.; Matyjaszewski, K., Nonleaching antibacterial glass surfaces via "Grafting Onto": The effect of the number of quaternary ammonium groups on biocidal activity. *Langmuir* **2008,** *24* (13), 6785-6795.

169. Bhattacharya, A.; Misra, B. N., Grafting: a versatile means to modify polymers - Techniques, factors and applications. *Progress in Polymer Science* **2004,** *29* (8), 767-814.

170. Kato, K.; Uchida, E.; Kang, E. T.; Uyama, Y.; Ikada, Y., Polymer surface with graft chains. *Progress in Polymer Science* **2003,** *28* (2), 209-259.

171. Dargaville, T. R.; George, G. A.; Hill, D. J. T.; Whittaker, A. K., High energy radiation grafting of fluoropolymers. *Progress in Polymer Science* **2003,** *28* (9), 1355-1376.

172. Matyjaszewski, K.; Tsarevsky, N. V., Nanostructured functional materials prepared by atom transfer radical polymerization. *Nature Chemistry* **2009,** *1* (4), 276-288.

173. Xu, F. J.; Neoh, K. G.; Kang, E. T., Bioactive surfaces and biomaterials via atom transfer radical polymerization. *Progress in Polymer Science* **2009,** *34* (8), 719-761.

174. Milovic, N. M.; Wang, J.; Lewis, K.; Klibanov, A. M., Immobilized N-alkylated polyethylenimine avidly kills bacteria by rupturing cell membranes with no resistance developed. *Biotechnology and Bioengineering* **2005,** *90* (6), 715-722.

175. Cheng, G.; Hong Xue; Zheng Zhang; Shengfu Chen; Shaoyi Jiang, A Switchable Biocompatible Polymer Surface with Self-Sterilizing and Nonfouling Capabilities. *Angewandte chemie-international edition* **2008,** *47,* 8831-8834.

176. Klibanov, A. M., Permanently microbicidal materials coatings. *Journal of Materials Chemistry* **2007,** *17* (24), 2479-2482.

177. Smith, A. W., Biofilms and antibiotic therapy: Is there a role for combating

bacterial resistance by the use of novel drug delivery systems? *Advanced Drug Delivery Reviews* **2005,** *57* (10), 1539-1550.

178. Lin, J.; Qiu, S. Y.; Lewis, K.; Klibanov, A. M., Bactericidal properties of flat surfaces and nanoparticles derivatized with alkylated polyethylenimines. *Biotechnology Progress* **2002,** *18* (5), 1082-1086.

179. Tew, G. N.; Clements, D.; Tang, H.; Arnt, L.; Scott, R. W., Antimicrobial activity of an abiotic host defense peptide mimic. *Biochimica et Biophysica Acta* **2006,** *1758* (9), 1387-1392

180. Kenawy, E. R.; Worley, S. D.; Broughton, R., The chemistry and applications of antimicrobial polymers: A state-of-the-art review. *Biomacromolecules* **2007,** *8* (5), 1359-1384.

181. Bagheri, M.; Beyermann, M.; Dathe, M., Immobilization Reduces the Activity of Surface-Bound Cationic Antimicrobial Peptides with No Influence upon the Activity Spectrum. *Antimicrobial Agents and Chemotherapy* **2009,** *53* (3), 1132-1141.

182. Imazato S; Russell R. R. B.; F., M. J., Antibacterial activity of MDPB polymer incorporated in dental resin. *Journal of Dentistry* **1995,** *23* (3), 177-181.

183. Stratton, T. R.; Garcia, R. E.; Applegate, B. M.; Youngblood, J. P., Application of a High Throughput Bioluminescence-Based Method and Mathematical Model for the Quantitative Comparison of Polymer Microbicide Efficiency. *Biomacromolecules* **2009,** *10* (5), 1173-1180.

184. Nurdin, N.; Helary, G.; Sauvet, G., Biocidal polymers active by contact. 2. Biological evaluation of polyurethane coatings with pendant quaternary ammonium-salts. *Journal of Applied Polymer Science* **1993,** *50* (4), 663-670.

185. Madkour, A. E.; Dabkowski, J. A.; Nusslein, K.; Tew, G. N., Fast Disinfecting Antimicrobial Surfaces. *Langmuir* **2009,** *25* (2), 1060-1067.

186. Jia, Z. S.; Shen, D. F.; Xu, W. L., Synthesis and antibacterial activities of quaternary ammonium salt of chitosan. *Carbohydrate Research* **2001,** *333* (1), 1-6.

187. Mao, S. R.; Shuai, X. T.; Unger, F.; Wittmar, M.; Xie, X. L.; Kissel, T., Synthesis, characterization and cytotoxicity of poly(ethylene glycol)-graft-trimethyl chitosan block copolymers. *Biomaterials* **2005,** *26* (32), 6343-6356.

188. Zhu, S. Y.; Qian, F.; Zhang, Y.; Tang, C.; Yin, C. H., Synthesis and characterization of PEG modified N-trimethylaminoethylmethacrylate chitosan

nanoparticles. *European Polymer Journal* **2007,** *43* (6), 2244-2253.

189. Degiorgi, C. F.; Pizarro, R. A.; Smolko, E. E.; Lora, S.; Carenza, M., Hydrogels for immobilization of bacteria used in the treatment of metal-contaminated wastes. *Radiation Physics and Chemistry* **2002,** *63* (1), 109-113.

190. Markowitz, M. A.; Turner, D. C.; Martin, B. D.; Gaber, B. P., Diffusion and transfer of antibody proteins from a sugar-based hydrogel. *Applied Biochemistry and Biotechnology* **1997,** *68* (1-2), 57-68.

191. Li, Q.; Wang, D. A.; Elisseeff, J. H., Heterogeneous-phase reaction of glycidyl methacrylate and chondroitin sulfate: Mechanism of ring-opening-transesterification competition. *Macromolecules* **2003,** *36* (7), 2556-2562.

192. Lim, S. H.; Hudson, S. M., Synthesis and antimicrobial activity of a water-soluble chitosan derivative with a fiber-reactive group. *Carbohydrate Research* **2004,** *339* (2), 313-319.

193. Flory, P. J.; Rehner, J., Statistical mechanics of cross-linked polymer networks I Rubberlike elasticity. *Journal of Chemical Physics* **1943,** *11* (11), 512-520.

194. Peppas, N. A.; Merrill, E. W., Crosslinked poly(vinyl-alcohol) hydrogels as swollen elastic networks. *Journal of Applied Polymer Science* **1977,** *21* (7), 1763-1770.

195. Ravindra, R.; Krovvidi, K. R.; Khan, A. A., Solubility parameter of chitin and chitosan. *Carbohydrate Polymers* **1998,** *36* (2-3), 121-127.

196. Safronov, A. P.; Zubarev, A. Y., Flory-Huggins parameter of interaction in polyelectrolyle solutions of chitosan and its alkylated derivative. *Polymer* **2002,** *43* (3), 743-748.

197. Yui, T.; Kobayashi, H.; Kitamura, S.; Imada, K., Conformational analysis of chitobiose and chitosan. *Biopolymers* **1994,** *34* (2), 203-208.

198. Runarsson, O. V.; Holappa, J.; Nevalainen, T.; Hjalmarsdottir, M.; Jarvinen, T.; Loftsson, T.; Einarsson, J. M.; Jonsdottir, S.; Valdimarsdottir, M.; Masson, M., Antibacterial activity of methylated chitosan and chitooligomer derivatives: Synthesis and structure activity relationships. *European Polymer Journal* **2007,** *43* (6), 2660-2671.

199. Sadovskaya, I.; Brisson, J. R.; Lam, J. S.; Richards, J. C.; Altman, E., Structural elucidation of the lipopolysaccharide core regions of the wild-type strain

PAO1 and O-chain-deficient mutant strains AK1401 and AK1012 from Pseudomonas aeruginosa serotype O5. *European Journal of Biochemistry* **1998,** *255* (3), 673-684.

200. Berger, J.; Reist, M.; Mayer, J. M.; Felt, O.; Peppas, N. A.; Gurny, R., Structure and interactions in covalently and ionically crosslinked chitosan hydrogels for biomedical applications. *European Journal of Pharmaceutics and Biopharmaceutics* **2004,** *57* (1), 19-34.

201. Ostuni, E.; Chapman, R. G.; Holmlin, R. E.; Takayama, S.; Whitesides, G. M., A survey of structure-property relationships of surfaces that resist the adsorption of protein. *Langmuir* **2001,** *17* (18), 5605-5620.

202. Fischbach, M. A.; Walsh, C. T., Antibiotics for Emerging Pathogens. *Science* **2009,** *325* (5944), 1089-1093.

203. Radzishevsky, I. S.; Rotem, S.; Bourdetsky, D.; Navon-Venezia, S.; Carmeli, Y.; Mor, A., Improved antimicrobial peptides based on acyl-lysine oligomers. *Nature Biotechnology* **2007,** *25* (6), 657-659.

204. Sovadinova, I.; Palermo, E. F.; Huang, R.; Thoma, L. M.; Kuroda, K., Mechanism of Polymer-Induced Hemolysis: Nanosized Pore Formation and Osmotic Lysis. *Biomacromolecules* **2011,** *12* (1), 260-268.

205. Li, P.; Poon, Y. F.; Li, W.; Zhu, H. Y.; Yeap, S. H.; Cao, Y.; Qi, X.; Zhou, C.; Lamrani, M.; Beuerman, R. W.; Kang, E. T.; Mu, Y.; Li, C. M.; Chang, M. W.; Jan Leong, S. S.; Chan-Park, M. B., A polycationic antimicrobial and biocompatible hydrogel with microbe membrane suctioning ability. *Nature Materials* **2011,** *10* (2), 149-156.

206. Kahne, D.; Leimkuhler, C.; Wei, L.; Walsh, C., Glycopeptide and lipoglycopeptide antibiotics. *Chemical Reviews* **2005,** *105* (2), 425-448.

207. Yu, H. J.; Wang, W. S.; Chen, X. S.; Deng, C.; Jing, X. B., Synthesis and characterization of the biodegradable polycaprolactone-graft-chitosan amphiphilic copolymers. *Biopolymers* **2006,** *83* (3), 233-242.

208. Yu, H. J.; Chen, X. S.; Lu, T. C.; Sun, J.; Tian, H. Y.; Hu, J.; Wang, Y.; Zhang, P. B.; Jing, X. B., Poly(L-lysine)-graft-chitosan copolymers: Synthesis, characterization, and gene transfection effect. *Biomacromolecules* **2007,** *8* (5), 1425-1435.

209. Wiradharma, N.; Khoe, U.; Hauser, C. A. E.; Seow, S. V.; Zhang, S. G.; Yang, Y. Y., Synthetic cationic amphiphilic alpha-helical peptides as antimicrobial agents. *Biomaterials* **2011,** *32* (8), 2204-2212.

210. Chou, H. T.; Kuo, T. Y.; Chiang, J. C.; Pei, M. J.; Yang, W. T.; Yu, H. C.; Lin, S. B.; Chen, W. J., Design and synthesis of cationic antimicrobial peptides with improved activity and selectivity against Vibrio spp. *International Journal of Antimicrobial Agents* **2008,** *32* (2), 130-138.

211. Thevissen, K.; Terras, F. R. G.; Broekaert, W. F., Permeabilization of fungal membranes by plant defensins inhibits fungal growth. *Applied and Environmental Microbiology* **1999,** *65* (12), 5451-5458.

212. Cabrini, G.; Verkman, A. S., Potential-sensitive response mechanism of DIS-C3-(5) in biological-membranes. *Journal of Membrane Biology* **1986,** *92* (2), 171-182.

213. Pandey, B. K.; Ahmad, A.; Asthana, N.; Azmi, S.; Srivastava, R. M.; Srivastava, S.; Verma, R.; Vishwakarma, A. L.; Ghosh, J. K., Cell-Selective Lysis by Novel Analogues of Melittin against Human Red Blood Cells and Escherichia coli. *Biochemistry* **2010,** *49* (36), 7920-7929.

214. Fischer, W., LIPOTEICHOIC ACID AND LIPIDS IN THE MEMBRANE OF STAPHYLOCOCCUS-AUREUS. *Medical Microbiology and Immunology* **1994,** *183* (2), 61-76.

215. Hancock, R. E. W., The bacterial outer membrane as a drug barrier. *Trends in Microbiology* **1997,** *5* (1), 37-42.

216. Chung, Y. C.; Su, Y. P.; Chen, C. C.; Jia, G.; Wang, H. I.; Wu, J. C. G.; Lin, J. G., Relationship between antibacterial activity of chitosan and surface characteristics of cell wall. *Acta Pharmacologica Sinica* **2004,** *25* (7), 932-936.

217. Chicharro, C.; Granata, C.; Lozano, R.; Andreu, D.; Rivas, L., N-terminal fatty acid substitution increases the leishmanicidal activity of CA(1-7)M(2-9), a cecropin-melittin hybrid peptide. *Antimicrobial Agents and Chemotherapy* **2001,** *45* (9), 2441-2449.

218. Qi, X. B.; Zhou, C. C.; Li, P.; Xu, W. X.; Cao, Y.; Ling, H.; Chen, W. N.; Li, C. M.; Xu, R.; Lamrani, M.; Mu, Y. G.; Leong, S. S. J.; Chang, M. W.; Chan-Park, M. B., Novel short antibacterial and antifungal peptides with low cytotoxicity: Efficacy and action mechanisms. *Biochemical and Biophysical Research Communications* **2010,** *398* (3), 594-600.

219. Sawai, M. V.; Waring, A. J.; Kearney, W. R.; McCray, P. B.; Forsyth, W. R.; Lehrer, R. I.; Tack, B. F., Impact of single-residue mutations on the structure and function of ovispirin/novispirin antimicrobial peptides. *Protein Engineering* **2002,** *15* (3), 225-232.

220. Dathe, M.; Nikolenko, H.; Klose, J.; Bienert, M., Cyclization increases the antimicrobial activity and selectivity of arginine- and tryptophan-containing hexapeptides. *Biochemistry* **2004,** *43* (28), 9140-9150.

221. Tam, J. P.; Lu, Y. A.; Yang, J. L., Antimicrobial dendrimeric peptides. *European Journal of Biochemistry* **2002,** *269* (3), 923-932.

222. Rinaudo, M., Chitin and chitosan: Properties and applications. *Prog. Polym. Sci.* **2006,** *31* (7), 603-632.

223. Geim, A. K.; Novoselov, K. S., The rise of graphene. *Nature Materials* **2007,** *6* (3), 183-191.

224. Becerril, H. A.; Mao, J.; Liu, Z.; Stoltenberg, R. M.; Bao, Z.; Chen, Y., Evaluation of solution-processed reduced graphene oxide films as transparent conductors. *Acs Nano* **2008,** *2* (3), 463-470.

225. Fowler, J. D.; Allen, M. J.; Tung, V. C.; Yang, Y.; Kaner, R. B.; Weiller, B. H., Practical Chemical Sensors from Chemically Derived Graphene. *Acs Nano* **2009,** *3* (2), 301-306.

226. Rafiee, M. A.; Rafiee, J.; Wang, Z.; Song, H. H.; Yu, Z. Z.; Koratkar, N., Enhanced Mechanical Properties of Nanocomposites at Low Graphene Content. *Acs Nano* **2009,** *3* (12), 3884-3890.

227. Stoller, M. D.; Park, S. J.; Zhu, Y. W.; An, J. H.; Ruoff, R. S., Graphene-Based Ultracapacitors. *Nano Letters* **2008,** *8* (10), 3498-3502.

228. Eda, G.; Fanchini, G.; Chhowalla, M., Large-area ultrathin films of reduced graphene oxide as a transparent and flexible electronic material. *Nature Nanotechnology* **2008,** *3* (5), 270-274.

229. Dreyer, D. R.; Park, S.; Bielawski, C. W.; Ruoff, R. S., The chemistry of graphene oxide. *Chemical Society Reviews* **2010,** *39* (1), 228-240.

230. Zhu, Y. W.; Murali, S.; Cai, W. W.; Li, X. S.; Suk, J. W.; Potts, J. R.; Ruoff, R. S., Graphene and Graphene Oxide: Synthesis, Properties, and Applications. *Advanced Materials* **2010,** *22* (35), 3906-3924.

231. Yang, K.; Zhang, S. A.; Zhang, G. X.; Sun, X. M.; Lee, S. T.; Liu, Z. A., Graphene in Mice: Ultrahigh In Vivo Tumor Uptake and Efficient Photothermal Therapy. *Nano Letters* **2010,** *10* (9), 3318-3323.

232. Zhang, W.; Guo, Z. Y.; Huang, D. Q.; Liu, Z. M.; Guo, X.; Zhong, H. Q.,

Synergistic effect of chemo-photothermal therapy using PEGylated graphene oxide. *Biomaterials* **2011,** *32* (33), 8555-8561.

233. Pan, Y. Z.; Bao, H. Q.; Sahoo, N. G.; Wu, T. F.; Li, L., Water-Soluble Poly(N-isopropylacrylamide)-Graphene Sheets Synthesized via Click Chemistry for Drug Delivery. *Advanced Functional Materials* **2011,** *21* (14), 2754-2763.

234. Das, M. R.; Sarma, R. K.; Saikia, R.; Kale, V. S.; Shelke, M. V.; Sengupta, P., Synthesis of silver nanoparticles in an aqueous suspension of graphene oxide sheets and its antimicrobial activity. *Colloids and Surfaces B-Biointerfaces* **2011,** *83* (1), 16-22.

235. Cai, X.; Tan, S. Z.; Lin, M. S.; Xie, A.; Mai, W. J.; Zhang, X. J.; Lin, Z. D.; Wu, T.; Liu, Y. L., Synergistic Antibacterial Brilliant Blue/Reduced Graphene Oxide/Quaternary Phosphonium Salt Composite with Excellent Water Solubility and Specific Targeting Capability. *Langmuir* **2011,** *27* (12), 7828-7835.

236. Ruiz, O. N.; Fernando, K. A. S.; Wang, B. J.; Brown, N. A.; Luo, P. G.; McNamara, N. D.; Vangsness, M.; Sun, Y. P.; Bunker, C. E., Graphene Oxide: A Nonspecific Enhancer of Cellular Growth. *Acs Nano* **2011,** *5* (10), 8100-8107.

237. Santos, C. M.; Tria, M. C. R.; Vergara, R.; Ahmed, F.; Advincula, R. C.; Rodrigues, D. F., Antimicrobial graphene polymer (PVK-GO) nanocomposite films. *Chemical Communications* **2011,** *47* (31), 8892-8894.

238. Bao, Q.; Zhang, D.; Qi, P., Synthesis and characterization of silver nanoparticle and graphene oxide nanosheet composites as a bactericidal agent for water disinfection. *Journal of Colloid and Interface Science* **2011,** *360* (2), 463-470.

239. Liu, L.; Liu, J. C.; Wang, Y. J.; Yan, X. L.; Sun, D. D., Facile synthesis of monodispersed silver nanoparticles on graphene oxide sheets with enhanced antibacterial activity. *New Journal of Chemistry* **2011,** *35* (7), 1418-1423.

240. Shen, J. F.; Shi, M.; Li, N.; Yan, B.; Ma, H. W.; Hu, Y. Z.; Ye, M. X., Facile Synthesis and Application of Ag-Chemically Converted Graphene Nanocomposite. *Nano Research* **2010,** *3* (5), 339-349.

241. Xu, W. P.; Zhang, L. C.; Li, J. P.; Lu, Y.; Li, H. H.; Ma, Y. N.; Wang, W. D.; Yu, S. H., Facile synthesis of silver@graphene oxide nanocomposites and their enhanced antibacterial properties. *Journal of Materials Chemistry* **2011,** *21* (12), 4593-4597.

242. Zhang, D. H.; Liu, X. H.; Wang, X., Green synthesis of graphene oxide sheets decorated by silver nanoprisms and their anti-bacterial properties. *Journal of*

Inorganic Biochemistry **2011,** *105* (9), 1181-1186.

243. Rai, M.; Yadav, A.; Gade, A., Silver nanoparticles as a new generation of antimicrobials. *Biotechnology Advances* **2009,** *27* (1), 76-83.

244. Zhuang, X. D.; Chen, Y.; Liu, G.; Li, P. P.; Zhu, C. X.; Kang, E. T.; Neoh, K. G.; Zhang, B.; Zhu, J. H.; Li, Y. X., Conjugated-Polymer-Functionalized Graphene Oxide: Synthesis and Nonvolatile Rewritable Memory Effect. *Advanced Materials* **2010,** *22* (15), 1731-+.

245. Salavagione, H. J.; Martinez, G.; Ellis, G., Recent Advances in the Covalent Modification of Graphene With Polymers. *Macromolecular Rapid Communications* **2011,** *32* (22), 1771-1789.

246. Li, Y. X.; Pan, Z.; Fu, Y. Y.; Chen, Y.; Xie, Z. Y.; Zhang, B., Soluble reduced graphene oxide functionalized with conjugated polymer for heterojunction solar cells. *Journal of Polymer Science Part a-Polymer Chemistry* **2012,** *50* (9), 1663-1671.

247. Li, P.; Poon, Y. F.; Li, W. F.; Zhu, H. Y.; Yeap, S. H.; Cao, Y.; Qi, X. B.; Zhou, C. C.; Lamrani, M.; Beuerman, R. W.; Kang, E. T.; Mu, Y. G.; Li, C. M.; Chang, M. W.; Leong, S. S. J.; Chan-Park, M. B., A polycationic antimicrobial and biocompatible hydrogel with microbe membrane suctioning ability. *Nature Materials* **2011,** *10* (2), 149-156.

248. Lee, K. Y.; Mooney, D. J., Hydrogels for tissue engineering. *Chemical Reviews* **2001,** *101* (7), 1869-1879.

249. Dash, M.; Chiellini, F.; Ottenbrite, R. M.; Chiellini, E., Chitosan-A versatile semi-synthetic polymer in biomedical applications. *Progress in Polymer Science* **2011,** *36* (8), 981-1014.

250. Hummers, W. S.; Offeman, R. E., Preparation of graphitic oxide. *Journal of the American Chemical Society* **1958,** *80* (6), 1339-1339.

251. Kovtyukhova, N. I.; Ollivier, P. J.; Martin, B. R.; Mallouk, T. E.; Chizhik, S. A.; Buzaneva, E. V.; Gorchinskiy, A. D., Layer-by-layer assembly of ultrathin composite films from micron-sized graphite oxide sheets and polycations. *Chemistry of Materials* **1999,** *11* (3), 771-778.

252. Nakajima, N.; Ikada, Y., MECHANISM OF AMIDE FORMATION BY CARBODIIMIDE FOR BIOCONJUGATION IN AQUEOUS-MEDIA. *Bioconjugate Chemistry* **1995,** *6* (1), 123-130.

253. Watcharotone, S.; Dikin, D. A.; Stankovich, S.; Piner, R.; Jung, I.; Dommett,

G. H. B.; Evmenenko, G.; Wu, S. E.; Chen, S. F.; Liu, C. P.; Nguyen, S. T.; Ruoff, R. S., Graphene-silica composite thin films as transparent conductors. *Nano Letters* **2007,** *7* (7), 1888-1892.

254. Lee, K. Y.; Jo, W. H.; Kwon, I. C.; Kim, Y. H.; Jeong, S. Y., Structural determination and interior polarity of self-aggregates prepared from deoxycholic acid-modified chitosan in water. *Macromolecules* **1998,** *31* (2), 378-383.

255. Jung, I.; Dikin, D.; Park, S.; Cai, W.; Mielke, S. L.; Ruoff, R. S., Effect of Water Vapor on Electrical Properties of Individual Reduced Graphene Oxide Sheets. *Journal of Physical Chemistry C* **2008,** *112* (51), 20264-20268.

256. McAllister, M. J.; Li, J.-L.; Adamson, D. H.; Schniepp, H. C.; Abdala, A. A.; Liu, J.; Herrera-Alonso, M.; Milius, D. L.; Car, R.; Prud'homme, R. K.; Aksay, I. A., Single Sheet Functionalized Graphene by Oxidation and Thermal Expansion of Graphite. *Chem. Mat.* **2007,** *19* (18), 4396-4404.

257. Spinelli, V. A.; Laranjeira, M. C. M.; Fávere, V. T., Preparation and characterization of quaternary chitosan salt: adsorption equilibrium of chromium(VI) ion. *Reactive and Functional Polymers* **2004,** *61* (3), 347-352.

258. Latge, J. P., The cell wall: a carbohydrate armour for the fungal cell. *Molecular Microbiology* **2007,** *66* (2), 279-290.

259. Li, P.; Li, X.; Saravanan, R.; Li, C. M.; Leong, S. S. J., Antimicrobial macromolecules: synthesis methods and future applications. *RSC Advances* **2012,** *2* (10), 4031-4044.

260. Li, D.; Muller, M. B.; Gilje, S.; Kaner, R. B.; Wallace, G. G., Processable aqueous dispersions of graphene nanosheets. *Nature Nanotechnology* **2008,** *3* (2), 101-105.

261. Ellman, G. L., Tissue sulfhydryl groups. *Archives of Biochemistry and Biophysics* **1959,** *82* (1), 70-77.

262. Liao, K. H.; Lin, Y. S.; Macosko, C. W.; Haynes, C. L., Cytotoxicity of Graphene Oxide and Graphene in Human Erythrocytes and Skin Fibroblasts. *Acs Applied Materials & Interfaces* **2011,** *3* (7), 2607-2615.

Appendix: List of Publications

Journal Papers:

1. Li, P.; Wang, J.; Chan-Park, M. B., Quaternized chitosan functionalized nanosheets with enhanced antimicrobial activities. *In preparation.*

2. Li, P.; Zhou, C. C; Rayatpisheh, S.; Ye, K.; Poon, Y. F.; Hammond, P. T.; Duan H.; Chan-Park, M. B., Cationic peptidopolysaccharides show excellent broad-spectrum antimicrobial activities and high selectivity. ***Advanced Materials*** 2012, *24* (30), 4130-4137.

3. Li, P.; Li, X.; Saravanan R.; Li, C. M.; Leong, S. S. J., Antimicrobial macromolecules: synthesis methods and future applications. ***RSC Advances*** 2012, *2* (10), 4031-4044.

4. Li, P.; Poon, Y. F.; Li, W. F.; Zhu, H. Y.; Yeap, S. H.; Cao, Y.; Qi, X. B.; Zhou, C. C.; Lamrani, M.; Beuerman, R. W.; Kang, E. T.; Mu, Y. G.; Li, C. M.; Chang, M. W.; Leong, S. S. J.; Chan-Park, M. B., A polycationic antimicrobial and biocompatible hydrogel with microbe membrane suctioning ability. ***Nature Materials*** 2011**,** *10* (2), 149-156.

5. Rayatpisheh, S.; Li, P.; Chan-Park M. B., Argon plasma induced ultrathin thermal grafting of thermoresponsive pNIPAm coating for Contractile Patterned Human Smooth Muscle Cell Sheet Engineering. ***Macromolecular Bioscience*** 2012, *12* (7), 937-945.

6. Zhou, C. C.; Li, P.; Qi, X. B.; Sharif, A. R. M.; Poon, Y. F.; Cao, Y.; Chang, M. W.; Leong, S. S. J.; Chan-Park, M. B., A photopolymerized antimicrobial hydrogel coating derived from epsilon-poly-L-lysine. ***Biomaterials*** 2011**,** *32* (11), 2704-2712.

7. Yan, L. Y.; Chen, H.; Li, P.; Kim, D.-H.; Chan-Park, M. B., Finely Dispersed Single-Walled Carbon Nanotubes for Polysaccharide Hydrogels. ***ACS Applied Materials & Interfaces*** 2012**,** *4* (9), 4610-4615.

8. Zhou, C. C.; Qi, X. B.; Li, P.; Chen, W. N.; Mouad, L.; Chang, M. W.; Leong, S. S. J.; Chan-Park, M. B., High Potency and Broad-Spectrum Antimicrobial Peptides Synthesized via Ring-Opening Polymerization of α-Aminoacid-N-carboxyanhydrides. ***Biomacromolecules*** 2010, *11* (1), 60-67.

9. Qi, X. B.; Zhou, C. C.; Li, P.; Xu, W. X.; Cao, Y.; Ling, H.; Chen, W. N.; Li, C. M.; Xu, R.; Lamrani, M.; Mu, Y. G.; Leong, S. S. J.; Chang, M. W.; Chan-Park, M. B., Novel short antibacterial and antifungal peptides with low cytotoxicity: Efficacy and action mechanisms. ***Biochemical and Biophysical Research Communications*** 2010**,** *398* (3), 594-600.

Conference Presentations:

1. Li, P.; Chan-Park, M. B., Antimicrobial coating and solutions. *5th Annual BioPharma Asia Convention*, **2012**, Singapore.
2. Li, P.; Chan-Park, M. B., Broad-spectrum and high selective antimicrobial cationic peptidopolysaccharides. 5th MRS-S Conference on Advanced Materials, **2012**, Singapore.
3. Li, P.; Poon, Y. F.; Zhou, C. C.; Chang, M. W.; Leong, S. S. J.; Chan-Park, M. B., A new class of contact active antimicrobial nanoporous hydrogel coating. *International conference on materials for advanced technologies*, **2011**, Singapore.
4. Li, P.; Zhou, C. C.; Chan-Park, M. B., Antimicrobial Peptides Synthesized via Ring-Opening Polymerization of α-Aminoacid-N-carboxyanhydrides. *International conference on materials for advanced technologies*, **2011**, Singapore.

Patents:

1. Chan M. B. E.; Li, P., Quaternized chitosan functionalized nanosheets with enhanced antimicrobial activities. *Pending.*
2. Chan M. B. E.; Li, P., Cationic peptidopolysaccharides with excellent broad-spectrum antimicrobial activities. *Pending*.
3. Chan M. B. E.; Zhou, C. C.; Leong, S. J. S.; Chang, M. W.; Li, P.; Qi, X.; Lamrani, M., Polymerizable composition for ophthalmic and medical use and antibacterial composition obtained by polymerizing. Pub. No.: WO2011149058.